Development of highly efficient polymer monolithic column with low flow resistance for high performance liquid chromatography

2013

Tomohiko HIRANO

高速液体クロマトグラフィーのための高分離性能かつ低流路抵抗のポリマーモノリスカラムの開発

近年，高速液体クロマトグラフィー（HPLC）の分離カラムとして，シリカゲルや有機高分子の連続多孔体を固定相とするモノリスカラムが注目されている。モノリスカラムは現在普及している微粒子充填カラムと比較して流路抵抗が低いという特徴をもつことから，高速送液による高速分離などに利用できるという利点がある。しかし，モノリスカラムにおいて低流路抵抗と高分離性能の両立は困難だった。そこで我々は，有機高分子多孔体を固定相とするポリマーモノリスカラムについて，その調製法の改良により，これまでにない高分離性能をもつ低流路抵抗ポリマーモノリスカラムを開発し，高速送液による高速分離に適用した。また，低流路抵抗ポリマーモノリスカラムの応用として，移動相送液に高圧送液ポンプを用いず，僅かなガス加圧で送液を行う低圧 HPLC の構築を行った。

第 1 章は序論であり，本研究の背景と目的について述べた。

第 2 章では，低温紫外線光重合によるポリメタクリル酸エステル系逆相ポリマーモノリスカラムの調製について述べた。カラム調製法として従来用いられてこなかった 0℃程度の低温下における紫外線光重合を導入し，理論段数 4 万段/m 程度の十分な分離性能と，3 気圧程度で送液可能という低い流路抵抗を併せ持つカラムの開発に成功した。また，このカラムを高速分離に用いたところ， 5 種類のアルキルベンゼンを従来の HPLC の 1/100 以下に相当する 8 秒以内に分離することに成功した。

第 3 章では，低温紫外線光重合による陰イオン交換ポリマーモノリスカラムの調製について述べた。カラム調製時の反応溶液に第四級アンモニウム基をもつモノマーを添加し，低温紫外線光重合により低流路抵抗かつ高分離性能の陰イオン交換ポリマーモノリスカラムの開発に成功した。このカラムを用い，5 種類の無機陰イオンを 20 秒以内に分離することに成功した。

第 4 章では，ポリマーモノリスのモノマー転換率の定量法について述べた。ポリマーモ

ノリスのモノマー転換率はカラム評価のために重要であるが，その転換率を直接定量する方法は確立されていなかった。そこで，ポリメタクリル酸エステルが熱により解重合する性質を利用し，熱分解ガスクロマトグラフィーを用いてモノマー転換率を直接定量する手法を開発した。

第 5 章では，低転換率低温紫外線光重合について述べた。低温紫外線重合のモノマー転換率を 10～20%程度に抑えることで，理論段数約 10 万段/m の高分離性能と，2 気圧程度の低い圧力で送液可能な低い流路抵抗をもつカラムの開発に成功した。また，調製したカラムを用い，1～2 気圧程度の僅かなガス加圧で送液を行い，高圧ポンプを用いない低圧 HPLC を構築した。これ用いて従来の HPLC と同程度である 10～20 分以内に，4～5 成分のアルキルベンゼン類やタンパク質を分離できることを示した。

第 6 章では，高濃度酸中での分離への低圧 HPLC の応用について述べた。金属回収プロセスにおいて，高濃度塩酸中における金属イオンと界面活性剤の相互作用の評価が求められている。先に述べた低圧 HPLC は高圧ポンプが不要なため，金属や酸化アルミニウム等の接液部が無く耐酸性が高い。そこで，低圧 HPLC において，移動相に高濃度塩酸を用い，界面活性剤をコートしたカラムで金属イオンを分離し，その保持を指標として金属イオンと界面活性剤の相互作用を評価する手法を開発した。

第 7 章では，これらの内容を総括した。

以上のように，本研究では重合法の改良により，これまでにない高分離性能と低流路抵抗を併せもつポリマーモノリスカラムを調製した。また，低流路抵抗性を生かし，従来の HPLC では実現困難な超高速分離や送液ポンプを必要としない低圧 HPLC の構築といった応用を可能とした。

Chapter 1 General introduction

1.1 Conventional separation columns in high performance liquid chromatography

High performance liquid chromatography (HPLC) is one of the most powerful separation methods for analyzing a liquid sample. In present day, the HPLC is widely used in many fields such as science, engineering, pharmacy, and medicine. Fig. 1-1 shows a schematic illustration of a general HPLC instrument. Typical HPLC consists of mobile phase reservoir(s), high pressure pump(s), an injector, a separation column, a detector, and a data-processing device. The mobile phase is continuously supplied to the separation column by the high pressure pump. The sample solution is introduced into the column using the valve injector, in general. In the column, the analytes are separated based on the difference in the magnitude of interaction(s) between each analyte and a stationary phase. Then, each analyte eluted from the column was detected and the obtained-signal is recorded by the data-processing device.

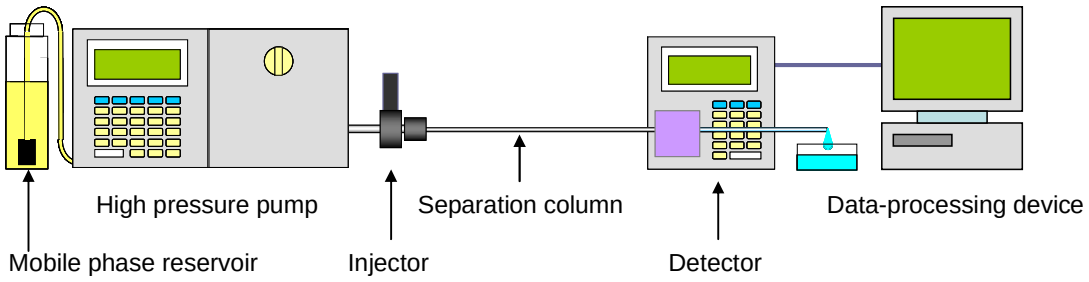

Fig. 1-1. Schematic illustration of HPLC.

Because success in HPLC separations depends strongly upon the efficiency of the separation column, large numbers of researches have been studied for advancement and development of highly efficient columns until today. In other

words, the enhancement of the column efficiency is one of the essential topics of progress in HPLC.

As measures of the column efficiency, both theoretical plate number, N and theoretical plate height, H are widely used. The relationship of two parameters is given by the following equation.

$$H = L/N \tag{1}$$

where L is column length. Large theoretical plate number, or low theoretical plate height, means column efficiency is high. In general, theoretical plate height is a function of a linear flow rate of mobile phase, u[1]:

$$H = Au + B/u + (C_s + C_m)u \tag{2}$$

where A, B, C_s, and C_m mean diffusion due to multi flow path, longitudinal diffusion, mass transfer in mobile phase, and mass transfer resistance to and from the stationary phase, respectively. This equation is called van Deemter equation.

The most popular column for HPLC is a packed column, which means the column closely packed with micro-beads. Chemically modified fully porous spherical silica particles are most frequently used as the micro-beads for HPLC. Especially for a packed column, Eq. 2 can be written as follows[2]:

$$H = 2\lambda d_p + \frac{2\gamma D_M}{u} + \frac{f_s(k)d_f^2}{D_s}u + \frac{f_M(k)d_p^2}{D_M}u \tag{3}$$

where d_p, d_f, k, D_S, D_M, and $f(k)$ are diameter of particle, thickness of stationary

phase, retention factor, diffusion coefficient in stationary phase, diffusion coefficient in mobile phase, and parameter related with k of analyte. The parameters of λ and γ are constants that depend on the quality of packing. This equation clearly shows that the efficiency of a packed column increases with a decrease in d_p. Actually, in order to accommodate the demand for enhancing the column efficiency, the particle diameter has become smaller and smaller. In early HPLC, the particle of a few tenth μm in diameter was used but in today, the particle of 3-5 μm in diameter mainly used. Furthermore, less than 3 μm particle down to 1.5 μm has been developed and gradually widespread.[3-10] On the other hand, however, a flow resistance of packed column drastically increased, when the smaller particles were used because the column resistance is inversely proportional to d_p^2. The flow resistance, R, and back pressure of column, P, can be given by the following equations:

$$R = P/u\eta L \quad \text{or,} \quad P = u\eta RL \tag{4}$$

where η is viscosity of a mobile phase. As shown in this equation, the back pressure is directly proportional to the flow resistance of the column, and therefore the recent decrease in the diameter of packed particles causes a serious increase in the back pressure. The column packed with 3-5 μm particles can generally be operated with a pressure up to 30-40 MPa using a conventional high pressure pump, but the column packed with less than 3 μm particle requires ultra high pressure pumps and highly pressure-resistant pipelines which are capable up to 130 MPa.[11-13] Such system is often called ultra high performance liquid chromatography (UHPLC).

Meanwhile, today, a core-shell type packed column has been studied as an

alternative technology to enhance the column efficiency with suppressing the serious increase in a flow resistance.[14-18] The core-shell particle is composed of a non-porous spherical core and a porous layer shell of less than 1 μm thickness surrounding the core. In comparison to fully porous spherical particle in the same diameter, the diffusion in the particle is restricted because core-shell particle contains non-porous core, and relatively higher column efficiency can be achieved. Therefore, in the case of the "core-shell column", relatively large particles, which suppresses serious increase in a column resistance, can be used to achieve the equivalent separation efficiency compared with a conventional column packed with full-porous particles. However, in order to obtain adequate column efficiency, less than 5 μm particle is generally required.[11-13] Therefore, back pressure of several to several tenth MPa is still needed to supply a mobile phase into a column packed with the core-shell type particles.

Beside the packed column, an open tubular capillary (OTC) column is sometimes used in HPLC.[19-24] The OTC column is a narrow capillary column whose inner wall is chemically or physically coated by thin layer such as liquid phase, supports, and porous materials. The OTC column is the most low flow resistance column used in HPLC. However, in order to obtain sufficient column efficiency, the diameter of OTC should be less than 10 μm or significant extending of the column length is required. A column with a narrow diameter causes a difficulty of sample injection and a decrease in sensitivity and the longer column results in a long analytical time. Moreover, in the OTC column, the surface area of stationary phase is smaller than that of the packed column, and thus both retention of analytes and sample loading capacity are limited. Therefore, the OTC column is seldom used in HPLC whereas that is common in GC.

1.2 Chromatographic limitation due to high pressure

Enhancement in column efficiency is indispensable for a progress in HPLC separation described above. The use of the column packed with smaller or core-shell particles is one of the solutions for this problem. Alternatively extension in a column length is sometime employed as the simple method to enlarge the column efficiency. However, as shown in Eq. 4, the back pressure is directly proportional to the column length. Therefore, the enhancement in a separation efficiency based on the extension in the column length has a limitation due to a capacity to resist pressure for a HPLC apparatus.

On the other hand, reducing the separation time, or high speed separation, is one of the most important agendas in HPLC.[25-27] The approaches to achieve the high speed separation are mainly divided into two categories. One method is reduction of a column length. However, it may cause insufficient separation of analytes and a column with the higher separation efficiency will be required, such as small particles-packed column with a high flow-resistance. Even though a short column packed with small particles is used, the pressure to supply a mobile phase to the column is generally enlarged. Another method for reducing a separation time is based on an increase in a linear flow rate of a mobile phase stream. In this method, however, the increase in a linear flow rate also induces an increase in a back pressure as shown in Eq. 4. Moreover, the column efficiency decreases with increase in a linear flow rate as shown Eq. 1. Since the third term of Eq. 1, or C-term, is directly proportional to the linear flow rate, the value of H almost linearly increases in a higher flow rate region.

One of the practical instances for the fast HPLC separation is a

combination of both two approaches mentioned above. Namely, a separation is performed using a short column packed with small particles with a high flow rate mobile phase. However, this approach results in drastic enhancement in the pressure for supplying a mobile phase.[11-13] Therefore, the fast separation also limited by barotolerance of a HPLC apparatus. Therefore, development the low flow resistance column with both high separation efficiency and high sample loading ability will be effective to solve the limitation due to the capacity to resist pressure for a HPLC apparatus.

1.3 Monolithic column

The monolithic column was developed as a HPLC column with a different internal structure from the conventional columns.[28-32] As shown in Fig. 1-2, the

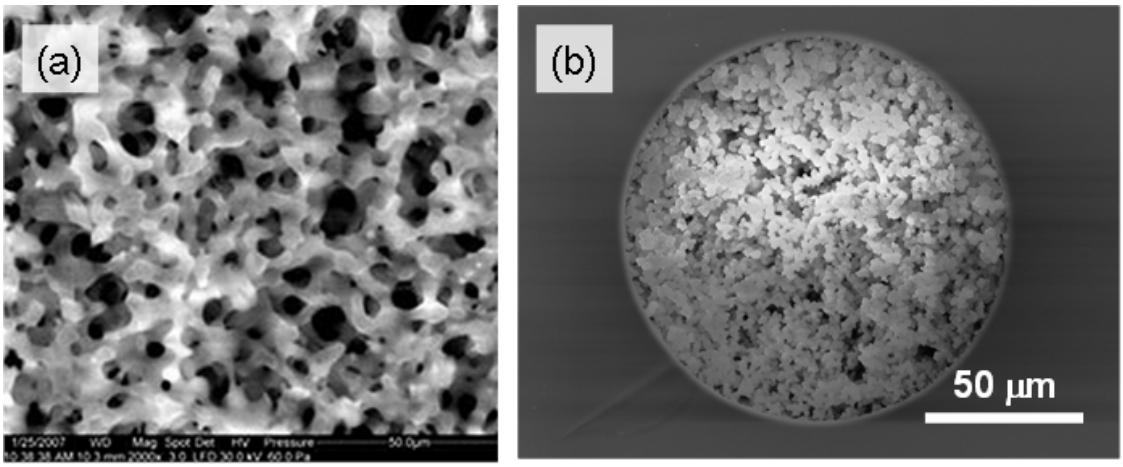

Fig. 1-2. SEM images of silica monolith (a) and polymer monolith (b)[38].

stationary phase of the monolithic column is a single-piece of three dimensional bicontinuous porous material. Because of the presence of relatively large flow through pore, the flow resistance of a monolithic column is lower than that of a packed column. Additionally, the decrease in the separation efficiency, or H in Eq. 1,

is lower than that for a packed column when the flow rate of a mobile phase increases, *i.e.*, *C*-term for a monolith column is smaller than that for a conventional packed-one.[33] Therefore, monolith columns have a potential to solve the pressure-based limitation to achieve both ultra-fast separation and ultra-efficient separation using a long column. Actually, the ultra-efficient separation using 3.5-12.4 m long monolith column[34,35] and ultra-fast separation at a flow rate of 87-100 mm s^{-1} ware previously reported.[36,37]

The monolithic columns can be divided into two types according to their material, *i.e.*, silica- and polymer-based monolithic columns.[28-32] The silica monolithic column was introduced by Minakuchi et al. in 1996.[39] It has some advantages over the polymer one, for instance, well controlled pore structure, good mechanical strength, and high column efficiency especially for small molecules.[40,41] However, since silica is decomposed in acidic or basic solutions, acceptable pH range is narrower than that of the polymer one. The techniques for the preparation and modification of silica monolithic columns have been extensively studied and their users are increasingly widespread.[40,41]

On the other hand, polymer monolithic column, which was introduced by Svec et al. in 1992,[42] has unique advantages such as an availability over a wide pH range and simplicity of preparation, that is, single-step *in situ* polymerization was frequently used.[43-49] As the material for polymer monoliths, methacrylate, acrylate, acrylamide, and styrene were often used and enhancement in the separation efficiency was frequently studied.[43-49] In general, however, the efficiency of polymer monolithic column is still lower than that of silica one especially for low molecule compounds. Recently, some new approaches achieving high efficiency polymer monolithic column, such as polycondensation of epoxy monomer[50] and a low

conversion thermal polymerization,[51-53] were developed. However, further progress in the preparation of polymer monolith was still desired.

1.4 Objective and contents of this thesis

As described in this chapter, the low flow resistance is one of the important factors to solve the pressure-based limitation in HPLC. In this study, therefore, development of highly efficient polymer monolithic columns with low flow resistance was objected. At first, the preparation method for poly(butyl methacrylate-*co*-ethylene dimethacrylate) monolith, which is one of the most common polymer monoliths, was studied. Here, ultra-violet (UV) photo-polymerization under low temperature was investigated for preparing the high performance reversed phase monolithic column with low flow resistance (chapter 2). Here, it was revealed that both lower temperature and higher UV irradiation intensity produced low flow resistance column with moderate separation efficiency. Furthermore, the prepared column was successfully applied to the ultra high speed separation over hundredfold faster than that of the conventional HPLC. Then, the low temperature UV photo-polymerization was also applied to the preparation of the highly efficient methacrylate-ester-based anion-exchange monolithic column (chapter 3). The anion-exchange column was used for a separation of inorganic anions including high speed separation.

Recently, it was reported that the low conversion polymerization led to the high column efficiency for polymer monolithic columns.[51-53] Moreover, we guess that the high column efficiencies achieved in chapters 2 and 3 would have some relations with the low conversion polymerization. However, there is no method to determine

the exact conversion of the monomers to a monolithic stationary phase fixed in the capillary column. Therefore, in chapter 4, the direct determination method for the monomer conversions using pyrolysis gas chromatography, which is generally used for analyses of polymers composition, was developed.

As described above, the low temperature UV photo-polymerization was effective to achieve a high performance and low flow resistance polymer monolith column. As the next step, further enhancement in both separation efficiency and low flow resistance were objected. Here, the low temperature UV photo-polymerization was combined with the low conversion polymerization. This polymerization method, namely low conversion low temperature UV photo-polymerization, for poly(butyl methacrylate-*co*-ethylene dimethacrylate) monolith was investigated and the superior performance in both separation efficiency and reduction in column flow resistance was achieved (chapter 5). Moreover, low pressure HPLC (LP-HPLC), in which the mobile phase stream was generated by vacuum or low gas-pressurization, was proposed using the developed monolith column as the simplest HPLC system.

In chapter 6, an application of a gas-pressure driven LP-HPLC was demonstrated. Since the gas-pressure driven LP-HPLC is free from metal and aluminum oxide parts generally used in a conventional chromatograph, this apparatus is highly acid-resistant. Here, styrene-based low flow resistance monolithic column was prepared by the low conversion thermal polymerization and the interactions between metal ions and surfactants coated on the monolith column in highly acidic solution were investigated chromatographically.

References

1 J.J. van Deemter, F.J. Zuiderweg, A. Klinkenberg, *Chem. Eng. Sci.,* **1956**, 5, 271.

2 J. C. Gidding, "Dynamics of chromatography", Marcel Dekker **1965**.

3 A.A. Mohammad, R. Panagiota, A. Vincent, W. Naijun, *J. Sep. Sci.*, **2008**, *31,* 2167.

4 G.D. Vaijanath, P.K. Pravin, P.R. Pilla, K. Ashok, *J. Pharm. Biomed. Anal.,* **2008**, *46,* 236.

5 R. Toporisic, A. Mlakar, J. Hvala, I. Prislan, L. Zupancic-Kralj, *J. Pharm. Biomed. Anal.,* **2010**,*52*, 294.

6 B.H. Prasad, W.L. Hae, L. Mi-sun, K. Eun-Hee, K. Sung-Doo, P. Jeonghyeon, L. Miran, H. Sung-Kyu, Y. Young-Ran, *J. Chromatogr. B,* **2010**, *878*, 1718.

7 H.K. Mayer, G. Fiechter, E. Fischer, *J. Chromatogr. A,* **2010**, *1217*, 3251.

8 .S. Sachin, I.A. Najar, S.C. Sharma, M.K. Verma, M.V. Reddy, R. Anand, R.K. Khajuria, S. Koul, R.K. Johri, *J. Chromatogr. B,* **2010**, *878*, 823.

9 L. Hong, D. Zhenxia, Y. Qipeng, *J. Chromatogr. B,* **2009**, *877*, 4159.

10 S. Fekete, K. Ganzler, J. Fekete, *J. Pharm. Biomed. Anal.*, **2009**, *51*, 56.

11 J. R. Mazzeo, U. D.Neue, M. Kele, and R. S. Plumb, *Anal. Chem.*, **2005**, *77*, 460A.

12 D. T.-T. Nguyen, D. Guillarme, S. Rudaz, and J.-L. Veuthey, *J. Sep. Sci.,* **2006**, *29*, 1836.

13 S. Fekete, E. Olah, J. Fekete, *J. Chromatogr. A,* **2012**, *1228*, 57.

14 J.H. Knox, *Anal. Chem.,* **1966**, *38*, 253.

15 C. Horvath, B.A. Preiss, S.R. Lipsky, *Anal. Chem.,* **1967**, *39*, 1422.

16 C. Horvath, S.R. Lipsky, *J. Chromatogr. Sci.*, **1969**, *7*, 109.

17 J.J. Kirkland, *Anal. Chem.,* **1969**, *41*, 218.

18 J.J. Kirkland, F.A. Truszkowski, C.H. Dilks Jr., G.S. Engel, *J. Chromatogr. A,* **2000**, *890*, 3.

19 D. Ishii, T. Takeuchi, *J. Chromatogr. Sci.*, **1980**, *18*, 462.

20 J. Yang, *J. Chromatogr. Sci.*, **1982**, *20*, 241.

21 P.R. Dluzneski, J.W. Jorgenson, *J. High Resolut. Chromatogr. Chromatogr. Commun.,* **1988**, *11*, 332.

22 K. Göhlin, A. Buskhe, M. Larsson, *Chromatographia,* **1994**, *39*, 729.

23 Y. Guo, L.A. Colón, *Chromatographia,* **1996**, *43*, 477.

24 X. Huang, J. Zhang, C. Horváth, *J. Chromatogr. A,* **1999**, *858*, 91.

25 D. Figeys, *Anal. Chem.*, **2003**, *75*, 2891.

26 D. Ryan and K. Robards, *Anal. Chem.*, **2006**, *78*, 7954.

27 J. C. Smith, J. -P. Lambert, F. Elisma, and D. Figeys, *Anal. Chem.*, **2007**, *79*, 4325.

28 C. Legido-Quigley, N.D. Marlin, V. Melin, A. Manz, N.W. Smith, *Electrophoresis,* **2003**, *24*, 917.

29 G. Guiochon, *J. Chromatogr. A,* **2007**, *1168*, 101.

30 R. Wu, L. Hu, F. Wang, M. Ye, H. Zou, *J. Chromatogr. A,* **2008**, *1184*, 369.

31 N.W. Smith, Z. Jiang, *J. Chromatogr. A,* **2008**, *1184*, 416.

32 D. Guillarme, J. Ruta, S. Rudaz, J.-L. Veuthey, *Anal. Bioanal. Chem.,* **2010**, *397*, 1069.

33 F. Gritti, G. Guiochon, J. Chromatogr. A, **2009**, *1216*, 4752.

34 K. Miyamoto, T. Hara, H. Kobayashi, H. Morisaka, D. Tokuda, K. Horie, K. Koduki, S. Makino, O. Núñez, C. Yang, T. Kawabe, T. Ikegami, H. Takubo, Y. Ishihama, N. Tanaka, *Anal. Chem.,* **2008**, *80*, 8741.

35 M. Iwasaki, S. Miwa, T. Ikegami, M. Tomita, N. Tanaka, Y. Ishihama, *Anal.*

Chem., **2010**, *82*, 2616.

36 D. Lee, F. Svec, J.M.J. Fréchet, *J. Chromatogr. A,* **2004**, *1051*, 53.

37 Y. Ueki, T. Umemura, Y. Iwashita, T. Odake, H. Haraguchi, K. Tsunoda, *J. Chromatogr. A,* **2006**, *1106*, 106.

38 H. Zhong, G. Zhu, P. Wang, J. Liu, J. Yang, Q. Yang, *J. Chromatogr. A,* **2008** *1190*, 232.

39 H. Minakuchi, K. Nakanishi, N. Soga, N. Ishizuka, N. Tanaka, *Anal. Chem.,* **1996**, *68*, 3498.

40 K. Cabrera, *J. Sep. Sci.,* **2004**, *27*, 843.

41 O. Núñez, K. Nakanishi, N. Tanaka, *J. Chromatogr. A,* **2008**, *1191*, 231.

42 F. Svec, J.M.J. Fréchet, *Anal. Chem.,* **1992**, *64*, 820.

43 K. Hosoya, N. Hira, K. Yamamoto, M. Nishimura, N. Tanaka, *Anal. Chem.,* **2006**, *78*, 5729.

44 Z. Kučerová, M. Szumski, B. Buszewski, P. Jandera, *J. Sep. Sci.,* **2007**, *30*, 3018.

45 H. Aoki, N. Tanaka, T. Kubo, K. Hosoya, *J. Sep. Sci.,* **2009**, *32*, 341.

46 M.W.H. Roberts, C.M. Ongkudon, G.M. Forde, M.K. Danquah, *J. Sep. Sci.,* **2009**, *32*, 2485.

47 E.G. Vlakh, T.B. Tennikova, *J. Chromatogr. A*, **2009**, *1216*, 2637.

48 F. Svec, *J. Chromatogr. A,* **2010**, *1217*, 902.

49 F. Svec, *J. Chromatogr. A,* **2012**, *1228*, 250

50 K. Hosoya,, N. Hira,,K. Yamamoto, M. Nishimura, and N. Tanaka, Anal. Chem., **2006**, *78*, 5792.

51 L. Trojer, C.P. Bisjak,W. Wieder, G. K. Bonn, *J. Chromatogr. A,* **2009**, *1216*, 6303.

52 I. Nischang, O. Brüggemann, *J. Chromatogr. A,* **2010**, *1217*, 5389.

53 I. Nischang, I. Teasdale, O. Brüggemann, *J. Chromatogr. A,* **2010**, *1217*, 7514.

Chapter 2 Methacrylate-ester-based reversed phase monolithic columns for high speed separation prepared by low temperature UV photo-polymerization

2.1 Introduction

As described in chapter 1, the progress in the polymer monolithic column is required in order to enhance the separation efficiency. General polymer-based monolithic columns are prepared by *in situ* polymerization of a reaction solution containing monomer, crosslinker, porogenic solvents, and initiator; the composition of this solution affects the characteristics of the produced monolithic columns, *i.e.*, backpressure, retention factor, and column efficiency.[1-5] The characteristics of the columns were also affected by the polymerization conditions, such as the polymerization temperature and time.[6-8] In other words, the efficiency of the polymer-based monolithic column can be improved by the optimization of polymerization conditions. The usual polymerization methods of the monolithic columns are thermal- and photo-polymerizations.[9-11] The thermal-polymerization is more commonly used than the photo-polymerization because of its simplicity. Ueki *et al.* prepared the low flow resistance polymer-based monolithic column using the thermal polymerization.[12] They achieved the high speed separation of the alkylbenzenes at a linear flow rate of 100 mm/s (100 times faster than the conventional HPLC) with 33 MPa back pressure, which is available on the conventional HPLC pump.

Meanwhile, the photo-polymerization has some advantages over the thermal-polymerization; the former can be achieved at a localized and targeted

region by controlling irradiation area. This advantage is essential to prepare polymer-based monolith in micro fluidic devices.[13,14] In addition, the radical generation rate in the photo-polymerization is able to be controlled independently of the polymerization temperature by varying the light source intensity. In other words, the polymerization temperature can also be changed without considering the radical generation rate. Thus, the photo-polymerization has wide latitude of the polymerization conditions. For the preparation of the photo-polymerized monolithic columns, however, the effects of the UV irradiation intensity and the polymerization temperature on the column efficiency have not been sufficiently studied. This is the case in particular for the preparations at lower temperatures, at which the thermal polymerization does not efficiently contribute.

In this chapter, we prepared butyl methacrylate-based reversed phase monolithic columns for the high speed separation, over 100 times faster than that in the conventional HPLC using photo-polymerization. In order to control the column properties, we independently varied two polymerization conditions, the UV irradiation intensity and the polymerization temperature. Their effects on the column efficiency and the back pressure, which are critical for the high speed separation, were investigated. Particularly, we focused on the polymerization at relatively low temperature. The performance and stability of the prepared monolithic column in the high speed separation were evaluated at flow rates up to 110 mm/s.

2.2 Experimental

2.2.1. Chemicals

Butyl methacrylate (BMA), ethylene dimethacrylate (EDMA), 1-decanol, cyclohexanol, 2,2-dimethoxyphenyl-2-acetophenone (DMPA), acetone, sodium hydroxide, hydrochloric acid, methanol, acetonitrile, uracil, naphthalene, anthracene, toluene, *n*-propylbenzene, *n*-butylbenzene, and *n*-pentylbenzene were purchased from Wako Pure Chemicals (Osaka, Japan). Ethylbenzene and 3-methacryloxypropyltrimethoxysilane were obtained from Tokyo Chemical Industry (Tokyo, Japan) and Shin-Etsu Chemicals (Tokyo), respectively. All chemicals were used as received. Distilled water was used for all experiments.

2.2.2. Column preparation

First, a UV-transparent fused silica capillary (100 μm i.d., 375 μm o.d., 20 cm long, GL science, Tokyo, Japan) filled with 1 M NaOH aqueous solution was kept in a water bath at 65°C for 1 h, and then sequentially flushed with distilled water, 1 M HCl aqueous solution, and distilled water. After drying with a N_2 stream for 1 h, the capillary was filled with 33% 3-methacryloxypropyltrimethoxysilane in acetone and then kept in water bath at 65°C for 3 h to introduce the anchor for attaching polymer-based-monolith to the capillary inner wall. After the treatment, the capillary was flushed with methanol and then dried with a N_2 stream for 1 h.

A polymerization mixture consisting of BMA (24 wt%, monomer), EDMA (16 wt%, crosslinker), 1-decanol (34 wt%, porogenic solvent), cyclohexanol (26 wt%, porogenic solvent), DMPA (1 wt% respect to monomers, photoinitiator) was poured into the pretreated capillary. The composition was decided empirically. Then a

photo-polymerization was performed using a UV illuminator (3UV Benchtop Trance Illuminator, Upland., CA) as a UV (254 nm) light source in an incubator (MIR-153, Sanyo, Osaka, Japan) under various polymerization conditions shown in Table 2-1.

Table 2-1 Photo-polymerization conditions of butyl methacrylate-based monolithic columns

Condition No.	UV lamp tubes	Reflector	UV irradiation intensity / mW cm^{-2}	UV irradiation time / min	Polymerization temperature / °
1	1	-	0.4	8	0
2	6	-	1	8	0
3	6	-	1	16	0
4	6	+	2.0[a]	8	0
5	6	+	2.0[a]	8	10
6	6	+	2.0[a]	8	20

a. Estimated value.

The capillary was irradiated at 5 cm distance from the UV illuminator, which has six UV lamp tubes. In the condition No. 1 of Table 2-1, the capillary was irradiated with the UV light from only one lamp. In the conditions Nos. 2 - 6, the UV light from all of six lamp tubes was irradiated to the capillary. In the conditions Nos. 4 - 6, semi-cylindrical reflector (diameter of 20 cm, length of 20 cm) was additionally placed over the capillary to enhance the UV irradiation intensity and homogeneity. The values of the UV intensities of the conditions Nos. 1 - 3 were measured by an UV meter (UVC-254, AS ONE, Osaka, Japan), and those of Nos. 4 - 6 were values estimated by considering the reflection. As shown in Table 2-1, the polymerizations were performed under the relatively lower temperature (0 - 20°C, ±2°C). After the polymerization, the capillary was immediately connected to a LC pump and then washed with methanol for at least 6 h at a flow rate of 2 μL/min. Finally, the column was cut to 10 cm long.

2.2.3. Chromatography

The capillary HPLC system used consisting of a pump (LC-10ADvp, Shimadzu, Kyoto, Japan), a sample injector (Model 7520, Rheodyne, Cotati, CA) with a 0.5 μL sample loop, a splitter for split injection (resistance capillary: 30 cm × 50 μm i.d.), and a UV/VIS detector (CE-1575, Jasco, Tokyo, Japan). The split ratio is about 20:1 except in case of the column prepared with the condition No. 6 (60:1) which has about three times higher flow resistance than the other five columns. All of chromatographic experiments were performed by isocratic elution using acetonitrile-water (50:50, v/v) as the mobile phase at room temperature (around 20°C). A linear flow rate was calculated from the elution time of uracil (t_0 marker) and the column length. Theoretical plate numbers were calculated using the half width and the retention time of each peak.

2.2.4. SEM measurement

The cutting planes of the monolithic columns were analyzed with a scanning electron microscope (SEM, JXA-8800, JEOL, Tokyo, Japan). After chromatographic measurements, the columns were washed with methanol at a flow rate of 2 μL for at least 12 h, followed by drying at ambient temperature for 3 days and N_2 purging for 3 h. Each dried capillary was cut into at least 3 pieces; Each piece was spattered with gold and then analyzed by SEM.

2.3 Results and Discussion

2.3.1. Effects of the UV irradiation intensity on the column efficiency

In a photo-polymerization, the UV irradiation conditions should directly affect the rate and the uniformity of the radical generation. Therefore, we investigated their effect on the column efficiency of the butyl methacrylate-based monolithic column. At first, several monolithic columns were prepared under various UV irradiation conditions (Nos. 1 - 4 in Table 2-1) at the polymerization temperature of 0°C. Then separations of a standard mixture (uracil, naphthalene, anthracene) using these columns were evaluated in the flow rate range of about 1 - 40 mm/s.

Fig. 2-1 shows separations of the standards using the columns prepared with various irradiation conditions of Nos. 1 - 4 at the linear flow rate of 1 mm/s. In comparison with the columns prepared at the same irradiation time for 8 min

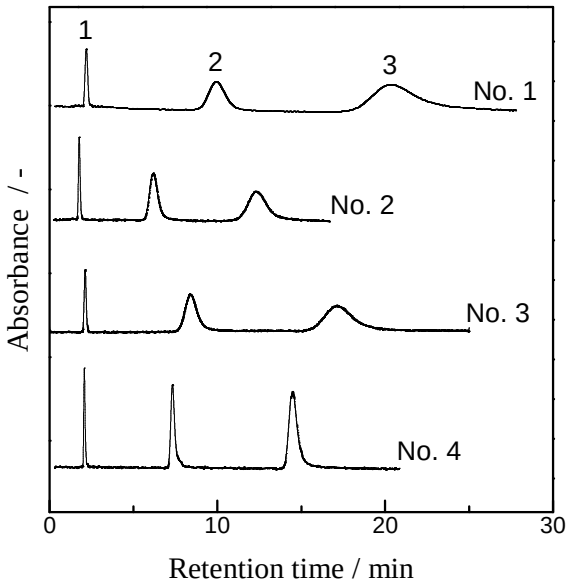

Fig. 2-1 Separations of polycyclic aromatics on the butyl methacrylate-based monolithic columns prepared with different UV irradiation conditions: (No. 1) UV irradiation intensity, 0.4 mW/cm^2; UV irradiation time, 8 min, (No. 2) 1 mW/cm^2, 8 min, (No.3) 1 mW/cm^2, 16 min, (No.4) 2 mW/cm^2, 8 min. Column size, 100 mm × 100 μm i.d.; mobile phase, acetonitrile-water (50:50, v/v); linear flow rate, 1 mm/s; UV detection at 217 nm. Analytes: (1) uracil (t_0 marker), (2) naphthalene, (3) anthracene. Analyte concentration: 1 mM.

(conditions of Nos. 1, 2, and 4), the column prepared at the higher UV intensity provided better efficiency, *i.e.*, narrower peaks. When the total UV irradiation energies were the same (conditions of Nos. 3 and 4), the column prepared with the higher UV irradiation intensity (No. 4) produced more efficient separation.

The effect of the linear flow rate on the column efficiency was also evaluated. Fig 2-2 shows the *H-u* plots for naphthalene using the columns prepared

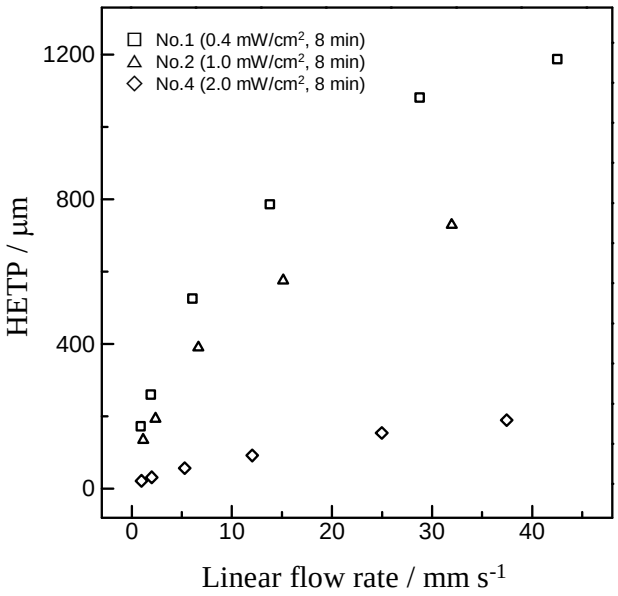

Fig. 2-2 *H-u* plots of the monolithic columns prepared with 8 min of the UV irradiation (Nos. 1, 2, and 4). Chromatographic conditions are the same as in Fig. 2-1. HETP was calculated from the naphthalene peak.

with eight minutes of the UV irradiation (Nos. 1, 2, and 4). As clearly shown in Fig. 2-2, the plots shift to the lower (HETP decreased) with increase in the UV irradiation intensity. The improvement of the column efficiency with the higher UV irradiation intensity was observed over the entire linear flow rate range of 1 - 40 mm/s and its magnitude at higher flow rate was larger than that at lower flow rate.

The chromatographic characteristics of the six columns prepared are described in Table 2-2. In comparison with the conditions Nos. 1 - 4, the UV irradiation conditions did not affect significantly the back pressure (flow resistance

Table 2-2 Chromatographic characteristics of monolithic columns prepared with different conditions

Condition No.	Back pressure[a] / MPa s mm^{-1}	k[b]	N/L[c] / m^{-1}
1	0.28	3.5	4000
2	0.25	2.5	9000
3	0.28	3.0	6000
4	0.31	2.5	45000
5	0.28	2.9	32000
6	0.91	4.0	16000

a. Slope value for flow rate-back pressure relation in the back pressure from 0.2 to 11 MPa ($r^2 > 0.999$).
b. The retention factor of naphthalene at a linear flow rate of 1 mm/s.
c. The theoretical plate numbers of the naphthalene peak at a linear flow rate of 1 mm/s.

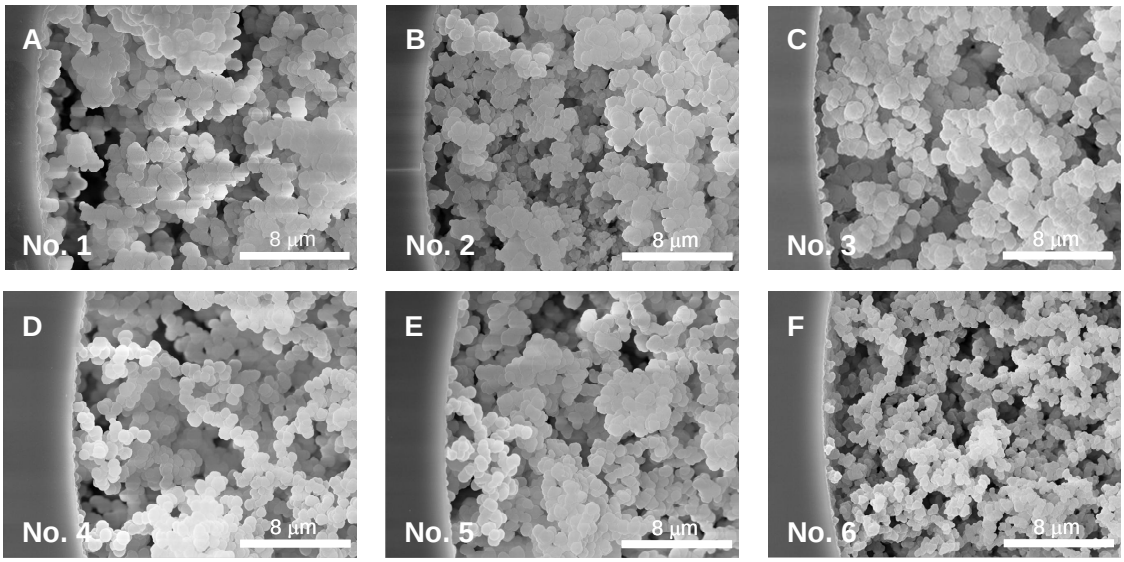

Fig. 2-3 SEM images of the monolithic columns prepared with different polymerization conditions in Table 2-1.

of the column), and thus did not affect the through pore structures of the monolithic columns. The SEM images of the monolithic columns prepared are shown in Fig. 2-3. It is clear that all of the monolithic columns in Fig. 2-3 have agglomerated

structures. Fig. 2-3A - D are the images of the columns prepared under the different UV irradiation conditions. These images show that the monolithic through pore structures, such as the sizes of the monolithic globules and the through pores, are comparable for the four columns. The retention factors are distributed in a range of 2.5 - 3.5 for the four columns, but no specific correlation between the retention factor and the UV irradiation conditions was observed. The theoretical plate numbers of the columns were significantly affected by the UV irradiation intensity, as clearly demonstrated in Fig. 2-1 and Table 2-2; the theoretical plate numbers increased with increase in the UV irradiation intensity. The directional uniformity of the UV irradiation also increases in the order of No. 1 < No. 2, 3 < No. 4. Not only the stronger UV irradiation but also its higher directional uniformity, therefore, might enhance the column efficiency. However, further studies are required to explain in detail such variations induced by the UV irradiation conditions.

2.3.2. Effects of the polymerization temperature on the column efficiency

The polymerization temperature changes the porogenic solvent's viscosity, the solubility of monolith polymer in the porogenic solvent, and the polymerization rate; such changes could affect the characteristics of the monolithic column. In this section, the effect of the polymerization temperature on the column efficiency with the constant UV irradiation intensity for the photo-polymerization was investigated. Here, we focused on the polymerization at the lower temperature, which the thermal-polymerization could not induce. Therefore, the monolithic columns were prepared in the relatively lower temperature range between 0 and 20°C (conditions of Nos. 4 - 6 in Table 2-1). Considering the results of the former section, we prepared

these columns at the UV irradiation intensity of 2 mW/cm^2 for 8 min. The *H-u* plots of the columns prepared with different polymerization temperatures (conditions Nos. 4 - 6) are shown in Fig. 2-4. With decreasing polymerization temperature, the column efficiency was enhanced. Especially the HETP was much more decreased from 20 to 10°C than from 10 to 0°C. Table 2-2 also shows the chromatographic

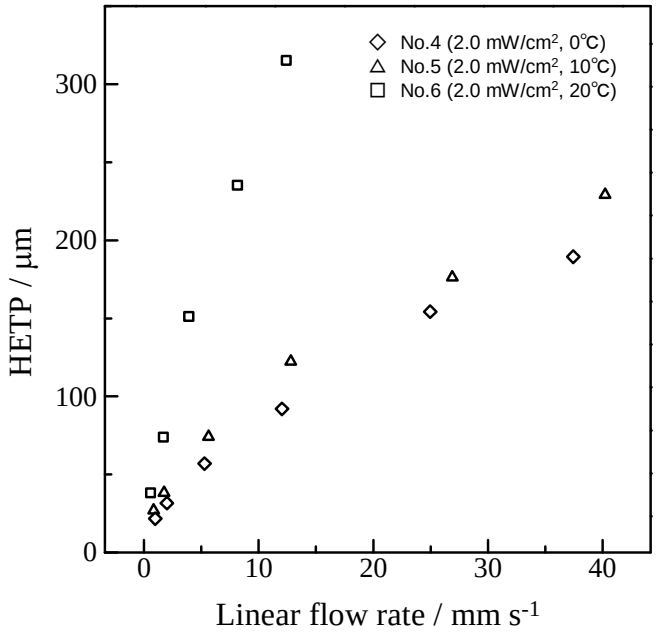

Fig. 2-4 *H-u* plots of the monolithic columns prepared with different polymerization temperatures. HETP values were calculated from naphthalene peak. Chromatographic conditions are the same as those in Fig. 2-1.

characteristics of the columns prepared with the conditions of Nos. 4 - 6. The highest back pressure value was observed for the column prepared at 20°C; those of the other columns (10 and 0°C) were significantly lower and nearly the same. The drastic difference in the back pressure between 20 and 10°C indicates that the polymerization temperature alters the base structure of the monolith, such as the sizes of through pore or the skeleton, which affect the back pressure directly. In fact, Fig. 2-3D - F revealed that the column prepared at 20°C had smaller through pores and globules than those at lower temperatures (the sizes of the column structure

prepared at 10°C were almost the same as those at 0°C). Whereas the temperature-induced changes in the porogenic solvent properties (*i.e.* solvency and viscosity), in the rates of the polymerization reaction, and in the differences in the heat diffusion rate of the reaction heat might affect the column properties, more studies are needed to explain the details.

The lower temperature and the higher UV irradiation intensity were found to enhance the column efficiency. Much higher UV irradiation intensity (> 2 mW/cm^2) and lower polymerization temperature (< 0°C) could not be applied because of limitation of our instruments. In this study, the best performance was achieved by the column prepared with the condition of No. 4 (2 mW/cm^2, 8 min, 0°C) in Table 2-1. The reproducibility (batch-to-batch) of the columns prepared in this condition was good, *i.e.*, the relative standard deviations (RSDs) of back pressure, retention factor, and theoretical plate number were 10, 4, and 6%, respectively (n = 5).

2.3.3. High speed separation of alkylbenzenes

The column prepared with the condition of No. 4 (2 mW/cm^2, 8 min, 0°C) was applied to the high speed separation, in which uracil (t_0 marker) and five alkylbenzenes (toluene, ethylbenzene, *n*-propylbenzene, *n*-butylbenzene, *n*-pentylbenzene) were separated at the linear flow rate of up to 110 mm/s.

The typical separations of alkylbenzenes with various linear flow rates are shown in Fig. 2-5. The theoretical plates numbers of alkylbenzenes (toluene, ethylbenzene, *n*-propylbenzene, *n*-butylbenzene, and *n*-pentylbenzene) at the linear flow rate of 1 mm/s were 45000, 45000, 42000, 40000, and 36000 plates/m,

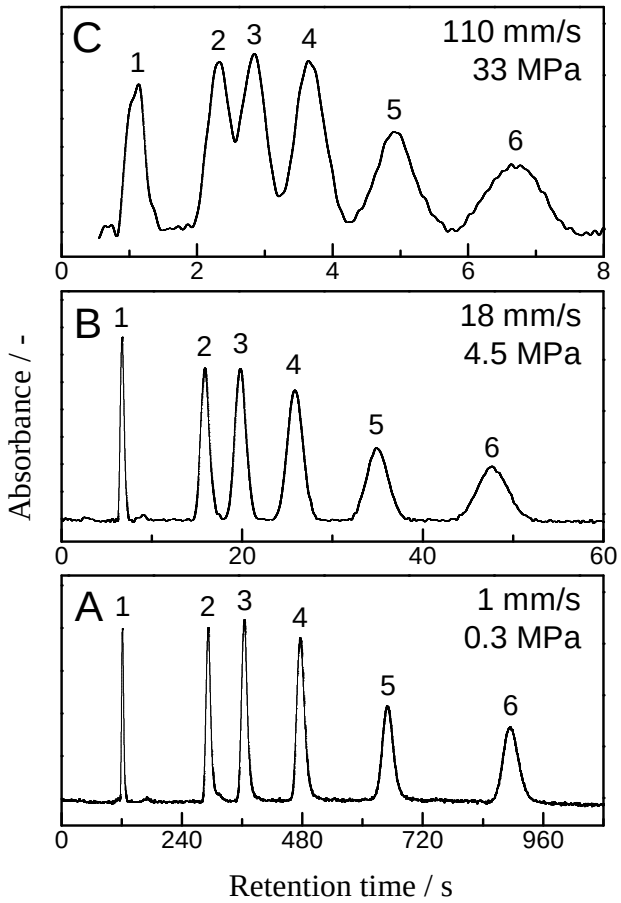

Fig. 2-5 Separations of alkylbenzenes on the monolithic column prepared with polymerization condition No. 4 (UV irradiation intensity, 2 mW/cm^2; UV irradiation time, 8 min; polymerization temperature, 0°C) at various flow rates. Analytes: (1) uracil (t_0 marker), (2) toluene, (3) ethylbenzene, (4) *n*-propylbenzene, (5) *n*-butylbenzene, (6) *n*-pentylbenzene. Analyte concentration: 0.3 mM (uracil), 1 mM (alkylbenzenes). UV detection at 190 nm. Other conditions are the same as those in Fig. 2-1.

respectively. Fig 2-5A shows the separation of alkylbenzenes at the linear flow rate of 1 mm/s, the standard linear flow rate for the conventional packed column, in which the back pressure was quite low (0.3 MPa). According to the increase in the flow rate, both the analytical period and the separation efficiency decreased. The baseline separations of the analytes were kept at the linear flow rate up to 18 mm/s, as shown in Fig. 2-5B. At this flow rate, the separation was completed within 60 s. With further increase in the linear flow rate, the peaks that eluted earlier were partially overlapped. Fig 2-5C shows the separation of the analytes at the linear

flow rate of 110 mm/s. At this extremely fast flow rate, the separation of toluene and ethylbenzene (peaks 2 and 3) was insufficient, but the peak top separation of the six analytes including t_0 marker was achieved within 8 s. Furthermore, the back pressure at the linear flow rate of 110 mm/s is 33 MPa, which can be achieved using a normal LC pump. The high speed separation at the linear flow rate of 110 mm/s could be performed at moderate back pressure, 33 MPa, but in order to achieve more efficient separation, we need more improvements of the column efficiency.

2.3.4. Stability of monolithic column on high back pressure

Generally, the mechanical strength of polymer-based monoliths with the agglomerated structures is relatively lower than those of silica-based ones. Under the higher back pressure, polymer-based monoliths would be compressed, which

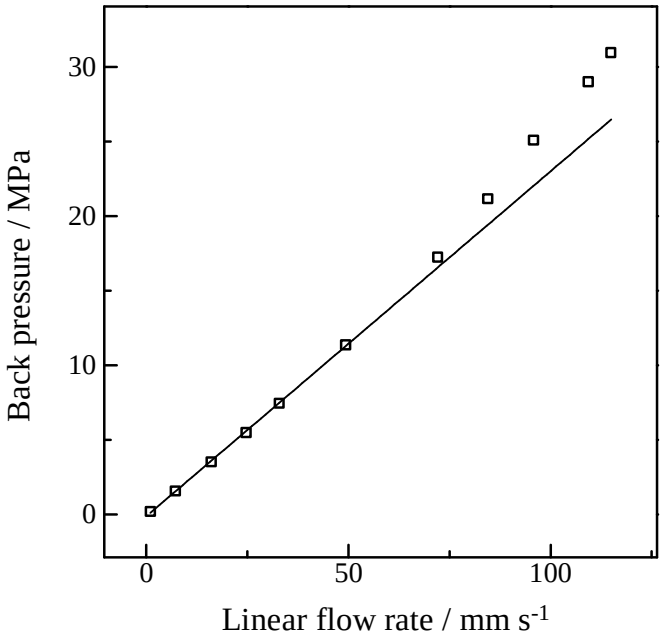

Fig. 2-6 Relationship between linear flow rate and back pressure (*P-u* plot) of the monolithic column prepared with condition No. 4 (UV intensity, 2 mW/cm^2; irradiation time, 8 min; polymerization temperature, 0°C). The line on the plot is the fitting line for six points in 1 - 50 mm/s. Chromatographic conditions are the same as those in Fig. 2-5.

causes a decrease in the column efficiency.[15] Therefore the stability of the polymer-based monolithic column in the higher pressure region is an important factor to keep column efficiency. In this section, we present the stability values of the column prepared with condition No. 4 at a linear flow rate of 1 - 110 mm/s (0.3 - 33 MPa).

Fig 2-6 shows a relationship between the back pressure and the linear flow rate (*P-u* curve). The *P-u* curve in Fig. 2-6 shows good linearity until a flow rate of 50 mm/s (11 MPa), and then the slope of the *P-u* curve gradually increases. This *P-u* curve shows that the through pore structure changed at 50 mm/s (11 MPa). Fig 2-7 shows the *H-u* plots of three alkylbenzenes (toluene, *n*-propylbenzene, and *n*-pentylbenzene) in a linear flow rate range of 1 - 110 mm/s. In the linear flow rate range of 1 - 50 mm/s (0.3 - 11 MPa), all three *H-u* plots showed similar behaviors. Beyond 50 mm/s (11 MPa), the slope of the *H-u* plot of toluene gradually increased.

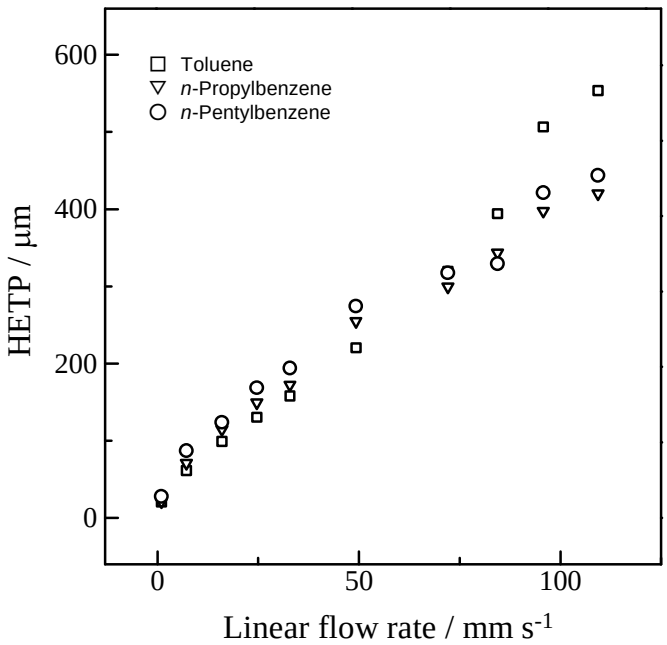

Fig. 2-7 *H-u* plots of the monolithic column prepared with condition No. 4 (UV intensity, 2 mW/cm^2; irradiation time, 8 min; polymerization temperature, 0°C). Chromatographic conditions are the same as those in Fig. 2-5.

On the other hands the values, those of *n*-propylbenzene and *n*-pentylbenzene hardly changed throughout the flow rate range tested. The relationships between the retention factors and the linear flow rate are shown in Fig. 2-8. The retention factors of all alkylbenzenes decreased with increases in the linear flow rate. The decrement was almost the same for every analyte, *i.e.*, the retention factor at 110 mm/s was about 75% of that at 1 mm/s. As is interesting to note, a decrease in the retention factor was observed over the flow rate of 20 mm/s. This value differed from the turning point of the *P-u* and *H-u* plot shown in Figs. 2-6 and 2-7. The mechanism for this difference is under study.

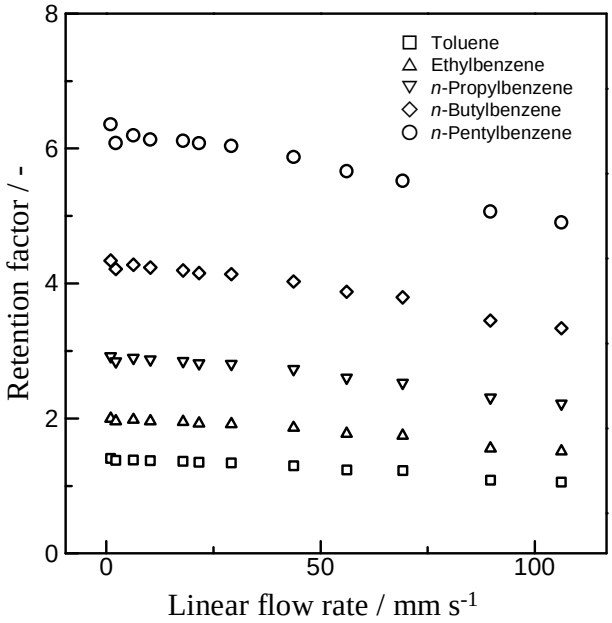

Fig. 2-8 Relationships between linear flow rate and retention factor of alkylbenzenes of the monolithic column prepared with condition No. 4 (UV intensity, 2 mW/cm^2; irradiation time, 8 min; polymerization temperature, 0°C). Chromatographic conditions are the same as those in Fig. 2-5.

These *P-u*, *H-u*, and *k-u* plots show that the structure of monolith gradually altered according to the increase in the back pressure. However, no visible change of the monolithic structure, such as compression, was observed after measurements at 33 MPa. Moreover, these chromatographic behaviors (*P-u*, *H-u*, and *k-u* relations) in

the region of 1 - 110 mm/s were reproduced in multi-cycle measurements. The structural changes would return to the original state after the high pressure was released.

2.4 Conclusion

We prepared the low flow resistance reversed phase-monolithic columns using low temperature UV photo-polymerization. We demonstrated that their separation performances at the flow rates over 100 mm/s are the same as or even better than that of the column prepared by thermal polymerization reported previously. The structural change under the high pressure is one of the possible disadvantages for the polymer-based monolithic column. Unfortunately, the structure of the column prepared in this study would be deformed under the high pressure caused by the fast flow rate. The suppression of the structural change is necessary to achieve more efficient high speed separation. Needless to say, the increase in the separation efficiency is also important for the high speed separation. The higher UV irradiation intensity and the lower polymerization temperature were found to be effective to enhance the column efficiency. Although our experimental system could not to be adjusted to the conditions for the column preparation at lower temperature and higher UV irradiation intensity, the photo-polymerization with such conditions would be suitable to enhance the separation efficiency of polymer-based monolithic columns.

References

1. D. Lee, F. Svec, and J. M. J. Fréchet, *J. Chromatogr.*, *A*, **2004**, *1051*, 53.
2. J. Grafnetter, P. Coufal, E. Tesařová, J. Suchánková, Z. Bosáková, and J. Ševčík, *J. Chromatogr.*, *A*, **2004**, *1049*, 43.
3. S. Eeltink, J. M. Herrero-Martinez, G. P. Rozing, P. J. Schoenmakers, and W. Th. Kok, *Anal. Chem.*, **2005**, *77*, 7342.
4. S. Eeltink, G. P. Rozing, P. J. Schoenmakers, and W. Th. Kok, *J. Chromatogr.*, *A*, **2006**, *1109*, 74.
5. S. Eeltink, L. Geiser, F. Svec, and J. M. J. Fréchet, *J. Sep. Sci.*, **2007**, *30*, 2814.
6. F. Svec and J. M. J. Fréchet, *Chem. Mater.*, **1995**, *7*, 707.
7. F. Svec and J. M. J. Fréchet, *Macromolecules*, **1995**, *28*, 7580.
8. C. Viklund, F. Svec, J. M. J. Fréchet, and K. Irgum, *Chem. Mater.*, **1996**, *8*, 744.
9. F. Svec, *J. Sep. Sci.*, **2004**, *27*, 1419.
10. S. Eeltink and F. Svec, *Electrophoresis*, **2007**, *28*, 137.
11. N. W. Smith and Z. Jiang, *J. Chromatogr.*, *A*, **2008**, *1184*, 416.
12. Y. Ueki, T. Umemura, Y. Iwashita, T. Odake, H. Haraguchi, and K. Tsunoda, *J. Chromatogr., A*, **2006**, *1106*, 106.
13. C. Yu, F. Svec, and J. M. J. Fréchet, *Electrophoresis*, **2000**, *21*, 120.
14. D. S. Peterson, T. Rohr, F. Svec, and J. M. J. Fréchet, *Anal. Chem.*, **2002**, *74*, 4081.
15. T. Jiang, J. Jiskra, H. A. Claessens, and C. A. Cramers, J. Chromatogr., A, **2001**, *923*, 215.

Chapter 3 Separation of small inorganic anions using methacrylate-based anion-exchange monolithic column prepared by low temperature UV photo-polymerization

3.1 Introduction

In the chapter 2, we proposed the low temperature UV photo-polymerization for preparation of reversed phase (RP) methacrylate-ester-based monolithic column. Here, this polymerization method was applied to the preparation of the column with different separation mode.

The ion-exchange mode is one of the most general separation modes in HPLC. Thus, the development of both cation- and anion-exchange monolithic columns has been frequently reported.[1-7] In the case of anion-exchange silica monolithic columns, a high separation efficiency (theoretical plate height, *H*, of 9-14 μm) has been achieved for small inorganic anions.[4] However, the separation efficiency of small inorganic anions on polymer monolithic columns is still not high as that on silica monolithic columns (theoretical plate number per meter, *N*, of <40000 plates m^{-1} or *H* of >25 μm).[2,5,7] Therefore, further advances in the separation efficiency of anion-exchange polymer monolithic columns are desired.

The preparative procedures for anion-exchange polymer monolithic columns can be divided into two categories: multi-step methods and single-step methods. In the multi-step method, a porous structure without anion-exchange ability is initially polymerized and the anion-exchange functionality is subsequently introduced. In the single-step method, the reaction solution containing anion-exchange functional materials is polymerized and a porous structure with anion-exchange functionality

is prepared as long as there are available monomers with the suitable functionalities. The advantages of the single-step method are that it is a relatively simple and time-efficient preparation procedure. In this chapter, therefore, the latter method was used to develop a rapid and simple method preparing an anion-exchange polymer monolithic column with a high separation efficiency and high permeability that achieves the fast separation of inorganic anions.

As described in chapter 2, we found that photo-initiated polymerization at low temperatures is effective for the preparation of highly efficient and highly permeable methacrylate-based RP monolithic columns.[9] Concurrently, Szumski and Buszewski also reported similar results.[10] In this chapter, we developed a single-step-preparation method for the construction of an anion-exchange polymer monolithic column by low-temperature UV photo-polymerization. The column efficiency was evaluated for small UV absorbable inorganic anions, and their rapid separation in both isocratic and gradient modes was demonstrated.

3.2 Experimental

3.2.1. Apparatus

The arrangement of the apparatus used for chromatography in this study was almost the same as that reported in our previous research.[8] The apparatus was composed of two pumps (LC-20AD, Shimadzu), a T-connector for mixing mobile phases, a splitter, a resistance tube (id. 0.05 mm × 50 mm), an injector (7520, Rheodyne), a capillary monolithic column, and a UV detector (CE-970, Jasco). The splitter was fitted at the outlet end of the injector and was used for split injection.

The pumps were operated at a constant flow rate (0.036-20.9 mL/min), and a large fraction of the mobile phase was removed as waste from the splitter.

3.2.2. Chemicals

Butyl methacrylate (BMA), ethylene dimethacrylate (EDMA), [2-(methacryloyloxy)ethyl]-trimethyl ammonium chloride (META), 1-decanol, cyclohexanol, 2,2-dimethoxyphenyl-2-acetophenone (DMPA), methanol, acetonitrile (ACN), uracil, sodium nitrate, sodium nitrite, potassium bromide, sodium iodide, and sodium iodate were purchased from Wako Pure Chemicals. 3-methacryloxypropyltrimethoxysilane was obtained from Shin-Etsu Chemicals (Tokyo).

3.2.3. Preparation of anion-exchange monolithic column

A UV-transparent fused-silica capillary (i.d. 0.1 mm, o.d. 0.375 mm, GL Science) was silanized with 3-methacryloxypropyltrimethoxysilane as described in our previous paper.[9] The capillary was cut to a length of 15 cm and filled with the reaction solution. The compositions of the reaction solutions are summarized in Table 1. Photo-polymerization was then carried out using a UV illuminator (3UV Bench top Trance Illuminator, Upland) as a UV light source (254 nm, 2 mW/cm^2) in an incubator (MIR-153, Sanyo) at -15 °C for 8 min.[9,10] Following polymerization, the capillary was immediately connected to an LC pump and then washed with methanol for at least 6 h at a flow rate of approximately 2 μL/min. Finally, the column was cut to a length of 10 cm.

Table 3-1 Mixing ratios in weight of reaction solutions for anion-exchange polymer monolith column. Values in parenthesis were the ratios in wt% unit.

	BMA	EDMA	META	1-propanol	1,4-butanediol
AX5	16 (15.8)	14 (13.8)	1.5 (1.5)	50 (49.3)	20 (19.7)
AX10	16 (15.5)	14 (13.6)	3.0 (2.9)	50 (48.5)	20 (19.4)
AX20	16 (15.1)	14 (13.2)	6.0 (5.7)	50 (47.2)	20 (18.9)

* 1 wt% DMPA to total wait of monomers was added as an initiator.

3.3 Results and Discussion

3.3.1. Effect of amount of META in reaction solution

The method for preparing the anion-exchange monolithic column used in this study was referenced to the method used for capillary electrochromatography (CEC) columns. For the preparation of a monolithic column for CEC, a small amount of ionic monomer is often added to the reaction solution to generate a stable electroosmotic flow. In this study, a solution containing a moderate amount of anion-exchangeable monomer was polymerized. A mixture composed of BMA (16 wt%), EDMA (14 wt%), 1-propanol (50 wt%), and 1,4-butanediol (20 wt%) was used as the base reaction solution.[7] META, an anion-exchange functional monomer, was added to the base solution in varying amounts of 5, 10, and 20 wt% relative to the total weight of BMA and EDMA. The compositions of the reaction solutions used in this study are listed in Table 1.

The permeability of the monolith column prepared using 20% META (AX20 in Table 1) was significantly lower than that of the monolithic column prepared using 5% and 10% META (AX5 and AX10). Because a column having a high flow

resistance is not suitable for fast separation, the performance of the AX20 column was not assessed in this study. The separation efficiencies of the AX5 and AX10 columns were evaluated using small UV-absorbable inorganic anions. As shown in Fig. 3-1, the retention times of the anions on the AX5 column were lower than those on the AX10 column, *i.e.*, the retention factor of NO_3^- on the AX10 column was about three times larger than that on the AX5 column. Increasing the amount of META in the reaction solution reasonably enhanced the retention ability of the columns for the analyte anions. Furthermore, the separation efficiency of the AX10 column was clearly superior to that of the AX5 column. The theoretical plate number per meter (N) of NO_3^- on the AX5 and AX10 columns was 7200 and 39000 plates m^{-1}, respectively. Therefore, the anion-exchange monolithic column prepared using 10% META was further investigated in this study.

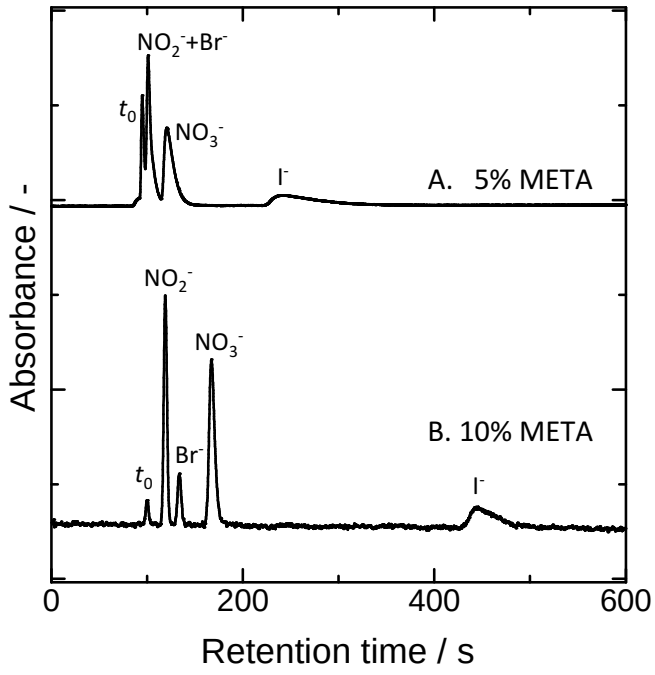

Fig. 3-1 Effect of META concentration in reaction solution on separation of small inorganic anions. Column: BMA-*co*-EDMA-*co*-META monolithic column (A. AX5 and B. AX10, i.d. 0.1 mm, length 100 mm); mobile phase: 100 mM NaCl aqueous solution; apparent flow velocity: 1 mm/s; detection: UV 210 nm; t_0 marker: uracil.

3.3.2. Effect of organic modifier in mobile phase

In this study, BMA, META, and EDMA were used in the copolymerization process for the preparation of the anion-exchange monolithic column. The BMA in the monolith has hydrophobic retention ability. Therefore, the content of an organic modifier, or acetonitrile (ACN), in the mobile phase was increased from 0% to 75% to assess the hydrophobic interaction. The separations of the inorganic anions using various mobile phases were shown in Fig. 3-2. In the case of the mobile phase without ACN (Fig. 3-2A), all analytes were completely separated. However, the elution time of the iodide anion, which is known as a relatively polarizable inorganic anion, was significantly longer and an unsymmetrical peak was obtained. As the concentration of ACN in the mobile phase was increased, the elution of the iodide anion was accelerated and the peak assumed a symmetrical shape as shown in Fig. 3-2. The suppression of the hydrophobic interaction between the iodide anion and the stationary phase provided the desired separation.

The addition of ACN to the mobile phase also influenced the separation behavior of other anions. The elution of all anions was slightly accelerated with the increase in the ACN content, similar to the iodide anion. The use of a mobile phase containing 75% ACN (Fig. 3-2D) resulted in overlap of Br^- and NO_3^- peaks. The separation efficiency, or the theoretical plate number per meter, of NO_2^- with the mobile phases containing 0, 25, 50, and 75% ACN were 54000, 68000, 82000, and 66000 plates m^{-1}, respectively. The column permeability (K) under these mobile phases was calculated by using the following equation: $K = \eta L u / P$ where η, L, u,

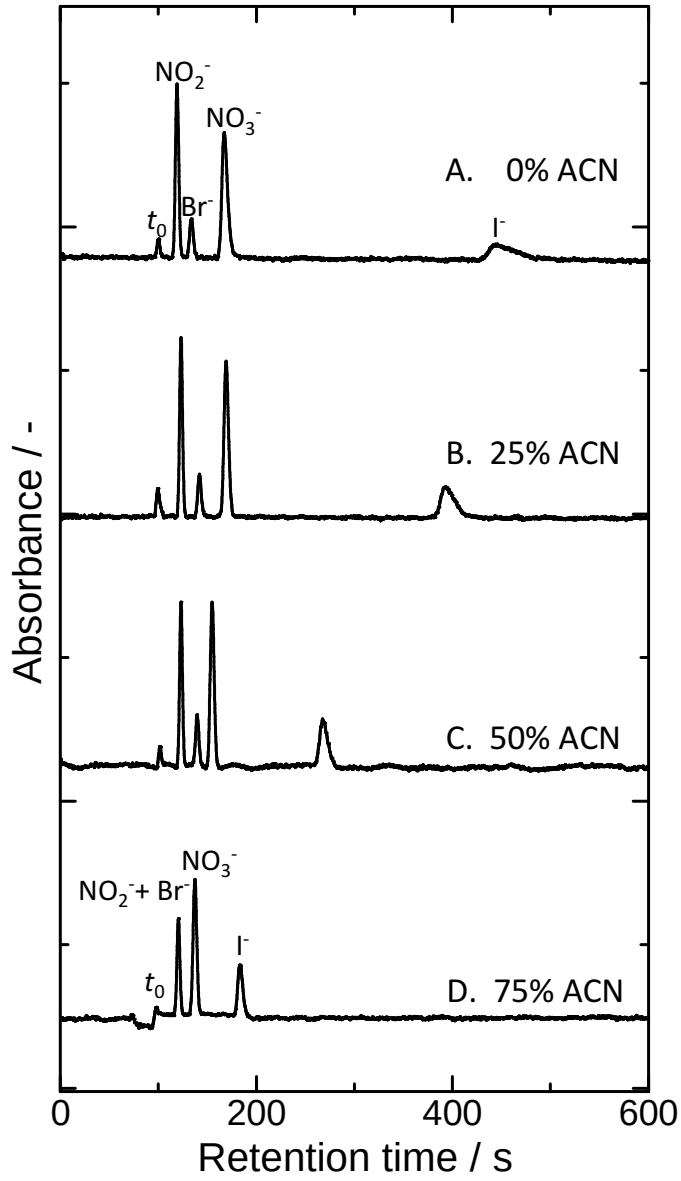

Fig. 3-2 Effect of acetonitrile concentration on separation of small inorganic anions. Column: BMA-*co*-EDMA-*co*-META monolithic column (AX10, i.d. 0.1 mm, length 100 mm); mobile phases: mixtures of acetonitrile (A. 0%, B. 25%, C. 50%, and D. 75%) and water containing 100 mM NaCl. The other conditions were the same as those for Fig. 3-1.

and P were viscosity, column length, t_0-based flow velocity ($u = L/t_0$), and backpressure, respectively.[12] The permeability was decreased with the increase in ACN concentration, *i.e.*, 3.5×10^{-13}, 2.9×10^{-13}, 2.7×10^{-13}, and 2.4×10^{-13} m^2 were calculated for the mobile phases containing 0, 25, 50, and 75% ACN, respectively. The results suggested that the monolith was swelled according to the increase in

the ACN concentration. The variation in the separation efficiency of NO_2^- would be provided by the change in the monolithic structure. In light of both the elution time and separation efficiency, the mobile phase containing 50% ACN was used for the following assays. The column had been used without any deterioration in the column efficiency for at least four months with the mobile phase containing 50% ACN. The organic solvent in the mobile phase did not aggravate the column stability or column life significantly.

3.3.3. Separation in isocratic elution mode

The inorganic UV-absorbable anions were separated using various flow rates as

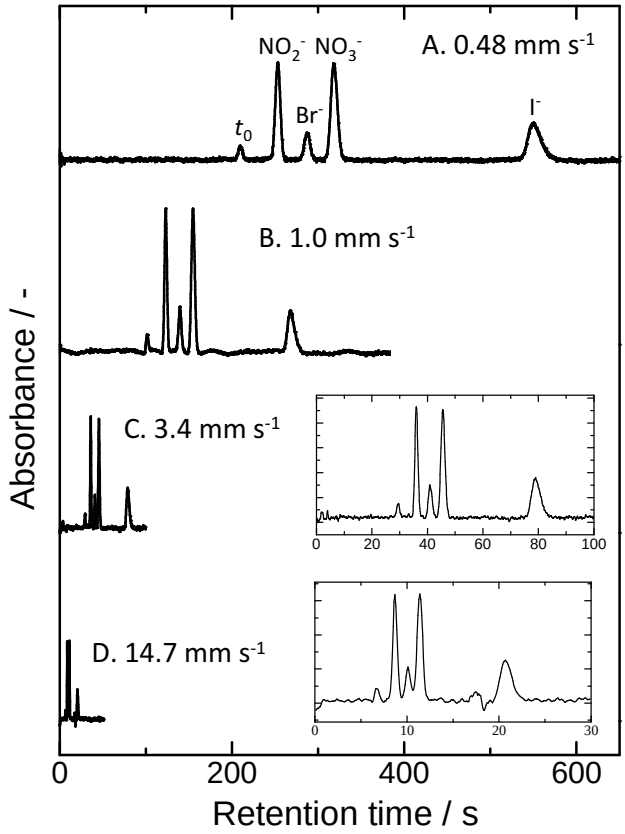

Fig. 3-3 Separation of small inorganic anions with various flow velocities of (A) 0.48 mm/s, (B) 1.0 mm/s, and (C) 3.4/mm, and (D) 14.7 /mm. Mobile phase: acetonitrile/water (50/50) containing 100 mM NaCl; the other conditions were the same those for as Fig. 3-1.

shown in Fig. 3-3. Moreover, the relationship between the flow rate and column efficiencies, or *H*-*u* plot, is shown in Fig. 3-4. The best column performance was achieved at a flow rate of 0.48 mm/s (Fig. 3-3A), *i.e.*, the theoretical plate heights of the anions were 12.2-15.6 μm (*N*, 64000-82000 plates m^{-1}; *k*, 0.2-1.6) and 9.4 μm (*N*, 110000 plates m^{-1}) for t_0. The separation efficiency of the anion-exchange polymer monolithic column prepared in this study was almost comparable to those of silica based monolithic columns (*N*, 69000-106000 plates m^{-1}; *k*, 0.1-2.5).[4] When the polymerization period was increased from 8 to 12 min, both the separation efficiency and permeability of the column were decreased. The similar behavior was also reported previously.[13-16] Therefore, low conversion polymerization would be a key to the high separation efficiency exhibited in this study. Baseline separation of all analytes was obtained up to a flow rate of 3.38 mm/s as shown in Fig. 3-3C. The five analytes were separated within 25 s at a flow rate of 14.7 mm/s (Fig. 3-3D), whereas the peaks of Br^- and NO_3^- were partially overlapped. The theoretical plate heights at

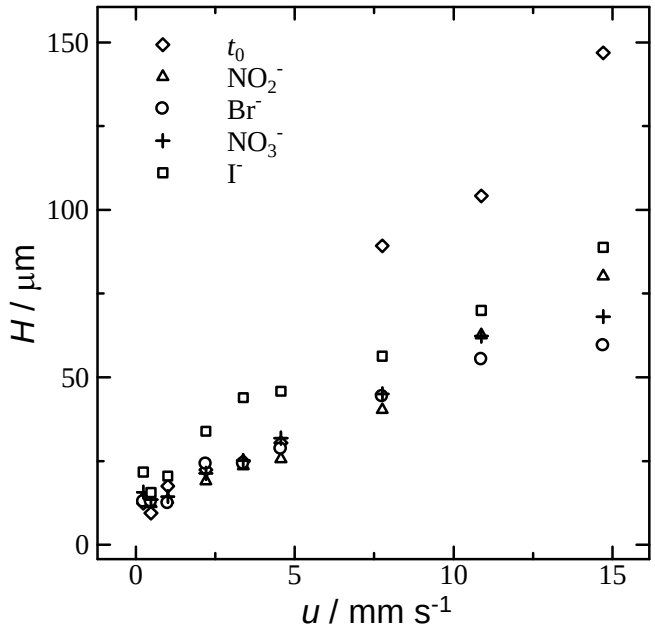

Fig. 3-4 Van Deemter plots of inorganic anions. Chromatographic conditions were the same as those for Fig. 3-3.

14.7 mm/s ranged from 60 to 89 μm (N, 12000-17000 plates m^{-1}) except for the t_0 marker.

In the flow rate range of 0.24-14.7 mm/s, the backpressure was proportional to the flow rate (r^2=0.998). This fact indicated that the monolithic structure was not deformed in this flow rate range, or under a pressure of less than 5 MPa (backpressure at 14.7 mm/s). In the liner relationship between the flow rate and backpressure, the slope (S_{P-u}) was 0.33 MPa/(mm/s), which corresponds to the pressure necessary to produce a flow rate of 1 mm/s using 50% ACN containing 100 mM of NaCl (η = 0.91 mPa·s) as the mobile phase. The column permeability in this condition was 2.7×10^{-13} m^2 as described previous section. The flow resistance and permeability of the anion-exchange monolithic column was roughly comparable with those of a RP monolithic column previously prepared by the current authors using photo-polymerization under low-temperature.[9] The preparation of the methacrylate-based monolithic column using UV photo-polymerization under low temperature is an effective method for producing a highly permeable column with high separation efficiency.

3.3.4. Separation in gradient elution mode

The separation of the anions was also performed using gradient elution. Fig. 3-5 shows the separation of the five UV absorbable inorganic anions, as well as the t_0 marker, using various flow rates with gradient elution. The concentration of NaCl in the mobile phase was increased from 10 to 200 mM over the course of the gradient to enhance the elution. The details of each gradient program are described in the figure caption. At flow rates of both 1.0 and 2.0 mm/s (Fig. 3-5A and B), the

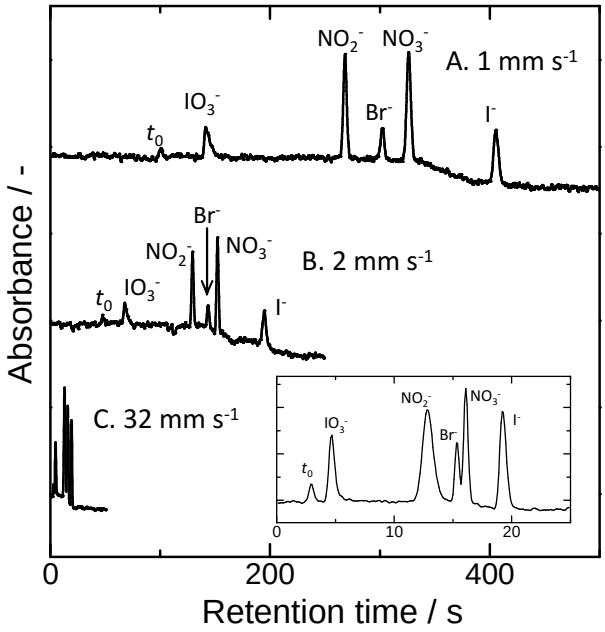

Fig. 3-5 Separation of small inorganic anions in gradient elution mode with various flow rates of (A) 1.0, (B) 2.0, and (C) 32 mm/s. Mobile phases: mixture of acetonitrile and water (50:50) containing (I) 10 mM NaCl and (II) 200 mM NaCl. Gradient programs: (A) 100% (I) in 120 s, 100%-0% (I) in 240 s; (B) 100% (I) in 60 s, 100%-0% (I) in 120 s; (C) 100% (I) in 3 s, 100%-0% (I) in 6 s; other chromatographic conditions were the same as those for Fig. 3-3.

analytes were separated completely. Based on the increase in the flow rate, the separation period in Fig. 3-5B was reduced to half the value of that in Fig. 3-5A. A flow rate of 32 mm/s resulted in separation of the analytes within 20 s as shown in Fig. 3-5C. The ultra-fast separation of small inorganic anions was, therefore, successfully achieved.

The repeatability of the fast separation was statistically evaluated. The values of the mean, SD, and %RSD for elution time, peak height, and relative peak height (uracil was regarded as an internal standard) under the separation conditions employed in Fig. 3-5C (n = 5) are listed in Table 2. The SD values for elution time were less than 0.25 s for all analytes and better repeatability in the elution time was exhibited for the analytes that were eluted at longer times. The %RSD values for the peak height were approximately 10% for all analytes. In

Table 3-2 Repeatability of analytes in fast separation at 32 mm s^{-1} (mean ± SD (%RSD), n = 5).

analyte	elution time (s)	peak height (a.u.)	relative peak height
uracil	3.1 ± 0.25 (8.1)	18.7 ± 1.9 (10.0)	(I.S.)
IO3-	4.8 ± 0.25 (5.2)	70.9 ± 6.7 (9.5)	3.79 ± 0.08 (2.2)
NO2-	13.0 ± 0.20 (1.5)	97.0 ± 9.0 (9.3)	5.18 ± 0.10 (2.0)
Br-	15.4 ± 0.12 (0.8)	62.1 ± 4.8 (7.7)	3.32 ± 0.16 (4.8)
NO3-	16.1 ± 0.14 (0.9)	122.1 ± 11.8 (9.7)	6.52 ± 0.14 (2.2)
I-	19.3 ± 0.19 (1.0)	102.3 ± 9.7 (9.5)	5.47 ± 0.10 (1.8)

* The chromatographic conditions were the same as those in Fig. 3-5C.

the case of relative peak height, the %RSDs were around 2% for all of the analytes except Br^-. The high precision of the fast separation using rapid gradient elution was thus confirmed.

3.4 Conclusions

A single-step UV photo-polymerization method was developed for the preparation of a methacrylate-based anion-exchange monolithic column at low temperature. The column exhibited good separation efficiency for some small inorganic anions. Under optimal conditions, a theoretical plate height of 9.4-15.6 μm (*N*, 64000-110000 plates m^{-1}) was achieved. This column efficiency was relatively high for a polymer monolithic column and was almost comparable with the efficiency of silica-based anion-exchange monolithic columns. The flow resistance of the column was acceptably low, and fast separation was successfully demonstrated with an apparent flow velocity up to 32 mm/s. In the gradient method, five inorganic anions

were separated rapidly with a high precision within 20 s. In this chapter, the anion-exchange monolith containing hydrophobic components was prepared in the capillary. The short optical pass length of the capillary column is disadvantageous to concentration sensitivity for analyses of real environmental aqueous samples. In a future work, a combination of a suitable pre-concentration method and a high performance anion-exchange column prepared with hydrophilic monomers will be essential to analyze real samples with the organic modifier free condition.

References

1. P. Hatsis and C. A. Lucy, *Anal. Chem.*, 2003, *75*, 995.
2. P. Zakaria, J. P. Hutchinson, N. Avdalovic, Y. Liu, and P. R. Haddad, *Anal. Chem.*, 2005, *77,* 417.
3. S. D. Chambe, K. M. Glenn, and C. A. Lucy, *J. Sep. Sci.*, 2007, *30,* 1628.
4. J. Jaafar, Y. Watanabe, T. Ikegami, K. Miyamoto, and N. Tanaka, *Anal. Bioanal, Chem.*, 2008, *319,* 2551.
5. C. J. Evenhuis, W. Buchberger, E. F. Hilder, K. J. Flook, C. A. Pohl, P. N. Nesterenko1, and P. R. Haddad, *J. Sep. Sci.*, 2008, *31,* 2598.
6. A. Nordborg and E. F. Hilder, *Anal. Bioanal. Chem.*, 2009, *394,* 71.
7. D. Connolly and B. Paull, *J. Sep. Sci.*, 2009, *32,* 2653.
8. R. Nakashima, S. Kitagawa, T. Yoshida, and T. Tsuda, *J. Chromatogr., A*, 2004, *1044,* 305.
9. T. Hirano, S. Kitagawa, and H. Ohtani, *Anal. Sci.*, 2009, *25,* 1107.
10. M. Szumski and B. Buszewski, *J. Sep. Sci.*, 2009, *32,* 2574.
11. Y. Huo, P. J. Schoenmakers, and W. Th. Kok, *J. Chromatogr.*, *A*, 2007, *1075,* 81.

12. S. H. Lubbad and M. R. Buchmeiser, *J. Sep. Sci.*, **2009**, *32,* 2521.

13. F. Svec, *J. Chromatogr. A,* **2012**, *1228*, 250

14. A. Greiderer, L. Trojer, C. W. Huck, and G. K. Bonn, *J. Chromatogr., A*, **2009**, *1216,* 7747.

15. I. Nischang and O. Brüggemann, *J. Chromatogr., A*, **2010**, *1217,* 5389.

16. I. Nischang, I. Teasdale, and O. Brüggemann, *J. Chromatogr., A*, **2010**, *1217,* 7514.

Chapter 4 Determination of monomer conversion in methacrylate-based polymer monoliths fixed in a capillary column by pyrolysis-gas chromatography

4.1 Introduction

In the last few years, the preparation of polymer monolithic columns *via* low-conversion polymerization has been reported by some research groups.[1-5] In these studies, low monomer conversion often led to a high separation efficiency with a low flow resistance. These results suggest that a relatively short polymerization period for monolith column preparation might impart superior column efficiency. On the other hand, in the chapters 2 and 3, we introduced the low temperature photo-polymerization to prepare low flow resistance polymer monolithic column with high efficiency. As described in these chapters, it was also suggested that the monomer conversion was an important factor to produce the highly efficient column with the low flow resistance. Therefore, it is essential to investigate the monomer conversion for further enhancement in both column efficiency and flow resistance in the low temperature UV photo-polymerization.

In general, monomer conversions are estimated by measuring the amount of unreacted monomers that are flashed out from the column after polymerization.[1-4] However, the exact conversion of the monomers to a monolithic stationary phase in the column cannot be measured using this method, because it does not account for small fragments of polymers that could be washed out from the column. Therefore, an alternative method is required to determine the exact monomer conversions to monolithic structures fixed in capillary columns for further progress in the

improvement of polymer monolith columns.

Pyrolysis-gas chromatography (Py-GC) is frequently used for analyses of synthetic polymers, even those that are insoluble.[6,7] In general, polymer monoliths are insoluble cross-linked polymers, and various monomers have been used for the syntheses.[8] Polymethacrylate is one of the most common base materials for polymer monoliths, and it is well-known that methacrylate-based polymers are readily depolymerized to the monomers at elevated temperatures.[9] Therefore, the composition of the methacrylate-based polymer can be determined directly from the peak intensities of the original monomers observed in the pyrogram. Furthermore, the amount of sample required for a Py-GC measurement is quite small (*i.e.*, generally less than 50 μg). Therefore, Py-GC is suitable for the compositional analysis of small amounts of polymer monolith synthesized in a capillary. In this chapter, we used Py-GC to determine the monomer conversion to methacrylate-based polymer monoliths fixed in a column without any pretreatment.

4.2 Experimental

4.2.1. Chemicals

Butyl methacrylate (BMA), ethylene dimethacrylate (EDMA), 1-decanol, cyclohexanol, 2,2-dimethoxyphenyl-2-acetophenone (DMPA), α-α'-azobisisobutyronitrile (AIBN), poly(ethyl methacrylate) (PEMA), methanol, and acetone were purchased from Wako Pure Chemicals (Osaka, Japan). 3-Methacryloxypropyltrimethoxysilane (MPTS) was obtained from Shin-Etsu Chemicals (Tokyo, Japan). All chemicals were used as received.

4.2.2. Preparation of monolith

Two types of poly(BMA-*co*-EDMA) monolith, *i.e.*, bulk monolith and that formed in a capillary column, were prepared from a reaction solution consisting of BMA (24 wt%), EDMA (16 wt%), 1-decanol (34 wt%), and cyclohexanol (26 wt%).[10] The molar ratio of BMA/EDMA in the reaction solution was 2.08/1. To synthesize the standard bulk monolith, AIBN (1 wt% respect to the total amount of monomers) was added to 1 mL of the reaction solution in a small vial (10 mm i.d.), and the solution was thermally polymerized at 65°C for 24 h. The resultant bulk monolith was washed with methanol to remove unreacted monomers, oligomers, and porogens (*i.e.*, 1-decanol and cyclohexanol), dried *in vacuo* for 2h, and cryomilled for 45 min. Finally, the obtained monolith powder was further washed with methanol and dried *in vacuo* for 2 h.

The capillary monolith columns were prepared by both thermal and photo-initiated polymerization in a fused-silica capillary (0.1 mm i.d.) with an MPTS-modified inner surface.[9] The thermal polymerization conditions were the same as those for the bulk solution. Photo-initiated polymerization (UV 254 nm, 2 mW cm^{-2}) was performed at low temperature (0°C) for various polymerization periods according to our previously reported method.[9] In this reaction, 1 wt% DMPA with respect to the amount of monomer was added to the reaction solution as photo initiator.

4.2.3. Py-GC measurement

A vertical microfurnace-type pyrolyzer (Frontier Laboratory PY-2020iD) was directly attached to the injection port of a gas chromatograph (G-6000, Hitachi) equipped with a flame ionization detector (FID). The monolith sample and PEMA (2.4 μg) as an internal standard (IS) were placed in a deactivated stainless-steel sample cup, and then introduced into the headed center of the pyrolyzer to depolymerize the poly(BMA-*co*-EDMA) monolith into BMA and EDMA. To analyze the bulk monolith, a weighted amount of the monolith (*ca.* 5 to 30 μg) was pyrolyzed with IS. To analyze the capillary monolith, a 10 ± 0.5 mm sample of the capillary column was cut into three pieces, which were placed in a sample cup with IS, and then dropped into the pyrolyzer to pyrolyze the monolith fixed in the fused-silica capillary (maximum about 30 μg). The Py/GC interface and the injection port of the GC were heated at 280˚C to prevent condensation of the pyrolysis products.

For separation of the degradation products, a metal capillary column (Ultra ALLOY^{+}-1701, 30 m × 0.25 mm i.d. × 0.25 μm coated with 14% cyanopropylphenyl-86% dimethylpolysiloxane) was used. A flow rate of 57 mL min^{-1} He carrier gas was used to rapidly sweep the pyrolysis products from the pyrolyzer to the separation column. The carrier gas flow was reduced to 1.14 mL min^{-1} at the inlet of the capillary column by means of a splitter. The temperature for the column was initially set at 40˚C, elevated up to 280ºC at a rate of 20ºC min^{-1}, and then maintained at 280ºC for 20 min.

4.3 Results and Discussion

4.3.1. Py-GC analysis of monolith

Generally, an IS is used for quantitative analyses. In this study, volatile compounds are not suitable for ISs because volatilization of the standard from a sample cup causes an instability of the analytical result. Therefore, PEMA, which is a methacrylate-based polymer that readily depolymerizes to EMA at elevated temperature, was used as the non-volatile IS for this study. A 4.0 μL aliquot of the standard solution (0.6 μg μL^{-1} acetone solution) was added to the sample cup using a microsyringe, and the acetone solvent was evaporated for about 30 s at room temperature before analysis.

Typical pyrograms of poly(BMA-*co*-EDMA) monoliths at 450°C with PEMA as the IS are shown in Fig. 4-1. The bulk monolith almost exclusively depolymerized into its constituent monomers, *i.e.*, BMA and EDMA, together with EMA from PEMA at 450°C (Fig. 4-1A). When the pyrolysis temperature was less than 400°C, the pyrogram peaks were slightly broader due to a decreased depolymerization rate. At pyrolysis

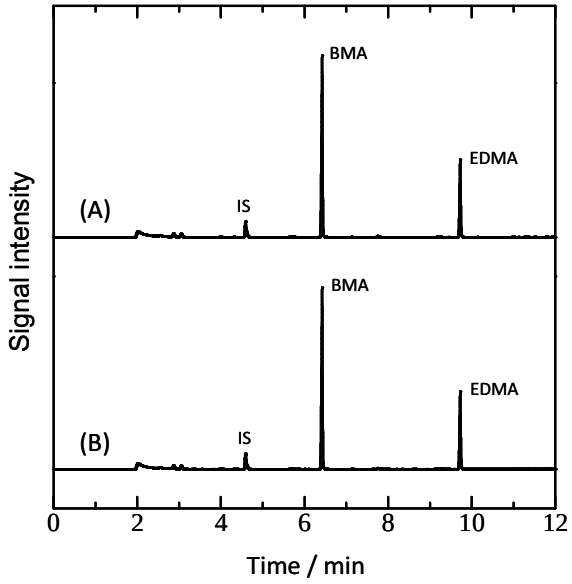

Fig. 4-1 Pyrograms of poly(BMA-*co*-EDMA) monolith at 450°C. (A) bulk monolith, 10.1 μg; (B) capillary monolith column prepared at 65°C for 24 h, 10 mm. PEMA (2.4 μg) was added as the IS.

temperatures above 500°C, undesired fragmentation (over decomposition) of the monolith was observed. Therefore, 450°C was employed as the pyrolysis temperature. The monolith fixed in the capillary column (0.1 mm i.d. × 10 mm) also decomposed to BMA and EDMA without any pretreatment before pyrolysis, as shown in Fig. 4-1B. After analyses, no residue was observed in the sample cup or inside the capillary. Almost all monoliths decomposed at the elevated temperature.

In analyses of the 10 mm long capillary monolith column, the repeatabilities of the peak intensities of IS, BMA, and EDMA were 3.3, 3.1, and 2.7% relative standard deviation (RSD; $n = 5$), respectively. The RSD values of the relative peak intensities for BMA/IS, EDMA/IS, and BMA/EDMA were 5.6, 5.3, and 0.7%, respectively. The precision of the yields of the BMA and EDMA monomers relative to the IS was about 5% RSD. The higher precision, *i.e.*, 0.7% RSD for the BMA/EDMA ratio, suggests that polymerization proceeded homogeneously in the capillary column.

4.3.2. Determination of conversion

The monomer conversion in poly(BMA-*co*-EDMA) monolith was assessed based on the amount of monomers produced during pyrolysis. BMA and EDMA were calibrated from the peak areas of the monomers from the bulk monolith relative to those from the IS (*i.e.*, BMA/IS and EDMA/IS) and the corresponding constituents contained in the monolith obtained at various amounts of monolith samples.

First, the copolymer composition of the bulk monolith, *i.e.*, molar ratio of BMA and EDMA, was evaluated using Py-GC. The average peak area ratio of BMA/EDMA from the Py-GC measurements of the bulk monolith was 2.45 ± 0.03 (*n*

= 6, with monolith amounts ranging from 5.8 to 23.6 μg). A mixture of BMA and EDMA standard (at a molar ratio of 2.08/1) was then subjected to GC analysis which resulted in a peak-area ratio of 2.16/1. Thus, the molar ratio of the BMA/EDMA composition of the bulk monolith was estimated to be 2.38/1 (1.71/1 in weight ratio).

The calibration curves for BMA and EDMA are shown in Figs. 4-2A and 4-2B, respectively. The top axes indicate the amount of bulk monolith used to construct the calibration curves, while the bottom axes correspond to the amounts of BMA or EDMA in the monolith, which were estimated using the BMA/EDMA composition of the bulk monolith. The left axes show the peak areas of the depolymerized monomers from the bulk monolith relative to those of the IS (*i.e.*, BMA/IS and EDMA/IS). Good linearity (R^2>0.998) was obtained in both calibrations, and the monoliths were depolymerized quantitatively in this range. The LODs (3 σ/S_a,

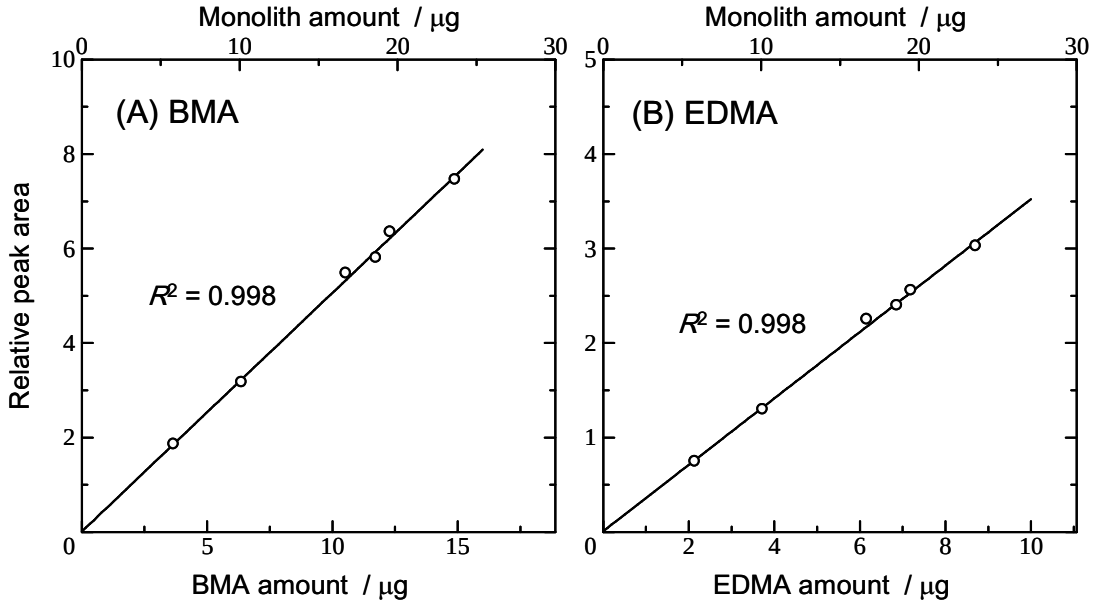

Fig. 4-2 Calibration curves for (A) BMA and (B) EDMA based on the relationship between the peak areas of the monomers from the bulk monolith relative to that of the IS (*i.e.*, BMA/IS and EDMA/IS) and the corresponding constituents of 5.8 - 23.6 μg monolith samples.

where S_a and σ are the slope and the standard deviation of the intercept, respectively) for BMA and EDMA were both 0.08 μg, and the LOQs ($10\ \sigma/S_a$) were 0.27 μg for BMA and 0.25 μg for EDMA. Using these calibration curves, the amounts of BMA and EDMA produced from the pyrolysis of monolith fixed in a capillary could be determined.

The conversion of the monolith formed in the capillary was then estimated as follows. The volume of the capillary (0.1 mm i.d. × 10 mm) was 78.5 nL, and the density of the reaction solution was 1.08 g mL^{-1} at room temperature. The contents of BMA and EDMA in the solution were 24 wt% and 16 wt%, respectively. Thus, 20.3 μg and 13.6 μg of BMA and EDMA, respectively, were fed into the capillary of 10 mm long. These values should correspond to 100% conversion, meaning that all monomers were converted to monolith in the capillary. Therefore, the conversions (*%C*) were estimated from the following equation:

$$\%C = \frac{\text{Amount of momomer determined by Py-GC of monolith sample}}{\text{Amount of momomer contained in the original solution}} \times 100$$

.

Based on the pyrogram shown in Fig. 4-1B and the calibration curves (Fig. 4-2), 17.5 ± 1.1 μg and 11.6 ± 0.7 μg ($n = 5$) of BMA and EDMA, respectively, were obtained from the monolith in the 10 mm column. Therefore, the *%C* values of BMA and EDMA were 86.3 ± 5.4% and 85.7 ± 5.1%, respectively. When the thermal polymerization period was extended from 24 h to 36 h, the conversions for the monolith in the capillary reached 103.8% for BMA and 99.8% for EDMA. The monomer conversions to poly(BMA-*co*-EDMA) monolith fixed in a capillary column were determined directly using Py-GC.

4.3.3. Relationship between polymerization period and monomer conversions

In our previous report, a poly(BMA-*co*-EDMA) monolithic capillary column was prepared *via* photo-polymerization with UV irradiation for 8 min at 0°C.[9] In this study, capillary monolith columns of UV-polymerized poly(BMA-*co*-EDMA) were prepared at 0°C with various polymerization periods of 4, 8, 12, and 16 min, and the relationship between monomer conversion and the polymerization period was elucidated. About 10 mm of each column and the IS were subjected to Py-GC measurements and the conversions of BMA and EDMA were determined. With a polymerization period of 4 min, the average conversions (n = 3) of BMA and EDMA were 23.8% and 43.2%, respectively (Fig. 4-3). The monomer conversions increased with increased polymerization periods and reached about 41.6% for BMA and 65.3%

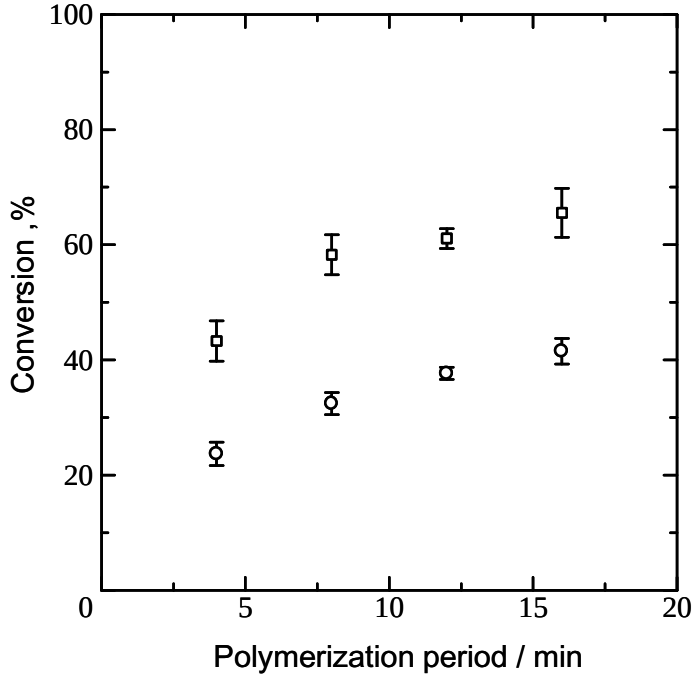

Fig. 4-3 Relationship between the polymerization period and conversions of BMA (○) and EDMA (□) determined by Py-GC. Sample: UV-polymerized poly(BMA-*co*-EDMA) monolithic column (0.1 mm i.d. × 10 mm). The error bars indicate the standard deviation (n = 3).

for EMDA with 16 min of polymerization. The greater conversion of EDMA compared to BMA indicates that the polymerization of EDMA proceeds at a faster rate under these polymerization conditions. A similar phenomenon was also reported for a thermally polymerized poly(BMA-*co*-EDMA) monolith.[3] Therefore, the bifunctional EDMA monomer polymerizes faster than the monofunctional BMA monomer.

4.4 Conclusions

Monomer conversions to poly(BMA-*co*-EDMA) monolith fixed in a capillary column were assessed *via* Py-GC without any sample pretreatment. The proposed method will be applicable for other types of polymer monolith columns. In the low-conversion poly(BMA-*co*-EDMA) monolith, the monomer composition did not match that of the reaction solution introduced into the capillary. A measurement of the actual monomer conversion is essential for further progress in improving polymer monolith columns. Studies of the correlation between the monomer conversion to polymer monoliths and various column properties are currently underway.

References

1. L. Trojer, C. P. Bisjak,W. Wieder, and G. K. Bonn, *J. Chromatogr. A*, **2009**, 1216, 6303.
2. A. Greiderer, L. Trojer, C. W. Huck, and G. K. Bonn, *J. Chromatogr. A*, **2009**, 1216, 7747.

3. I. Nischang and O. Brüggemann, *J. Chromatogr. A*, **2010**, 1217, 5389.
4. I. Nischang, I. Teasdale, and O. Brüggemann, *J. Chromatogr. A*, **2010**, 1217, 7514.
5. M. Takahashi, T. Hirano, S. Kitagawa, and H. Ohtani, *J. Chromatogr. A*, **2012**, 1232, 123.
6. T. P. Wampler (ed.), "*Applied Pyrolysis Handbook, Second Edition*", **2006**, CRC Press, Boca Raton.
7. S. Tsuge, H. Ohtani, and C. Watanabe, "*Pyrolysis-GC/MS Data Book of Synthetic Polymers -Pyrograms, Thermograms and MS of Pyrolyzates-*", **2011**, Elsevier, Amsterdam.
8. E. F. Hilder, F. Svec, and J. M. Fréchet, *Electrophoresis*, **2002**, 23, 3934.
9. H. Ohtani, T. Asai, and S. Tsuge, *Macromolecules*, **1985**, 18, 1148.
10. T. Hirano, S. Kitagawa, and H. Ohtani, *Anal. Sci.*, **2009**, 25, 1107.

Chapter 5 Low-flow-resistance methacrylate-based polymer monolithic column prepared by low-conversion ultraviolet photo-polymerization at low temperature

5.1 Introduction

As described previous chapters, the low flow resistance polymer monolithic columns with high efficiency were successfully prepared by the low temperature photo polymerization. Moreover, it was also suggested that reducing monomer conversion of polymer monolith would enhance the column efficiency and decrease in flow resistance in this photo polymerization method. Actuary, it was reported that the preparation of polymer monoliths by relatively short time thermal-polymerization resulted in increased porosity and specific surface area of the monolith, and column efficiency for small molecules was enhanced along with decreased flow resistance in the thermal polymerization,[1-3] As described in chapter 4, we developed the evaluation method for the monomer conversion to the monolith, which is necessary to control and evaluate the properties of polymer monolithic columns. Here, a low-conversion low temperature UV photo-polymerization was developed to prepare the polymer monolithic column with further higher efficiency and further lower flow resistance than those of the columns prepared in the chapters 2 and 3.

Meanwhile, a low-flow-resistance HPLC column has the potential to construct HPLC systems without the need for conventional HPLC high-pressure pumps to supply the mobile phase. An open tubular capillary column is the most permeable (lowest flow resistance) column used in HPLC. Kiplagat et al., using an open tubular capillary column, demonstrated the separation of inorganic anions

using a light-weight portable LC system in which the mobile phase was supplied to the column by siphoning with a difference in height of 2 m.[4] Monolithic columns can be used in a similar HPLC system without the need for a high-pressure pump, utilizing gas and/or vacuum pressure-driven pumps instead, when the flow resistance of the monolithic column is sufficiently low and the column efficiency is adequately high. Particularly, a vacuum pressure-driven capillary HPLC with a direct injection method has a potential to construct the simplest chromatograph.

In this chapter, low-conversion low temperature UV photo-polymerization was investigated to prepare reversed phase methacrylate-based polymer monolithic columns. As described in the chapter 2, we found that an increase in irradiation intensity in the range from 0.3 to 2.0 mW cm^{-2} resulted in enhancement of both column efficiency and permeability.[5] Accordingly, a high-pressure Hg lamp (an irradiation intensity of 170 mW cm^{-2}) was used as a high-power light source for photo-polymerization in the preparation of the monolithic columns at low polymerization temperature. Here, the effects of the conversion on the chromatographic properties of the prepared columns, such as flow resistance and separation efficiency, were evaluated by varying the polymerization time. Using the fabricated low-flow-resistance monolith column, then we demonstrated the separation of alkyl benzenes in a vacuum-driven low-pressure HPLC without the need for a conventional high-pressure HPLC pump.

5.2 Experimental

5.2.1. Chemicals

Butyl methacrylate (BMA), ethylene dimethacrylate (EDMA), 1-decanol, cyclohexanol, 2,2-dimethoxyphenyl-2-acetophenone (DMPA), methanol, acetonitrile (ACN), uracil, toluene, *n*-propylbenzene, *n*-butylbenzene, and *n*-pentylbenzene were purchased from Wako Pure Chemicals (Osaka, Japan). Ethylbenzene was obtained from Tokyo Chemical Industry (Tokyo, Japan). 3-Methacryloxypropyltrimethoxysilane (MAPS) was obtained from Shin-Etsu Chemicals (Tokyo). BODIPY FL C_{16} was obtained from Molecular Probes, Inc. (Eugene, OR). All chemicals were used as received.

5.2.2. Column preparation

A UV-transparent fused silica capillary (100 μm i.d., 375 μm o.d., GL Science, Tokyo, Japan) was silanized with MAPS as described in our previous report.[5] The capillary was cut to 15 cm long and filled with reaction solution consisting of BMA (monomer, 24 wt%), EDMA (cross-linker, 16 wt%), 1-decanol (porogen, 34 wt%), cyclohexanol (porogen, 26 wt%), and DMPA (photoinitiator, 1 wt% with respect to the monomers),[5-7] and the solution was photopolymerized using a high-pressure Hg lamp (170 mW cm^{-2}, 365 nm, HLR100T-2, SEN LIGHT Corporation, Osaka, Japan) for 1.5-16 min in an incubator (MIR-153, Sanyo, Osaka, Japan) at -15, 0, and, 15°C. After polymerization, the columns were immediately washed with methanol to remove unreacted reagents, unfixed-polymer fragments, and porogens.

5.2.3. Chromatographs

A conventional capillary HPLC system consisting of a pump (LC-10ADvp, Shimadzu,

Kyoto, Japan), a sample injector (Model 7520, Rheodyne, Cotati, CA, USA), a T connector equipped with a resistance tube for split injection (split ratio, 1:50), and a UV/Vis detector (CE-1575, Jasco, Tokyo, Japan) was used to evaluate the column characteristics (flow resistance, column efficiency, and retention) with an isocratic elution in the reversed phase (RP)-HPLC mode.

A low pressure-HPLC (LP-HPLC) system without a conventional HPLC pump was also used in this experiment. Here, two types of LP-HPLC were constructed, *i.e.*, vacuum- and gas pressure-driven system. Fig. 5-1 shows the

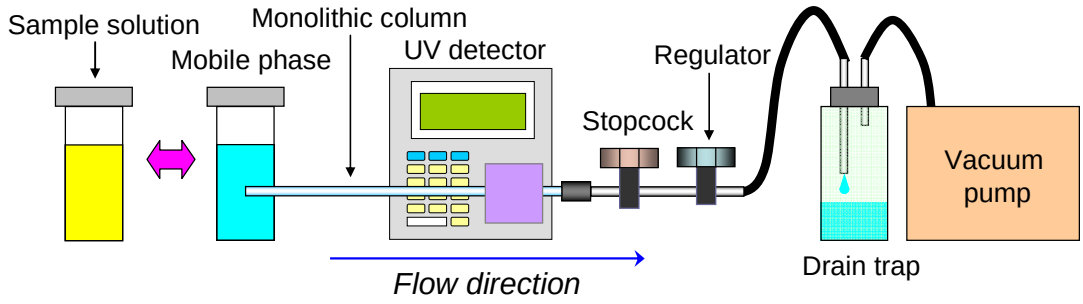

Fig. 5-1 Schematic illustration of a vacuum pressure-driven HPLC system.

vacuum-driven system, which comprised of a sample solution reservoir, a mobile phase reservoir, a polymer monolithic column polymerized for 2 min, a UV/Vis detector (CE-1575), a regulator, a stopcock, and a vacuum pump (DAP-6D, ULVAC KIKO Inc., Miyazaki, Japan). Meanwhile, a gas pressure-driven HPLC system, shown in Fig. 5-2, consists of a sample solution reservoir, a mobile phase reservoir, a polymer monolithic column polymerized with the optimum condition, a UV/Vis detector (CE-1575), a pump (LC-10ADvp) for supplying mobile phase for gradient (not for pressurizing), and a helium gas cylinder equipped with a pressure-regulator. As shown in the Fig. 5-2, the monolithic column, He gas line (0.1-0.2 MPa), and mobile phase line (only for gradient elution) in the inlet reservoir were sealed by the

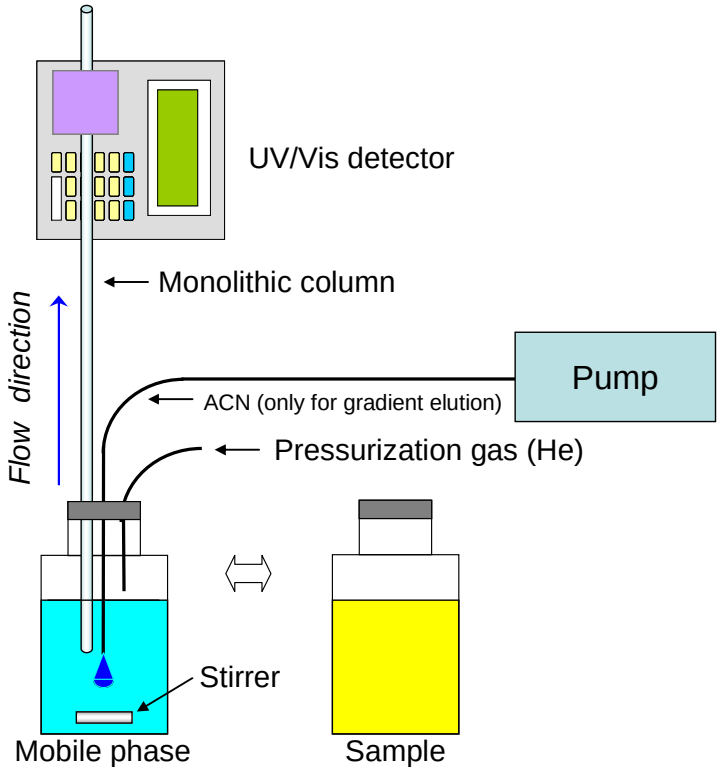

Fig. 5-2 Schematic illustration of a gas pressure-driven HPLC system

rubber septa. A direct injection method of 5 s pressurization, analogous with capillary electrophoresis, was used to introduce sample solution to the column. In the case of gradient elution, the initial composition of the mobile phase in the reservoir was water-rich, and ACN was continuously supplied to the reservoir by a pump. The solution in the reservoir was stirred and the mixture was supplied to the capillary column by the gas-pressure. Note that the pump was only used for the supplying ACN to the reservoir for the gradient elution and did not contribute to supplying the mobile phase to the capillary column.

All chromatographic experiments were performed at room temperature.

5.2.4. Calculation of porosity and permeability of monolithic columns

In general, the linear flow velocity is inversely proportional to the column porosity

at a constant volumetric flow velocity. Therefore, column porosity ε can be estimated by the following equation:

$$\varepsilon = \frac{u_{sf}}{u_0} \quad (1)$$

where u_{sf} and u_0 are the t_0-based linear flow velocities for an open tubular capillary without a monolith (superficial velocity) and for the monolithic column (chromatographic linear flow velocity), respectively.

The permeability K of a prepared monolithic column can be calculated using the following equation:[8]

$$K = \frac{u_{sf}\eta L}{\Delta P} \quad (2)$$

where η, L, and ΔP are the viscosity of the mobile phase, the column length, and the pressure drop, respectively.

5.2.5. Observation of the column cross-section

A longitudinal cross-section of the prepared column was observed using confocal laser scanning microscopy (CLSM, an inverted microscope, TE2000E, Nikon, Tokyo, Japan) combined with a confocal laser scanning system (Digital Eclipse C1, Nikon).[9,10] A fluorescent dye was adsorbed onto the monolith according to the following procedure: first, the column was filled with 0.01% BODIPY FL C_{16} in ACN

to stain the monolith, followed by flushing with 50% ACN aqueous solution (v/v), which is the same composition used for the mobile phase in the isocratic separation mode. The teflon outer coating of the capillary was removed, and the column was cut into pieces about 5 mm in length. A piece of the column was dipped in a 62% KSCN aqueous solution during the CLSM (×40 objective lens) observation to suppress distortion of the images.

5.2.6. Determination of conversion of the polymer monolith

Pyrolysis gas chromatography (Py-GC) was employed for determination of the monomer conversions and BMA/EDMA ratio of polymer monolith fixed in the column.[11] A vertical microfurnace-type pyrolyzer (PY2020iD, Frontier-Lab, Koriyama, Japan) was directly attached to the injection port of a gas chromatograph (G-6000, Hitachi) equipped with a flame ionization detector. The outer coating of the capillary monolithic column was removed and the bare column was cut to 5 mm long. A piece of the monolithic column was placed in a sample cup and then introduced into the pyrolyzer heated to 450°C under a flow of helium carrier gas (57 mL min^{-1}). At the elevated temperature, the poly(BMA-*co*-EDMA) monolith fixed in the column was depolymerized to the constituent monomers, BMA and EDMA. The thermal decomposition products were directly introduced into a GC separation column (1:50 split ratio) through an injection port maintained at 320°C. For the separation of the degradation products, a metal capillary column (Ultra ALLOY^{+} 1701, Frontier-Lab, 30 m × 0.25 mm i.d. × 0.25 μm coated with 14% cyanopropylphenyl/86% dimethylpolysiloxane, Koriyama, Japan) was used. The temperature of the column was initially set to 40°C, then elevated to 280°C at a rate of 20°C min^{-1}, and

maintained at 280°C for 20 min.

The copolymer composition by weight (wt% ratios for BMA and EDMA are denoted as r_{BMA} and r_{EDMA}, respectively) constituting the monolith was determined based on the peak area ratio of BMA and EDMA in the observed pyrogram.[11] The total weight of the poly(BMA-*co*-EDMA) monolith contained in a 5 mm length of column was determined as follows: first, a 5 mm section of monolithic column without the outer coating was weighed by micro-balance (UMT2, Mettler Toledo, Greifensee, Switzerland), incinerated using a gas burner to combust the monolith, and weighed again. The weight differential before/after incineration was defined as the total weight of the monolith, *w,* fixed in the capillary. We estimated the mass of BMA and EDMA in the reaction solution loaded into the 5 mm capillary as W_{BMA} and W_{EDMA}, respectively, according to the composition and density of the reaction solution and the volume of the 5 mm capillary. W_{BMA} and W_{EDMA} would correspond to the weight of monolith in 100% conversion. The conversion $\%C$ of each compound was estimated using the following equation:

$$\%C = \frac{w \times r_{\text{BMA or EDMA}}}{W_{\text{BMA or EDMA}}} \times 100 \quad (3)$$

5.3 Results and Discussion

5.3.1. Characterization of prepared monolithic column

Poly(BMA-*co*-EMDA) monolithic columns were polymerized by UV irradiation for various time periods (1.5, 2, 4, 8, and 16 min) at -15°C. The monolith prepared with

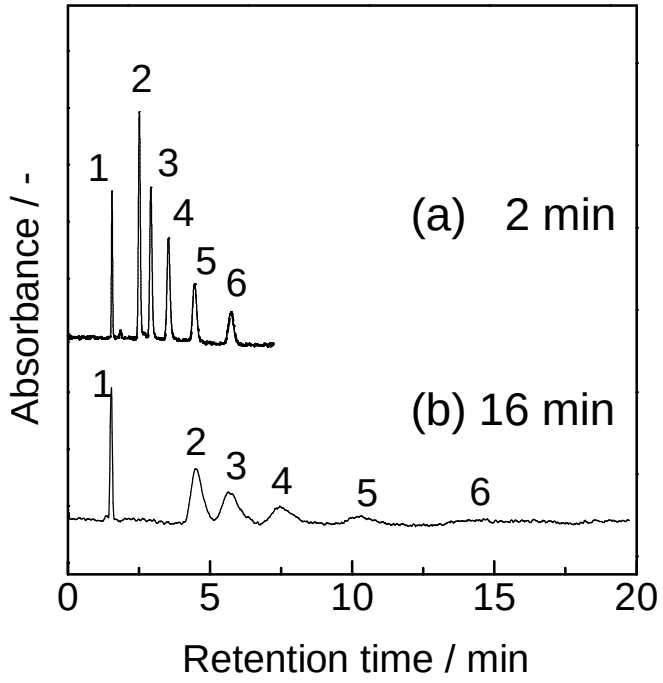

Fig. 5-3 Separation of alkylbenzenes at a linear flow rate of 1.0 mm s^{-1} using the columns polymerized for 2 and 16 min at -15°C. Conditions: column length 90 mm; mobile phase 50:50 acetonitrile:water (v/v); analytes (1) uracil (t_0 marker), (2) toluene, (3) ethylbenzene, (4) *n*-propylbenzene, (5) *n*-butylbenzene, and (6) *n*-pentylbenzene; UV detection at 190 nm.

the shortest irradiation time (1.5 min) broke during the washing procedure and was washed out of the capillary. Therefore, the columns polymerized for the other time period were evaluated. These prepared columns at -15°C were used to separate five alkylbenzenes (toluene to *n*-pentylbenzene) and t_0 marker (uracil) in the isocratic mode, resulting in the observation of the chromatograms shown in Fig. 5-3. When the analytes were separated using the column polymerized for 16 min (Fig. 5-3b), terribly broadened peaks were obtained for alkylbenzenes. In contrast, the separation using the column polymerized for 2 min produced sharp peaks for all five alkylbenzenes (Fig. 5-3a). The relationship between polymerization time and theoretical plate numbers for uracil, toluene, and *n*-propylbenzene at a chromatographic linear flow velocity of 1.0 mm s^{-1} are shown in Fig. 5-4. The column efficiencies for the retained analytes, toluene and *n*-propylbenzene, increased with

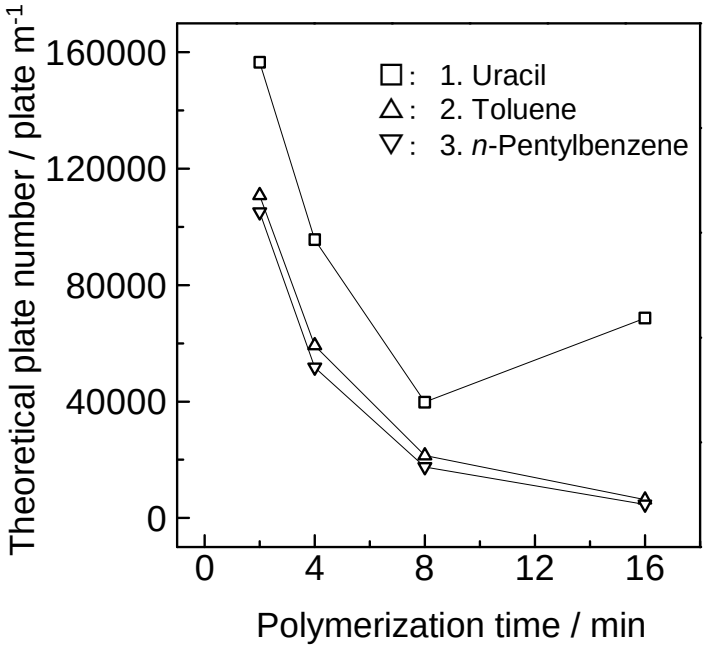

Fig. 5-4 Relationships between polymerization time and theoretical plate number for uracil, toluene, and *n*-propylbenzene using the columns polymerized for 2-16 min at -15°C; linear flow rate was 1.0 mm s^{-1}.

decreasing polymerization time. The theoretical plate numbers for toluene and *n*-propylbenzene using the column polymerized for 2 min were 111,000 and 105,000 plates m^{-1}, respectively. However, the column polymerized with 16 min UV irradiation exhibited deteriorated efficiencies, falling to 6,300 and 4,700 plates m^{-1} for toluene and *n*-propylbenzene, respectively. For uracil, which was not retained on the column, the best efficiency was also achieved using the column polymerized for 2 min, and the lowest theoretical plate number was obtained with the column polymerized for 8 min. For columns prepared by UV photopolymerization at low temperatures, decreasing the polymerization time (and, consequently, monomer conversions) enhanced the separation efficiency in a manner analogous to that observed for thermal polymerization.[1-3]

Additionally, the monolithic columns polymerized at 0°C and 15°C for 2 min were also prepared and evaluated under the same chromatographic conditions. The

theoretical plate numbers for the alkylbenzenes were around 30,000 plates m^{-1} for 0°C and 5,000 plates m^{-1} for 15°C at a linear flow rate of 1 mm s^{-1}. Moreover, an increase of polymerization temperature increased the flow resistance of the column; *i.e.*, the back pressure of the columns prepared at -15, 0, and 15°C were 0.14, 0.20, and 3.0 MPa at a linear flow rate of 1 mm s^{-1}, respectively. Since the objective of this study was preparation of high-efficient and low-flow resistance polymer monolithic column, further investigations were focused on the columns prepared at -15°C.

The conversion of both BMA and EDMA in the columns polymerized for 2, 4, 8, and 16 min at -15°C was determined using Py-GC. Fig. 5-5 shows that the relationships between the polymerization time and the conversions of BMA and EDMA. Conversion for both constituents increased with increasing polymerization time. By UV irradiation for 2 min, the conversions of BMA and EDMA come around to 10 and 21%; for 16 min, they reached 79 and 83%, respectively. As clearly shown

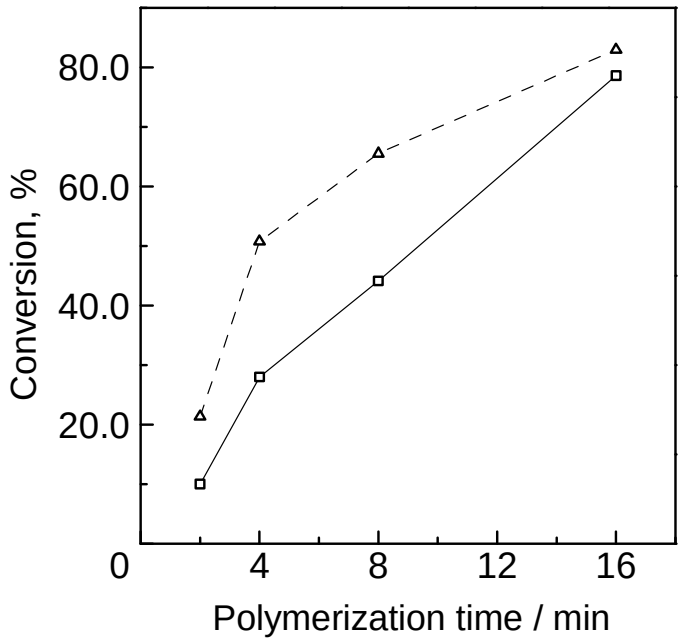

Fig. 5-5 Relationships between polymerization time and conversion of BMA (□) and EDMA (△) in the columns polymerized for 2-16 min at -15°C.

in Fig. 5-5, the polymerization of EDMA proceeded faster than that of BMA, consistent with previous reports.[1-3] At the shortest polymerization time, only about 6% of total monomer mass in the capillary (24 wt% × 10% + 16 wt% × 21%) reacted to form the polymer monolith fixed in the capillary.

The relationships between polymerization time and porosity/permeability of the monolith columns are shown in Fig. 5-6. The porosity ε, which was directly affected by the extent of polymerization, decreased with increasing polymerization time. At the shortest polymerization time of 2 min, the porosity was determined to be 92%, Since the total monomer conversion at this condition was 6%, the porosity of 92%, or $1-\varepsilon = 8\%$, is a reasonable value.

The permeability of the columns polymerized at -15°C determined using the elution time of t_0 marker and equation 2 is also shown in Fig. 5-6. The permeability was increased with a decrease of the polymerization time, similarly to porosity.

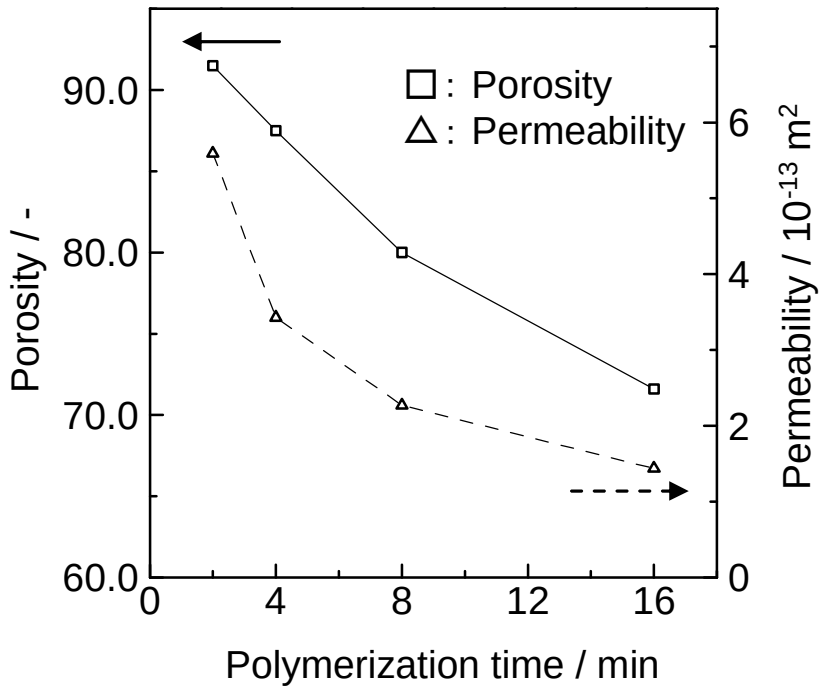

Fig. 5-6 Relationships between polymerization time and porosity (□) or permeability (△) of the columns polymerized for 2-16 min at -15°C.

Polymerization for 2 min produced a column with a high permeability of 5.6×10^{-13} m^2. This value is over an order of magnitude larger than that of a 3 μm particle packed column and twice as large as that of the monolithic column prepared by UV irradiation in our previous study (2.0 mW cm^{-2}, 8 min at 0°C; *%C*: 32% for BMA, 58% for EDMA).[5,11]

The monolithic column polymerized for 2 min at -15°C showed superior performance in terms of both separation efficiency and permeability. The characteristics of this column were further investigated. Fig. 5-7 shows *H-u* plots for this column using symbols; along with the results for the column prepared in our previous study (2.0 mW, 8 min, 0°C) shown with lines for comparison. At a linear flow rate of 1.0 mm s^{-1}, the height equivalence to a theoretical plate (HETP) values for uracil and toluene were 6.4 and 9.0 μm, respectively, using the column prepared in this study, while the values for the column in our previous study were approximately 2-3 times larger (about 25 μm for uracil and 22 μm for toluene). For

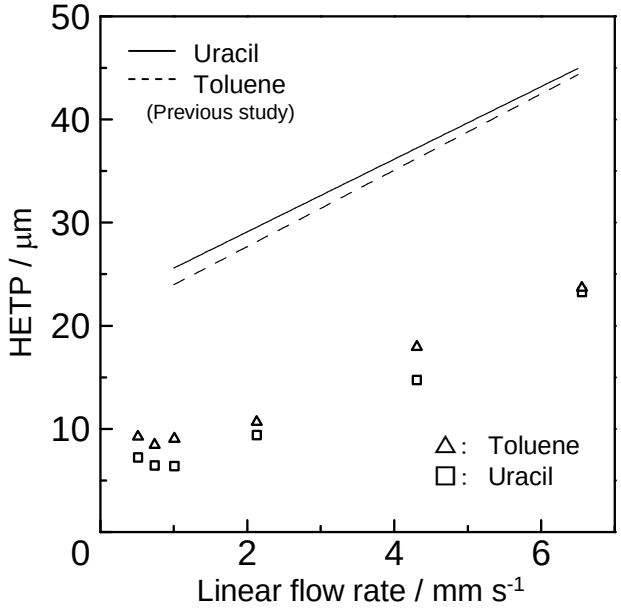

Fig. 5-7 Relationships between linear flow rate and the height equivalent to a theoretical plate (HETP) (*H-u* plots) for uracil and toluene. Chromatographic conditions were the same as those in Fig. 5-1.

the column in this study, the minimum HETPs were determined to be 6.4 μm for uracil at a linear flow rate of 1.0 mm s^{-1} and 8.4 μm for toluene at 0.7 mm s^{-1} toluene, corresponding to 157,000 and 118,000 plates m^{-1}, respectively. The *H*-*u* plots for the column in this study (marked by symbols in Fig. 5-7) are parallel to those for the column prepared previously (marked by lines) but are shifted down to lower HETP values in the range from 1.0 to 6.5 mm s^{-1}. This suggests that the reduction in the *A*-term in the *H*-*u* plot can be achieved using the current column preparation method to cause greater homogeneity of the column structure.

The peak capacity, *n*, in an isocratic mode (ACN/water=50/50, v/v) was also calculated by the following equation[12]:

$$n = 1 + \frac{\sqrt{N}}{4} \ln\left(\frac{t_R}{t_0}\right) \quad (4)$$

where *N*, and t_0 and t_R are theoretical plate number, and retention time of the first and the last eluted peak, respectively. Here, the retention times of uracil and *n*-pentylbenzene were used as t_0 and t_R, respectively, and the average theoretical plate number of uracil and *n*-pentylbenzene in each chromatogram was adopted as *N* value. The *n* values obtained for the column in present and the chapter 2[5] were almost comparable (34 and 33, respectively) because of the larger retention factor, or elution time, of *n*-pentylbenzene for the previous column (k=6.4) compared with that for the present one (k=2.8) in the same mobile phase condition.

CLSM observation was then performed to evaluate the morphology of the monolithic columns under the HPLC separation condition; *i.e.*, the columns used for the observation were filled with 50% ACN aqueous solution corresponding to the mobile phase used in this study. Fig. 5-8 shows CLSM images of the longitudinal

cross-section of the columns polymerized for (a) 2 min and (b) 16 min as well as (c) that of a column prepared under the conditions used in our previous study. The monolithic structure of the column polymerized for 2 min (Fig. 5-8a) was more

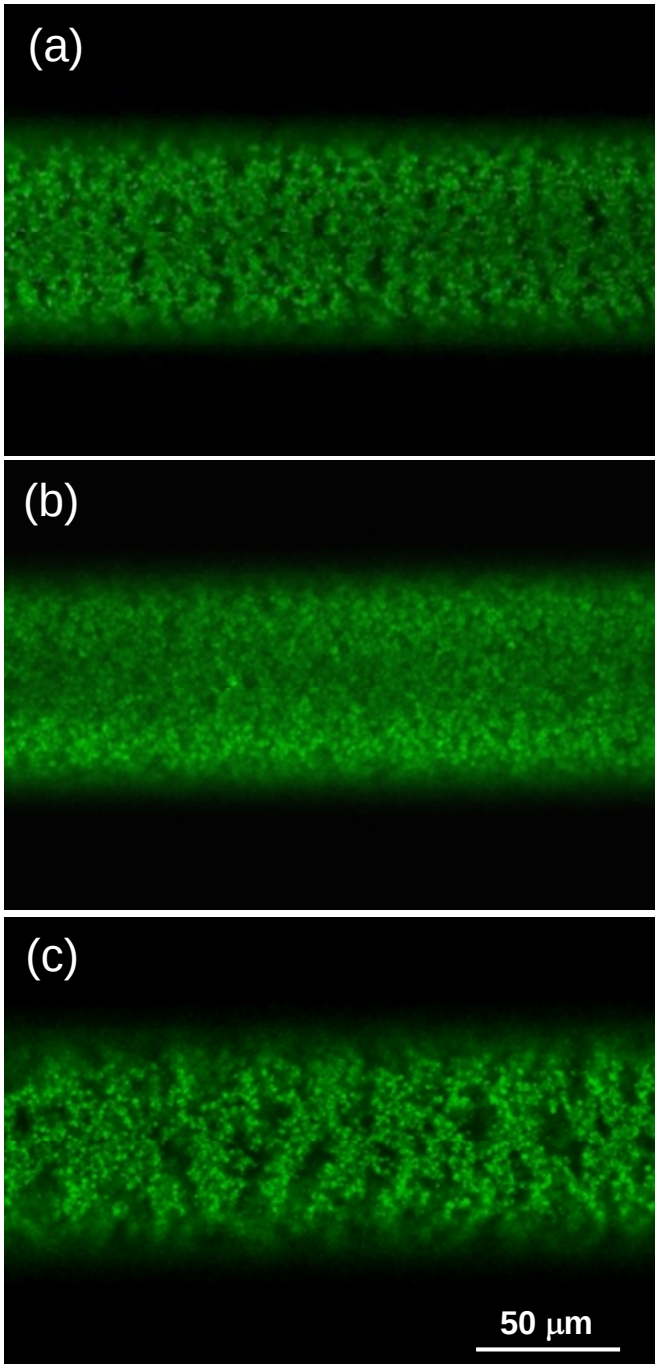

Fig. 5-8 CLSM images of longitudinal cross-sections of the columns polymerized for (a) 2 min and (b) 16 min at -15°C, compared with (c) the column in the chapter 2.[5]

homogeneous than that prepared in our previous study (Fig. 5-8c). Greater homogeneity should give rise to enhanced separation efficiency (Fig. 5-7) and a reduction in the *A*-term.

On the other hand, as shown in Fig. 5-8b, the density of the polymer monolith polymerized for 16 min appeared to be higher than that polymerized for 2 min (Fig. 5-8a), corresponding to the difference in monomer conversion. Meanwhile it seemed that the degree of homogeneity of the monolithic structures polymerized for 16 min and 2 min observed in the CLSM images (Fig. 5-8a and 5-8b) were almost identical. As mentioned above, however, the theoretical plate numbers for the separation of toluene and *n*-propylbenzene using the column polymerized for 2 min were about twenty times larger than the corresponding values obtained for the column polymerized for 16 min. Here it should be noted that the copolymer composition of the monolith varied as the polymerization process proceeded as shown in Fig. 5-5. This fact suggests that compositional heterogeneity would increase with increasing monomer conversion, potentially leading to the decrease in the column efficiency for retained analytes. It was also reported that the specific surface area of the polymer monolith was decreased with increasing of polymerization time.[1-3,13] Similar phenomenon would arise in the polymerization process in this work and affect the separation efficiency. The detailed study to clarify the relation between the copolymer compositions of the monolith and the column performance should be essential in the future work.

5.3.2. Repeatability, reproducibility, and stability of the low-flow-resistance column

The run-to-run repeatability, column-to-column reproducibility, and mechanical

stability for the column polymerized for 2 min at -15°C were evaluated. At the linear flow rate of 1.0 mm s^{-1}, the RSD for the run-to-run repeatability of retention time, retention factor, and HETP values for *n*-propylbenzene were 1%, 1% and 5% (n=3), respectively. Moreover, the RSD for column-to-column reproducibility of the retention time, retention factor, and HETP values for *n*-propylbenzene at 1.0 mm s^{-1} were 4%, 5% and 11%, respectively, and those of the flow resistance was within 9% (n=4).

In addition, the column was mechanically stable up to the linear flow rate at least 16 mm s^{-1} (1.9 MPa as back pressure); *i.e.*, a good linear relationship between the flow rate and backpressure was obtained (correlation coefficient = 0.999). Furthermore, no change in chromatographic property was observed during the continuous use of the column within a month at least.

5.3.3. Separations in vacuum and gas pressure-driven HPLC

The low-flow-resistance polymer monolithic column with high separation efficiency was successfully prepared using 2 min polymerization at -15°C as described in the previous section. Here, using prepared column, we constructed the two types of low-pressure HPLC (LP-HPLC) without a conventional HPLC pump to supply a mobile phase. At first, vacuum pressure-driven LP-HPLC, which would be the simplest LP-HPLC, was employed for the isocratic separation of alkylbenzenes. A direct injection method using suction (-0.045 MPa, 10 s), similar to capillary electrophoresis (CE), was employed. After sample loading, the mobile phase in the inlet reservoir was aspirated into the column by vacuum (-0.045 MPa). As a result,

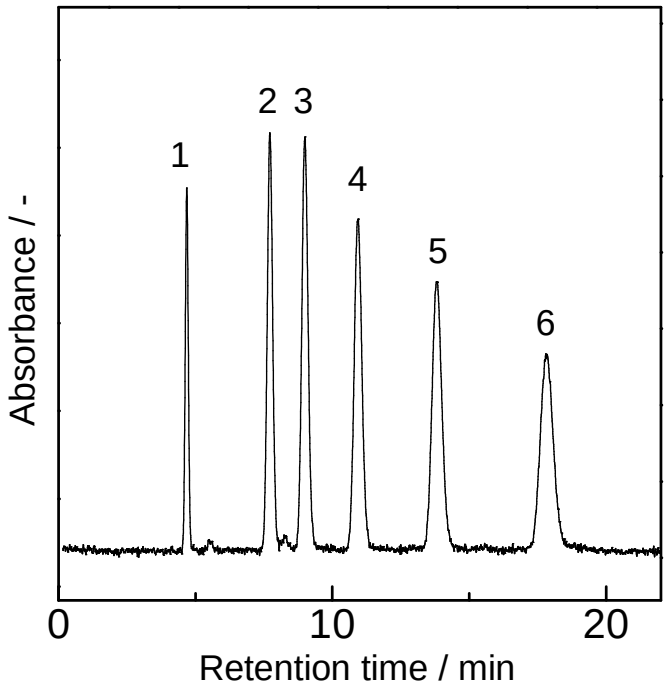

Fig. 5-9 Separation of alkylbenzenes using vacuum-driven HPLC. Pressure of vacuum: -0.045 MPa. Other conditions were the same as those in Fig. 5-1.

the analytes were separated and detected as shown in Fig. 5-9. The sample solution was successfully injected and transferred to the outlet by the vacuum at the column outlet end. The flow rate under the vacuum was 0.3 mm s^{-1} and the separation efficiency was 70,000-85,000 plates m^{-1}. The RSDs for run-to-run repeatability of linear flow rate, the retention factor, and the HETP values for *n*-propylbenzene were 2%, 0.3%, and 1%, respectively (n=3).

Secondly, the gas pressure-driven HPLC was used for both isocratic and gradient separations. Here, direct injection method by the gas pressure was employed (0.10-0.15 MPa). As shown in Fig. 5-10a, the five alkylbenzenes were well separated in both the isocratic and gradient elution by the gas pressure-driven LP-HPLC (0.15 MPa). In the isocratic elution, the RSDs for run-to-run repeatability of linear flow rate, the retention factor, and the HETP values for *n*-propylbenzene were 0.4%, 1%, and 5%, respectively (n=3). Meanwhile in the gradient elution, the

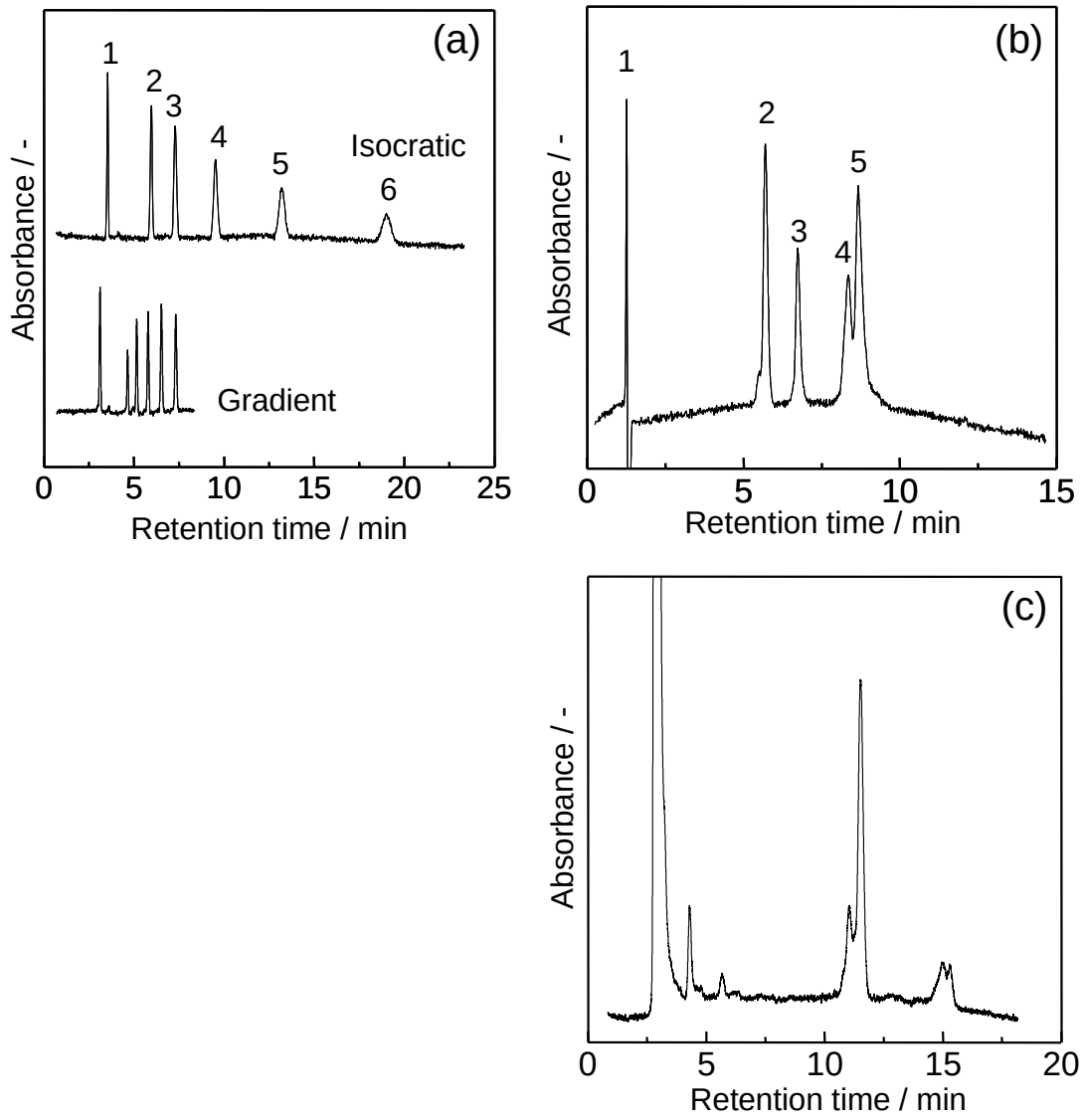

Fig. 5-10 Separation of alkylbenzenes (a), standard proteins (b) and whey (c) using gas pressure-driven HPLC. Conditions: column length 90 mm; UV detection at 190 nm. (a) Pressure 0.15 MPa; Mobile phase 40/60 ACN/water (v/v) for isocratic elution, 40/60 to 60/40 (v/v) in 10 min; analytes (1) uracil (t_0 marker), (2) toluene, (3) ethylbenzene, (4) *n*-propylbenzene, (5) *n*-butylbenzene, and (6) *n*-pentylbenzene. (b) Pressure 0.15 MPa; Mobile phase ACN/water =20/80 to 50/50 (v/v) in 15 min (0.5% TFA). (1) uracil (t_0 marker), (2) lysozyme, (3) lactalbumin, (4) bovine serum albumin, (5) myoglobin. (c) Pressure 0.10 MPa; Mobile phase ACN/water =20/80 to 55/45 (v/v) in 20 min (0.5% TFA).

RSDs for run-to-run repeatability of linear flow rate, the retention time and half maximum full-width for *n*-propylbenzene were 3%, 1%, and 2%, respectively (n=4). Moreover, this system was applied to the separation of proteins. The separation of four standard proteins is shown in Fig. 5-10b with a pressure of 0.15 MPa. Although

the peaks of bovine serum albumin and myoglobin were partially overlapped, sharp peak for each analyte were obtained. The RSDs for run-to-run repeatability of linear flow rate, the retention time, and half maximum full-width for lactalbumin were 4%, 2%, and 2%, respectively (n=3). Furthermore, a whey sample, which was prepared by filtration of a yogurt with 0.45 μm membrane filter, was separated as an application to a real sample. As shown in Fig. 5-10c, whey was successfully separated in LP-HPLC with a pressure of 0.10 MPa.

Hence, both vacuum and gas pressure-driven HPLC demonstrated high performance with good repeatability by using the low-flow-resistance column polymerized for 2 min at -15°C. Moreover, it was also shown that the prepared monolithic column exhibited good separation efficiency not only for alkylbenzenes but also for proteins.

5.4 Conclusions

In this chapter, a low-flow-resistance poly(BMA-*co*-EDMA) monolithic column was successfully developed by combining low-conversion and low-temperature polymerization. A UV photo-polymerization lasting 2 min was used to prepare the column at a low temperature of -15°C. The column exhibited a high column efficiency of >100,000 plates m^{-1} with a high permeability of 5.6×10^{-13} m^2 in the RP-HPLC mode. CLSM images revealed that the prepared monolith structures were more homogenous than those prepared in our previous study. Compositional copolymerization homogeneity was apparently enhanced by reducing the polymerization time, with improving the separation efficiency for retained analytes. Using the prepared column, a vacuum and gas pressure-driven low-pressure HPLC

systems was used without the need for a conventional HPLC pump to separate alkylbenzenes and proteins under a pressure of -0.045 MPa (vacuum) and 0.10-0.15 MPa (gas pressure). Additional researches characterizing both the chemical and material properties of the monolith to understand their relationship to the separation efficiency are currently in progress in our laboratory.

References

1. L. Trojer, C. P. Bisjak,W. Wieder, and G. K. Bonn, *J. Chromatogr., A,* **2009**, *1216*, 6303.
2. I. Nischang and O. Brüggemann, *J. Chromatogr., A,* **2010**, *1217*, 5389.
3. I. Nischang, I. Teasdale, and O. Brüggemann, *J. Chromatogr., A,* **2010**, *1217*, 7522.
4. I. K. Kiplagat, P. Kubáň, P. Pelcová, and V. Kubáň, *J. Chromatogr., A*, **2010**, *1217*, 5116.
5. T. Hirano, S. Kitagawa, and H. Ohtani, *Anal. Sci.,* **2009**, *25*, 1107.
6. D. Lee, F. Svec, and J. M. J. Fréchet, *J. Chromatogr., A,* **2004**, *1051*, 53.
7. Y. Ueki, T. Umemura, Y. Iwashita, T. Odake, H. Haraguchi, and K. Tsunoda, *J. Chromatogr., A,* **2006**, *1106*, 106.
8. P. Carman, *"Flow of Gases through Porous Media"*, Butterworth, London, **1956**.
9. H. Saito, K. Kanamori, K. Nakanishi, and K. Hirao, *J. Sep. Sci.,* **2007**, *30*, 2881.
10. S. Bruns, T. Müllner, M. Kollmann, J. Schachtner, A. Höltzel, and U. Tallarek, *Anal. Chem.,* **2010**, *82*, 6569.
11. T. Nakaza, A. Kobayashi, T. Hirano, S. Kitagawa, and H. Ohtani, *Anal. Sci.,* **2012**, *28*, 917.

12. J. C. Giddings, *Anal. Chem.* **1967**, *39*, 1027.

13. F. Svec and J. M. J. Fréchet, *Chem. Mater.,* **1995**, *7*, 707.

Chapter 6 Evaluation of interaction between metal ions and nonionic surfactant in high concentration HCl using low pressure-high performance liquid chromatography with low flow resistance polystyrene-based monolithic column

6.1 Introduction

As described the chapter 5, we have successfully prepared the methacrylate-based polymer monolithic column with high column efficiency and low flow resistance and developed a low pressure-HPLC (LP-HPLC) without use of conventional high-pressure pumps.[1] Here, we notice that the gas-pressure driven LP-HPLC has a potential of a highly acid-resistance HPLC because it is free from metal and aluminum oxide which are used in a conventional chromatograph. Therefore, in this chapter, the LP-HPLC was employed for evaluating interactions in strongly acidic solution.

In recent year, a demand for recovering valuable metals from wastes has been grown since the price of valuable metals has highly risen on a global scale.[2-4] One of the conventional recovery methods for the metals is a solvent extraction from acidic leaching solution of waste.[5-13] In solvent extraction, however, high cost and environment load are of problems because it uses a large amount of organic solvent. Therefore other recovery method free from such problem is required.

Recently, continuous counter-foam separation (CCFS) has been developed as a method for metal recovers from diluted solution without a use of organic solvent.[14-16] In CCFS, the target metal ion is separated from non-target metal ion(s) (matrix) based on the difference in an interaction between metal ions and

surfactant.[14-16] The schematic illustration of the separation mechanism of CCFS is shown in Fig. 6-1. As shown in Fig. 6-1, air is continuously pumped into a solution containing surfactant at the lower position of the bubble column and a foam stream from the bottom migrates up toward the top of the column. A metal solution containing both target and matrix ions is supplied to the middle point of the column. The metal ions interacting with the surfactant on the bubble surface rise up to the column top with the foam stream. A surfactant solution is also dropped from the relatively higher point of the column and non- and less-interactive ions in interstitial water are washed down gravitationally to the column bottom. Consequently, the metal ion strongly interacting with the surfactant, or target ion, is separated from the matrix and corrected continuously from the top end of the bubble column. CCFS was successfully applied to the recovery of Au from diluted aqueous solution containing Cu[14,15] and of Ga from the zinc refinery residue.[16]

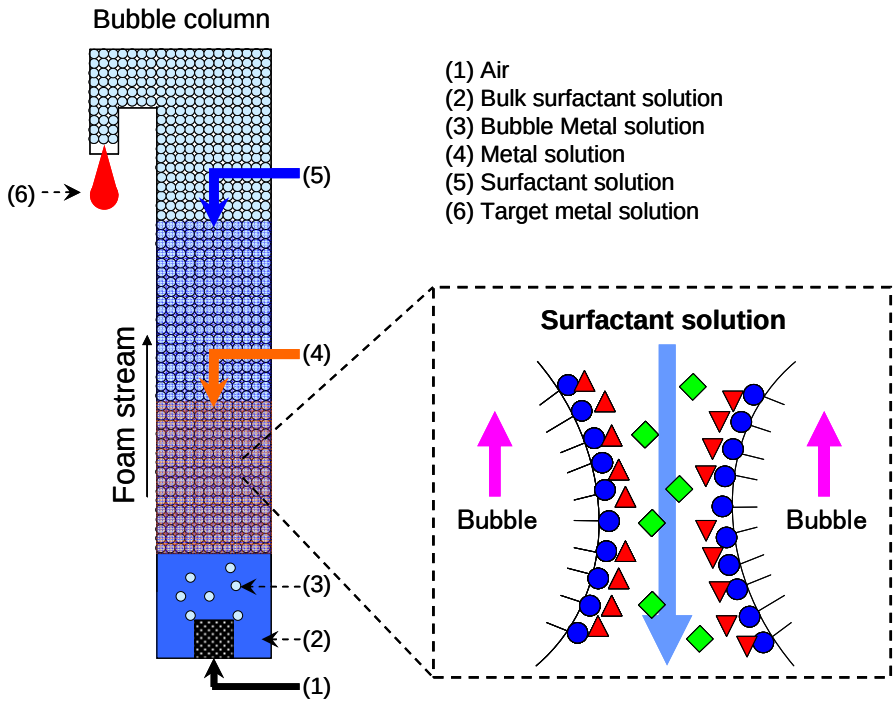

Fig. 6-1 Schematic illustration of CCFS

In CCFS, both separation and recovery efficiencies are strongly depended on the magnitude of the interaction between the metal ions and the surfactant in an aqueous phase.[14-16] Therefore, development of simple and rapid method to evaluate the interaction between metal ions and surfactant in an aqueous solution, particularly for highly acidic solution, is desired. Since high performance liquid chromatography (HPLC) is the separation method based on the interaction between analytes and a stationary phase, it has a potential to evaluate the interaction between metal ions and surfactants. For instance, a column coated by surfactants will be effective in evaluating the interaction of surfactants with metal ions injected to the column. That is, the magnitude of the interaction is simply evaluated by the retention time, or capacity factor, of the metals eluted from the HPLC column. However, it should be noted that CCFS for metal recoveries generally required a solution of high concentration acid, typically several mol L^{-1} (M) of hydrochloric acid (HCl).[14-16] Therefore, a highly acid-resistant HPLC system is essential for this evaluation, but HPLC systems commercially available are not suitable for this purpose because the general HPLC contains less acid-resistant parts such as aluminum oxide and/or stainless steel.

Therefore, in this chapter, we tried to develop the method for an evaluation of the interaction between metal ions and nonionic surfactant in high concentration HCl using a gas pressure-driven LP-HPLC. As mentioned above, the LP-HPLC has a highly acid-resistance potential because the LP-HPLC does not need the high pressure pump for supplying mobile phase. However, the methacrylate-based monolithic column, which was used in the previous chapter, will be damaged by hydrolysis of ester bonding in the solution containing high concentration acid. Actuary, the chromatographic behavior for the methacrylate-based monolithic

column was unstable in the continuous use of 6 M HCl as a mobile phase. Therefore, at a first step of this study, we optimized a preparation of a low flow resistance poly(styrene (ST)-*co*-divinylbenzene (DVB)) based monolithic column suitable for LP-HPLC as more acid-resistance stationary phase. Here, low conversion thermal polymerization was employed to achieve the low flow resistance column with suitable separation efficiency.[17-19] The column prepared with the optimized condition was coated with surfactants (polyoxyethylene nonylphenyl ether) and the interaction with chloride complex ions of metal ions (Au(III), Ga(III), Cu(II), Fe(III), Zn(II)) in 6 M HCl, that were used in past CCFS[14-16] was evaluated in a gas-pressure driven LP-HPLC. The effect of polyoxyethylene (POE) chain length on the interaction was mainly investigated.

6.2 Experimental

6.2.1. Chemicals

Styrene (ST), Divinylbenzene (DVB), 1-dodecanol (DDOL), toluene (TOL), 2,2-Azobis(isobutyronitrile) (AIBN), sodium hydroxide, hydrochloric acid (HCl), acetonitrile (ACN), tetrahydrofuran (THF), uracil, *n*-propylbenzene, *n*-butylbenzene, *n*-pentylbenzene, polyoxyethylene nonylphenyl ether (PONPE, *n*=7.5, 15, 20), sodium tetrachloroaurate (III) dihydrate, zinc chloride, iron (III) chloride hexahydrate, and copper (II) chloride dehydrate were purchased from Wako Pure Chemicals (Osaka, Japan). Ethylbenzene and gallium (III) chloride was obtained from Tokyo Chemical Industry (Tokyo, Japan). 3-Methacryloxypropyltrimethoxysilane (MAPS) was obtained from Shin-Etsu

Chemicals (Tokyo). All chemicals were used as received.

6.2.2. Column preparation

A fused silica capillary (100 μm i.d., 375 μm o.d., GL Science, Tokyo, Japan) was silanized with MAPS as described in our previous report.[20] The capillary was cut to 20 cm long and filled with reaction solution consisting of ST (monomer, 21.9 wt%), Divinylbenzene (cross-linker, 14.6 wt%), 1-dodecanol (porogen, 44.5 wt%), toluene (porogen, 19.1 wt%), and AIBN (initiator, 1 wt% with respect to the reaction solution)[19], and thermalpolymerized for 0.5-24 hours in an GC oven at 65°C was performed. After polymerization, the columns were immediately washed with THF to remove unreacted reagents, unfixed-polymer fragments, and porogens. Then the column was cut to 8 cm and connected to 10 cm of a Teflon-coated UV transparent fused silica capillary (100 μm i.d., 375 μm o.d., GL Science, Tokyo, Japan) for UV detection via a Teflon tubing. The analyte(s) was detected on the UV-trance parent coated capillary at 25 mm from outlet end of the connected column.

6.2.3. SEM measurement

The cross-sections of the monolithic columns were observed with a scanning electron microscope (SEM, JXA-8800, JEOL, Tokyo, Japan). After washing with THF, the columns were cut to 6 mm length, following drying at ambient temperature for 1 day at least. Each piece was spattered with Pt-Pd and then analyzed by the SEM.

6.2.4. Determination of conversion of the polymer monolith

Pyrolysis gas chromatography (Py-GC) was employed for determination of ST/DVB ratio and their conversions of polymer monolith fixed in the column.[21] A vertical microfurnace-type pyrolyzer (PY2020iD, Frontier-Lab, Koriyama, Japan) was directly attached to the injection port of a gas chromatograph (5890, Agilent Technologies, CA) equipped with a flame ionization detector. The outer coating of the capillary monolithic column was removed and the bare column was cut to 10 mm long. A piece of the monolithic column was placed in a sample cup and then introduced into the pyrolyzer heated to 600°C under a flow of helium carrier gas (57 mL min-1). At the elevated temperature, the poly(ST-*co*-DVB) monolith fixed in the column was depolymerized to its component ST and DVB monomers. The thermal degradation products were directly introduced into a GC separation column (1:50 split ratio) through an injection port maintained at 320°C. For the separation of the degradation products, a metal capillary column (Ultra ALLOY^{+} 17, Frontier-Lab, 30 m × 0.25 mm i.d. × 1.0 μm coated with 50% phenylmethylpolysiloxane, Koriyama, Japan) was used. The temperature of the column was initially set to 50°C, then elevated to 320°C at a rate of 10°C min^{-1}, and maintained at 320°C for 20 min.

The copolymer composition by weight (wt% ratios for ST and DVB are denoted as r_{ST} and r_{DVB}, respectively) constituting the monolith was determined based on the peak area ratio of ST and DVB in the observed pyrogram.[21] The total weight of the poly(ST-*co*-DVB) monolith contained in a 10 mm length of column was determined as follows: first, a 10 mm section of monolithic column without the outer coating was weighed by micro-balance (UMT2, Mettler Toledo, Greifensee, Switzerland), incinerated using a gas burner to consume the monolith, and weighed

again. The weight differential before/after incineration was defined as the total weight of the monolith, w, fixed in the capillary. We estimated the mass of ST and DVB in the reaction solution loaded into the 10 mm capillary as W_{ST} and W_{DVB}, respectively, according to the composition and density of the reaction solution and the volume of the 5 mm capillary. W_{ST} and W_{DVB} would correspond to the weight of monolith in 100% conversion. The conversion $\%C$ of each compound was estimated using the following equation:

$$\%C = \frac{w \times r_{\text{ST or DVB}}}{W_{\text{ST or DVB}}} \times 100 \quad (1)$$

6.2.5. Chromatographs

For the optimization of the column preparation, a capillary HPLC system consisting of a pump (LC-10ADvp, Shimadzu, Kyoto, Japan), a sample injector (Model 7520, Rheodyne, Cotati, CA, USA), a T connector equipped with a resistance tube for split injection (split ratio, 1:50), and a UV/Vis detector (CE-1575, Jasco, Tokyo, Japan) was used to evaluate the column characteristics (flow resistance, column efficiency, and retention) with an isocratic elution in the reversed phase (RP)-HPLC mode.[1]

A gas pressure-driven low-pressure HPLC (LP-HPLC) system without a conventional HPLC pump was also used in this experiment. A schematic illustration of LP-HPLC system is shown in Fig. 6-2. The apparatus comprised a sample solution reservoir, a mobile phase reservoir, a polymer monolithic column polymerized with the optimum condition, a UV/Vis detector (CE-1575), and a helium gas cylinder equipped with a pressure-regulator. As shown in Fig. 6-2, the

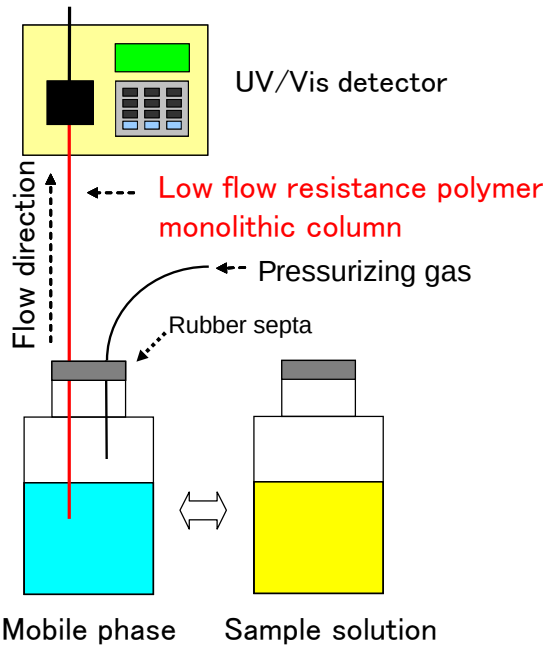

Fig. 6-2 Schematic illustration of LP-HPLC.

monolithic column and He gas line (0.2 MPa) in the inlet reservoir were sealed by the rubber septa. A direct injection to the column for 5 s, analogous with capillary electrophoresis, was used to introduce sample solution to the column.

All chromatographic experiments were performed at room temperature.

6.2.6. PONPE coating for monolithic column

The prepared ST-*co*-DVB monolithic column was coated with PONPE as follows. Firstly, the column was washed by 0.5 μL min^{-1} of water for 30 min (with the He gas pressure of 0.2 MPa). Then, 0.5 mM PONPE aqueous solution was supplied to the column with the same flow rate and the solution eluted from the column was monitored at 190 nm until the increased-absorbance became constant. The amount of PONPE coated on the column, N_{PONPE}, was estimated from this breakthrough curve. The column coated with PONPE was again washed by 0.5 μL min^{-1} of water

for 30 min.

6.2.7. Loading capacity of Au(III) to PONPE coated column

A solution of 0.5 mM Au(III) in 6 M HCl was supplied to the column coated with PONPE at a flow rate of 0.5 μL min^{-1} (He gas pressure of 0.2 MPa) after equilibration with 6 M HCl for 30 min. The solution eluted from the column was monitored at 220 nm to obtain a breakthrough curve of chloride complex of Au(III) and a loading capacity of Au(III) to the PONPE coated column was estimated using this breakthrough curve. Please note that the chloride complex of metal ion, M(x), in 6 M HCl was indicated as M(x) in the following part of this paper for simplify.

6.3 Results and Discussion

6.3.1. Preparation of low flow resistance styrene-co-divinylbenzene-based monolithic column.

The low flow resistance ST-*co*-DVB monolithic column for LP-HPLC was prepared by low-conversion thermal polymerization. In this preparation method, a polymerization time is the key to achieve desired characteristics. Therefore, ST-*co*-DVB-based monolithic columns were prepared with various polymerization times of 0.5, 1.0, 1.5, 3.0, 4.5, 9.0, and 24 hours.

Fig 6-3 shows the cross-sectional SEM images of the columns prepared with various polymerization times. The polymer monolith was entirely prepared in the

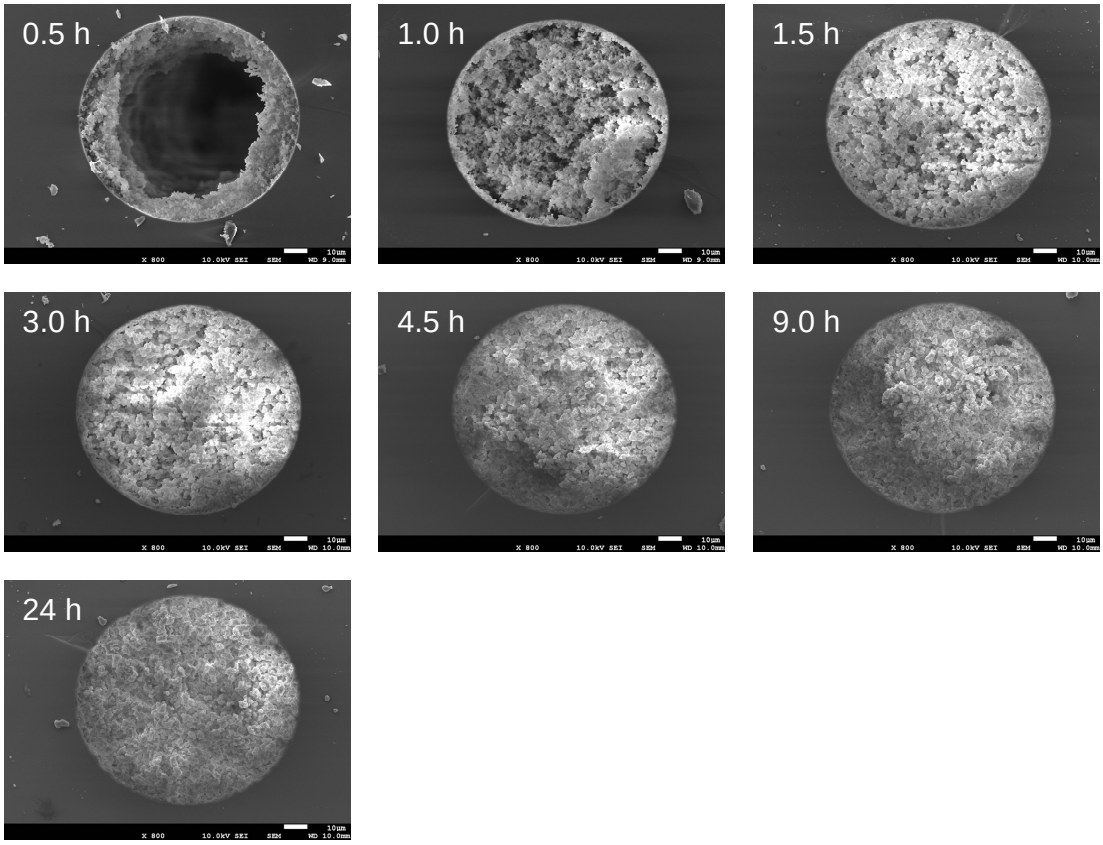

Fig. 6-3 Cross-sectional images of the columns polymerized for 0.5-24 h.

capillary with the polymerization time of 1.0-24 h (Fig. 6-3b-g) except for that of 0.5 h (Fig. 6-3a). The shortest polymerization time failed to construct a rigid polymer monolith and did not used for the further evaluation in this study. The through pore diameter observed by the SEM (Fig. 6-3b-g) decreased with an increase of polymerization time. It would reflect the increase in the polymer synthesis due to expanding the polymerization time. Fig. 6-4 shows the relationships between polymerization time (1.0-24 h) and conversions for monomers determined by Py-GC. At the shortest polymerization time of 1 h, the conversions for ST and DVB were 18% and 35%, respectively. According to the increase in polymerization time, the both conversions reasonably increased and reached 98% for ST and 97% for DVB at the longest polymerization time of 24 h. The conversion rate of bifunctional

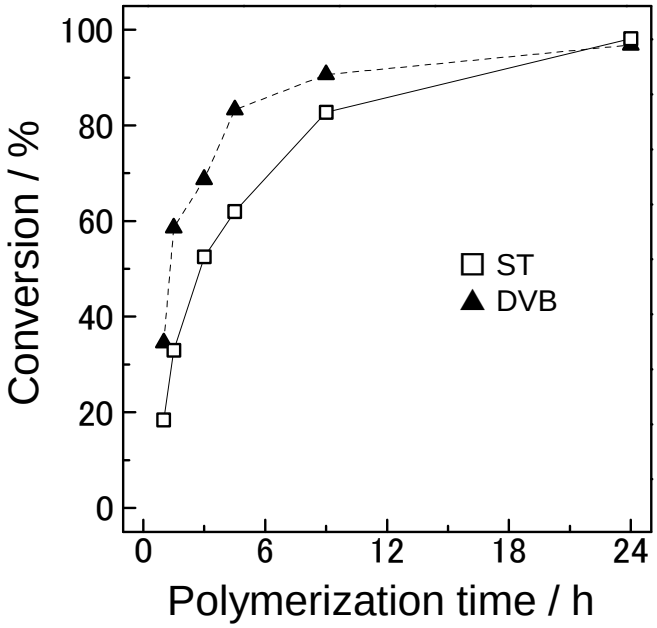

Fig. 6-4 Relationships between the polymerization time and the conversions for ST and DVB determined by Py-GC.

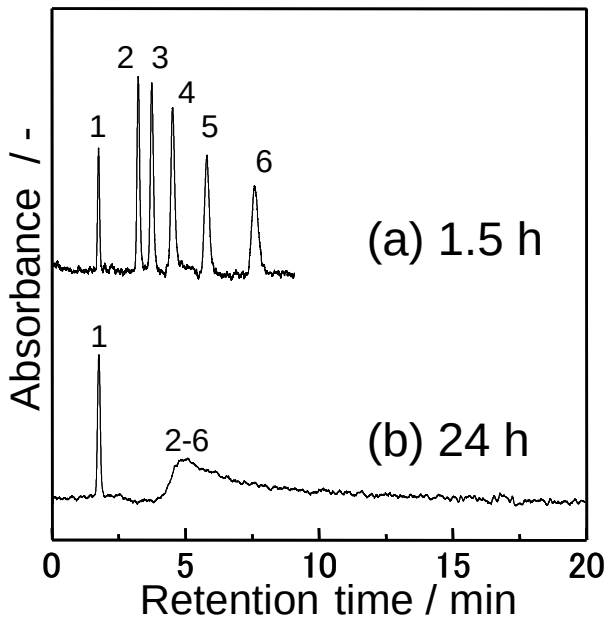

Fig. 6-5 Separations of alkylbenzenes at a linear flow rate of 1.0 mm s^{-1} using the columns polymerized for 1.5 h (a) and 24 h (b). Conditions: column length 80 mm; mobile phase acetonitrile/water = 70/30 (v/v); analytes (1) uracil (t_0 marker), (2) toluene, (3) ethylbenzene, (4) *n*-propylbenzene, (5) *n*-butylbenzene, and (6) *n*-pentylbenzene; UV detection at 190 nm.

monomer of DVB was faster than that of monofunctional monomer of ST, similarly to the previous studies.[1,17-19]

The mixture of five alkylbenzenes (toluene to *n*-pentylbenzene) and t_0 marker (uracil) was separated in the isocratic mode (ACN/water = 70/30, v/v) to evaluate the column efficiency and the flow resistance. Fig. 6-5 shows the resulting chromatograms at a linear flow rate of 1 mm s^{-1} using the columns polymerized for 1.5 and 24 h. When the column polymerized for 24 h was used (Fig. 6-5b), five alkylbenzenes were eluted as a single broadened peak. In contrast, the separation using the column polymerized for 1.5 h produced sharp peaks for all five alkylbenzenes (Fig. 6-5a). The relationship between the polymerization time and theoretical plate numbers for uracil, toluene, and *n*-propylbenzene at a chromatographic linear flow rate of 1 mm s^{-1} are shown in Fig. 6-6. The maximum theoretical plate numbers of toluene and n-propylbenzene were 65000 and 64000 plates m^{-1}, respectively, and obtained at 1.5 h. The plate numbers decreased with an increase in polymerization time and the theoretical plate numbers for toluene and

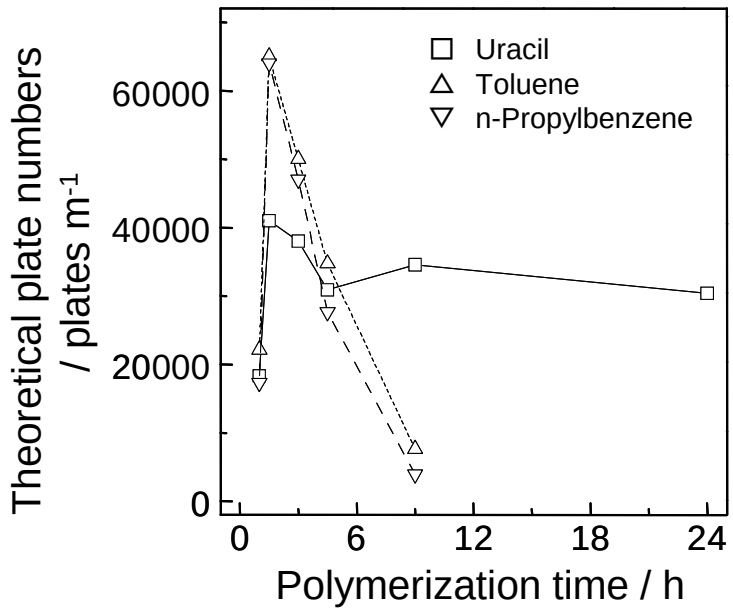

Fig. 6-6 Relationships between the polymerization time and the theoretical plate number at a linear flow rate of 1.0 mm s^{-1} for uracil, toluene, and *n*-propylbenzene. Chromatographic conditions were the same as those in Fig. 6-5.

n-propylbenzene were 7600 and 3900 plates m^{-1}, respectively at polymerization for 9 h. For non-retained analyte of uracil, maximum theoretical plate number of 40000 plates m^{-1} was obtained at polymerization time of 1.5 h and also decreased moderately with the increase in the polymerization time (reached to 31000 plates m^{-1} at 24 h). It was often observed that the column preparation with relatively short polymerization time produced the higher column efficiency in the low conversion polymerization of monoliths.[1,17-19]

The relationship between the polymerization time and the back pressure at a linear flow rate of 1 mm s^{-1}, or flow resistance of the column, is show in Fig. 6-7. The back pressure increased with the increase in polymerization time and this result agreed with the result of the SEM observation (Fig. 6-3). At the 1.5 h, where the highest theoretical plate number was obtained (Fig. 6-6), the back pressure was

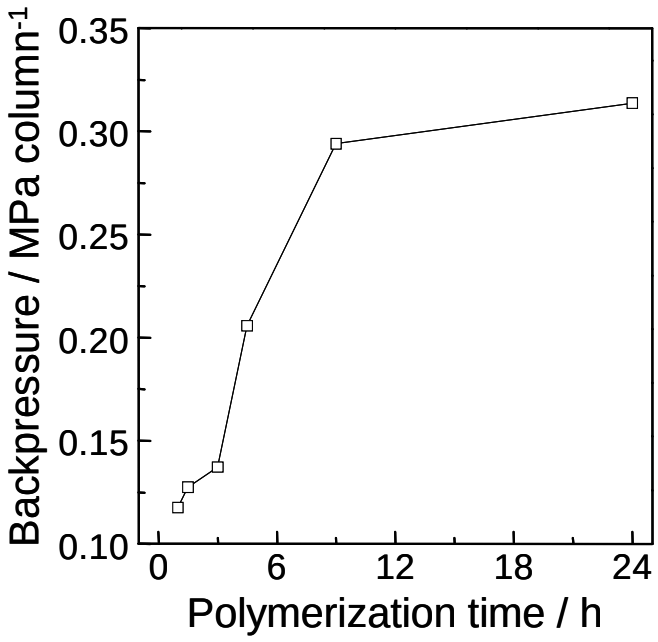

Fig. 6-7 Relationships between the polymerization time and the back pressure at a linear flow rate of 1.0 mm s^{-1}, Chromatographic conditions were the same as those in Fig. 6-5.

0.14 MPa and this permeability is sufficiently low for the use in LP-HPLC.[18]

The run-to-run repeatability, column-to-column reproducibility, and acidic stability were evaluated for the column polymerized for 1.5 h. At the linear flow rate of 1.0 mm s^{-1}, the RSD for the run-to-run repeatability of retention time, retention factor, and theoretical plate number for *n*-propylbenzene were 0.01%, 0.2% and 3% (n=5), respectively. Moreover, the RSD for column-to-column reproducibility of the retention time, retention factor, and theoretical plate number for *n*-propylbenzene at 1.0 mm s^{-1} were 0.5%, 1% and 4%, respectively, and those of the back pressure was 10% (n=3). Moreover, the monolithic column polymerized for 1.5 h was stably used in the 6 M HCl at least within 2 weeks.

On the view of separation efficiency, flow resistance, reproducibility and acid-resistance of the column, the polymerization for 1.5 h was employed to preparing the column to evaluate the metal ion-surfactant interaction using LP-HPLC.

6.3.2. Effect of POE chain length on loading capacity of Au(III) to PONPE coated column

The column prepared with the optimum condition was coated by PONPE with various POE chain length (n=7.5, 15, 20). Amounts of both PONPE coated on the column and loading capacity of Au(III) in 6 M HCl for each column were measured using the breakthrough curves and the results were summarized in Fig. 6-8. The amount of PONPE coated on the column decreased with the increase in the POE chain length. This phenomenon would result in the increase in hydrophilia of PONPE molecule and/or the volume of hydrophilic part with the increase in the

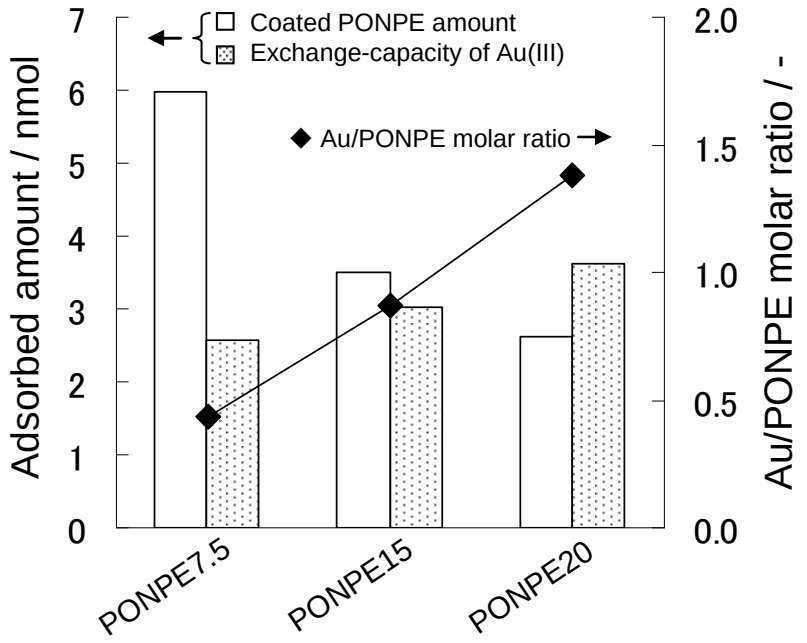

Fig. 6-8 Amounts of both PONPE coated on the column and loading capacity of Au(III) for PONPE7.5, 15 and 20 in 6 M HCl (left axis, bar graph). The ratios of loading capacity of Au(III)/ PONPE amount were also presented (right axis, line graph).

POE chain length. As is interesting to note, the loading capacity of Au(III) per column increased with the increase in POE chain length whereas the amount of PONPE coated on the column, N_{PONPE}, decreased.

The molar ratios of Au(III) loading capacity/N_{PONPE} in each column are also presented in Fig. 6-8. The molar ratio of Au(III)/N_{PONPE} enlarged by the elongation of POE chain, *i.e.*, the Au(III)/N_{PONPE} ratio on the column coated with PONPE7.5 was 0.4 and that with PONPE20 was 1.4 (about three times lager). This result indicates that PONPE with longer POE chain strongly interacted with Au(III). As the further investigation, the amounts of oxyethylene (OE) in mole unit per column (N_{OE}, N_{PONPE} × average OE unit numbers in single PONPE molecule) were calculated and shown in Fig. 6-9. The ratios of Au(III) amount to N_{OE}, *i.e.*, Au(III)/N_{OE}, are also calculated for each column. In contrast to Au(III)/N_{PONPE} ratios

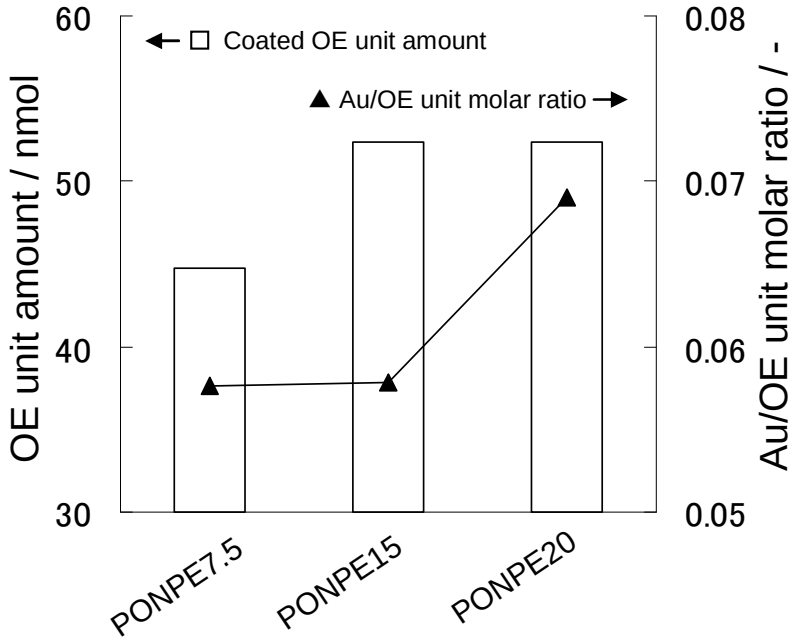

Fig. 6-9 Variation in amount OE coated on the column and its ratio to loading -capacity to Au(III).

shown in Fig. 6-8, the difference in Au(III)/N_{OE} ratios between PONPE7.5 and PONPE20 was about 20%. The interaction of single OE unit to Au(III) for PONPE20 would be slightly higher than that for other PONPEs. The difference for PONPE20 may arise from the difference in the flexibility of the POE chain. Consequently, the difference in loading capacity of Au(III) shown in Fig. 6-8 mainly given by the difference in number of OE unit coated on the column. Further study is necessary to elucidate the effect of the POE chain length on the interaction.

6.3.3. Chromatographic evaluation of interactions of PONPE with chloride complex ions of various metal ions

The interactions between chloride complex ions of Ga(III), Fe(III), Cu(II), and Zn(II) with the column coated with PONPE7.5, 15 and 20 were evaluated in the mobile

phase of 6 M HCl containing 0.5 mM Au(III). Here, Au(III) was added to the mobile phase both for enhancement in elution of analytes and for indirect absorbance measurement of Ga(III) and Zn(II). Uracil was added to each metal ion sample solution as a non-retained solute (t_0 marker).

Fig. 6-10 shows resulting chromatograms of four metal ions using the column coated with PONPE15 and a bare column as a reference. Here, uracil (t_0 marker), Cu(II), Fe(III), and Au(III) were detected as positive peaks and both Zn(II)

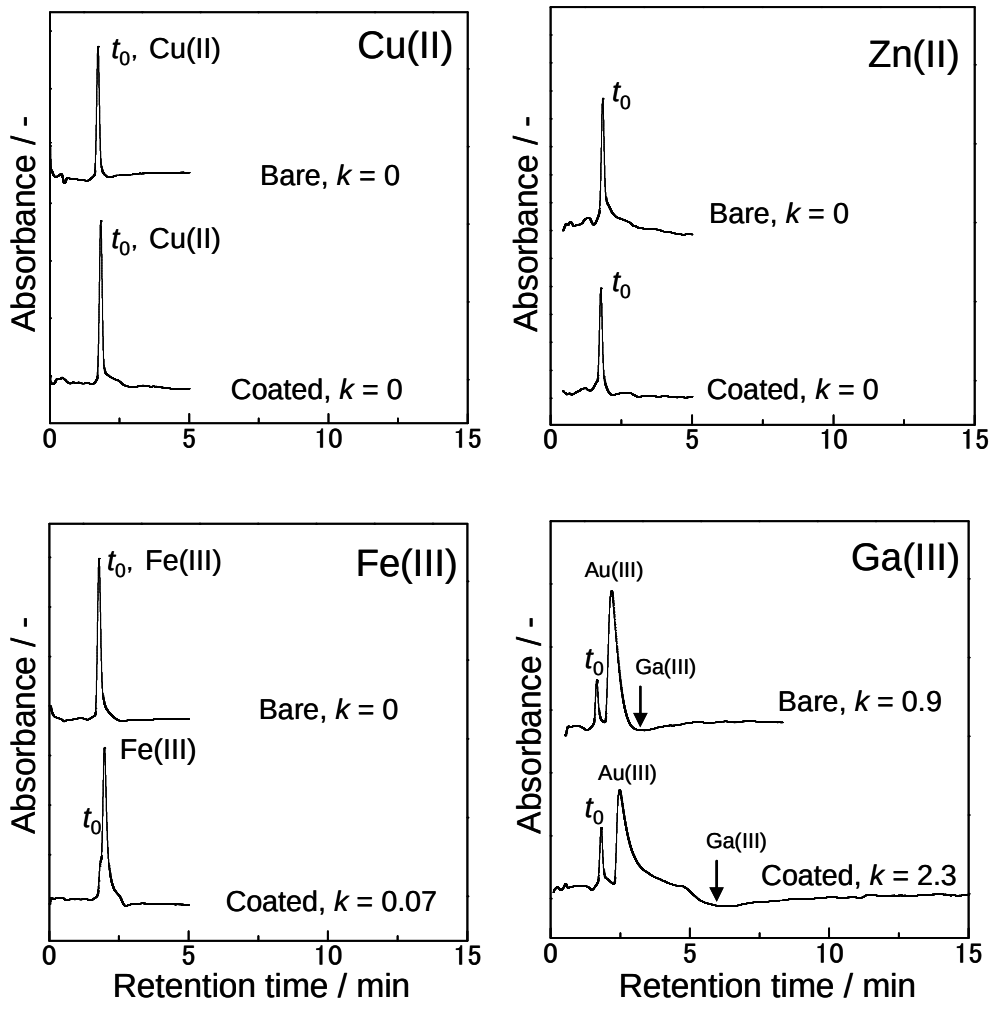

Fig. 6-10 Chromatograms of Ga(III), Fe(III), Cu(II), and Zn(II) using the gas pressure-driven LP-HPLC. Conditions: Mobile phase 0.5 mM Au(III) in 6 M HCl; Pressure 0.2 MPa; UV detection at 220 nm. Uracil was added as a t_0 marker.

and Ga(III) were as dip peaks. As shown in Fig. 6-10, Cu(II) was not retained in both the columns with and without PONPE15 coating. Although Fe(III) was not retained in the bare column, the coated column slightly retained Fe(III) (k=0.09). Ga(III) was retained weakly (k=0.9) in the bare column whereas the detailed interaction for the retention was not clear. When Ga(III) was injected to the PONPE15 coated column, the retention was clearly enhanced (k=2.3). Note that, the relatively large positive peak around 2.5 min is originated in the Au(III) release form the column induced by Ga(III) injection. In other words, Au(III) interacted with the POE chains exchanged with Ga(III). On the other hands, Zn(II) was not detected on both bare and PONPE-coated chromatogram. Moreover, the exchange-based Au(III) peak was also not detected. Thus we deemed that Zn(II) was not interacted the PONPE on the column.

The capacity factors of four metal ions in the column coated PONPE7.5, 15, and 20 were listed in Table 6-1. The capacity factor of Ga(III) increased by 3-4 times in any PONPE coated columns in comparison with bare one. Fe(III) was slightly retained (<0.1 in k) in each PONPE coated column and both Cu(II) and Zn(II) were not retained in any columns. The magnitude of the PONPE-metal ion

Table 6-1 Capacity factor for Ga(III), Fe(III), Cu(II), and Zn(II) on the column coated with PONPE7.5, 15, and 20.

	Capacity factor, k / -			
	Bare	PONPE7.5	PONPE15	PONPE20
Ga(III)	0.88	2.4	2.3	3.6
Fe(III)	0.0	0.073	0.072	0.12
Cu(II)	0.0	0.0	0.0	0.0
Zn(II)	0.0	0.0	0.0	0.0

Chromatographic conditions were the same as those in Fig. 6-10.

interactions, observed in this study, was Cu(II), Zn(II) (= 0) < Fe (III) < Ga(III), in the 6 M HCl containing 0.5 mM Au(III). This order agrees with that reported previously in the experiment of solvent extraction using 6 M HCl.[13] Therefore, the present method is effective to determinate the interaction between metals and surfactants.

Here, we calculated the differential capacity factor between coated and bare column, Δk (k_{PONPE} - k_{Bare}), in each column coated with different PONPEs. The Δk is the indicator for the PONPE-originated retention and the values of Δk divided by N_{PONPE}, *i.e.* $\Delta k/N_{PONPE}$, was also calculated. As shown in Fig. 6-11, $\Delta k/N_{PONPE}$ values for both Ga(III) and Fe(III) increased with the increase in the POE chain length. These enhancements in the retention would be produced by the increase in N_{OE} as described in the previous section. On the other hand, Fig. 6-12 shows the relationship between $\Delta k/N_{PONPE}$ for Ga(III) and Fe(III). Since the plot was in linear relation (r^2 = 0.980), $\Delta k/N_{PONPE}$ ratio of Ga(III)/Fe(III) in any columns were almost

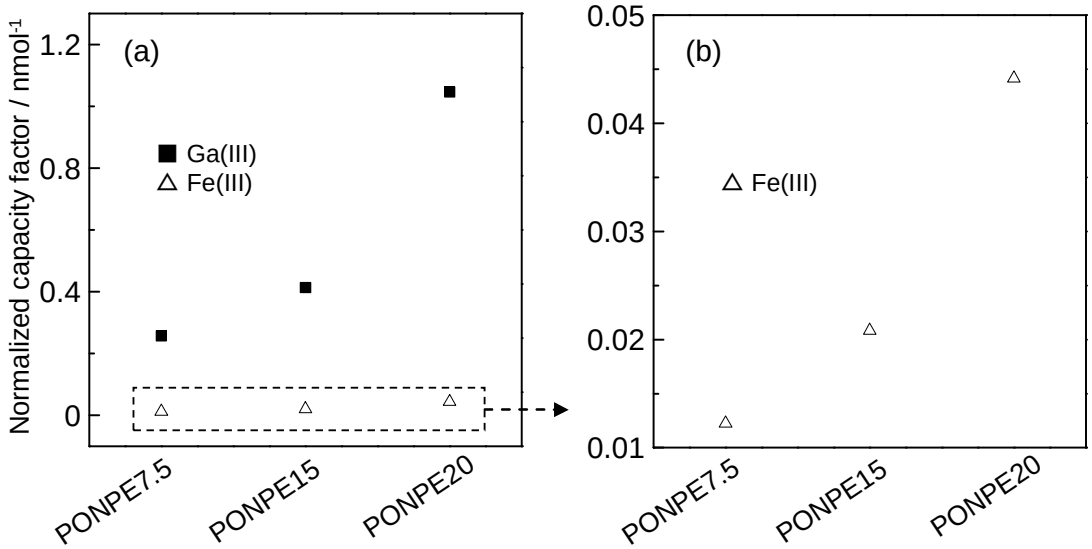

Fig. 6-11 Variations in retention factor of Ga(III) and Fe(III), which were normalized by amount of PONPEs coated on the column . Chromatographic conditions were the same as those in Fig. 6-10.

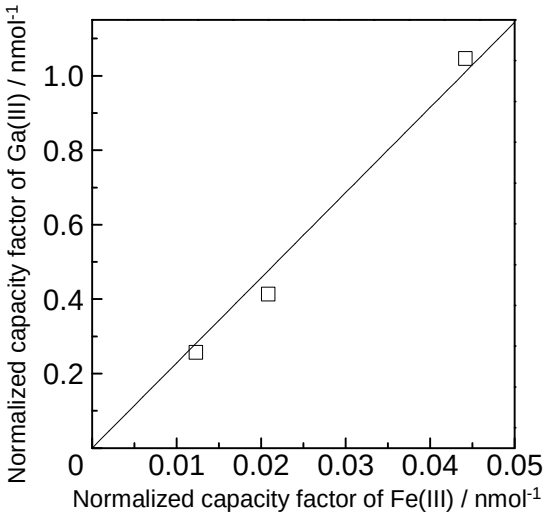

Fig. 6-12 Relationship of normalized retention factor of Ga(III) and Fe(III). Chromatographic conditions were the same as those in Fig. 6-10.

constant, about 22:1. In this case, the selectivities for Ga(III) and Fe(III) did not depend on the length of POE chain coated on the column.

6.4 Conclusion

In this chapter, we developed a method to evaluate the interaction between metal ions and nonionic surfactants in an aqueous solution containing high concentration HCl using gas pressure-driven LP-HPLC as acid-resistance HPLC system. Prior to the construction of the LP-HPLC, a short time thermal polymerization of styrene-*co*-divinylbenzene-based low flow resistance monolithic column was investigated and the polymerization for 1.5 h allowed the preparation of the column with both high separation efficiency of 60000 plates m^{-1} for alkylbenzenes and quite low back pressure of 0.14 MPa at a linear flow rate of 1 mm s^{-1}. The column prepared with the optimized condition was coated with the nonionic surfactant of PONPE with various POE chain lengths and applied for evaluation of the

interaction of PONPEs with metal ions in 6 M HCl. The interactions between PONPEs and metal ions of Au(III), Ga(III), Fe(III), Zn(II) and Cu(II) were successfully evaluated using both breakthrough and chromatographic methods. The interaction order for the metal ions obtained in this study was agree with the previously reported one. Furthermore, the study for the effect of POE length revealed that the magnitude of the interaction mainly depended on the amount of OE unit, not the chain length. The evaluation of interactions of metal ions and surfactants were successfully achieved by the present method using LP-HPLC. The combination of the proposed method using LP-HPLC and elementary analysis methods, such as ICP-AES or -MS, will permit a high throughput evaluation of interactions between surfactants and numerous metal ions in various conditions. These types of studies will be necessary for the progress in CCFS for recovering valuable metals from wastes.

References

1. T. Hirano, A. Kobayashi, T. Nakaza, S. Kitagawa, H. Ohtani, K. Nagayama, and T. Matsumoto, *Anal. Sci.,* **2013**, *29*, in Press.
2. K. Halada, Mater. Cycles Waste Manage. Res., **2009**, *20,* 49.
3. T. Nakamura, Mater. Cycles Waste Manage. Res., **2009**, *20,* 70.
4. S. Morimoto, Energy Resour., **2009**, *30,* 383.
5. I. Mihaylov and P. A. Distin, *Hydrometallurgy,* **1992**, *28,* 13.
6. J. Jayachandran and P. Dhadke, *Hydrometallurgy,* **1998**, *50,* 117.
7. H. S. Lee and C. W. Nam, *Hydrometallurgy,* **1998**, *49,* 125.
8. G. V. K. Puvvada, *Hydrometallurgy*, **1999**, *52,* 9.

9. K. Yamamoto and N. Katoh, *Anal. Sci.*, **1999**, *15,* 1013.

10. N. Hirayama, Y. Horita, S. Oshima, K. Kubono, H. Kokusen, and T. Honjo, *Talanta,* **2001**, *53,* 857.

11. M. S. Lee, J. G. Ahn, and E. C. Lee, *Hydrometallurgy,* **2002**, *63,* 269.

12. B. Bhattacharya, D. K. Mandal, and S. Mukherjee, *Sep. Sci. Technol.*, **2003**, *38,* 1417.

13. T. Kinoshita, S. Akita, S. Nii, F. Kawaizumi, and K. Takahashi, *Sep. Purif. Technol.*, **2004**, *37*, 127.

14. T. Kinoshita, Y. Ishigaki, K. Yamaguchi, S. Akita, Y. Yamada, S. Nii, K. Takahashi, and F. kawaizumi, *Sep. Purif. Technol.,* **2006**, *52,* 357.

15. T. Kinoshita, S. Akita, Y. Ishigaki, K. Yamaguchi, Y. Yamada, S. Nii, F. kawaizumi, and K. Takahashi, *IChemE Part A: Chem. Eng. Res. Des.*, **2007**, *85*, 229.

16. T. Kinoshita, Y. Ishigaki, N. Shibata, K. Yamaguchi, S. Akita, S. Kitagawa, H. Kondou, and S. Nii, *Sep. Purif. Technol.,* **2011**, *78,* 181.

17. L. Trojer, C. P. Bisjak, W. Wieder, and G. K. Bonn, *J. Chromatogr., A,* **2009**, *1216*, 6303.

18. I. Nischang and O. Brüggemann, *J. Chromatogr. A,* **2010**, *1217*, 5389.

19. I. Nischang, I. Teasdale, and O. Brüggemann, *J. Chromatogr., A,* **2010**, *1217*, 7514.

20. T. Hirano, S. Kitagawa, and H. Ohtani, *Anal. Sci.,* **2009**, *25*, 1107.

21. T. Nakaza, A. Kobayashi, T. Hirano, S. Kitagawa, and H. Ohtani, *Anal. Sci.,* **2012**, *28*, 917.

Chapter 7 Conclusions

The enhancement in separation efficiency of a column is one of the indispensable topics for the further progress in HPLC and the column with low flow resistance is also required as describe in chapter 1. In this study, highly efficient polymer monolithic columns with a low flow resistance for HPLC were successfully developed by new polymerization methods. Moreover, the prepared columns were applied to the ultra high speed separation and low pressure-HPLC, which are never carried out by the conventional packed and monolithic columns.

In chapter 2, the low flow resistance poly(butyl methacrylate (BMA)-*co*-ethylene dimethacrylate (EDMA))-based reversed phase monolithic columns was prepared by photo-polymerization. Here, the effects of the polymerization conditions (UV irradiation intensity and polymerization temperature) on the column characteristics were investigated and it was revealed that both the higher UV irradiation intensity and the lower polymerization temperature lead to the superior column efficiency. The column prepared with the optimized condition showed moderate separation efficiency around 40000 plates m^{-1} for alkylbenzenes at a linear flow rate of 1 mm s^{-1} and the low flow resistance was also achieved (the back pressure at this flow rate was 0.3 MPa). This column was applied to the ultra high speed separation of five alkylbenzene and separation within 8s was successfully demonstrated at a linear flow rate of 110 mm s^{-1}, which is corresponding to over a hundredfold faster speed than that in the conventional HPLC.

In chapter 3, the low temperature UV photo-polymerization, developed for the preparation of RP column described in chapter 2, was applied to preparing the

low flow resistance anion-exchange methacrylate-based monolithic column. The column prepared with UV photo-polymerization at -15°C exhibited the low flow resistance with the remarkably high separation efficiency similarly to the RP column. Under optimal conditions, a theoretical plate height of 9.4-15.6 μm (*N*, 64000-110000 plates m^{-1}) was achieved for some small inorganic anions. This column efficiency was relatively high for a polymer monolithic column and was almost comparable with the efficiency of silica-based anion-exchange monolithic columns. The flow resistance of the column was acceptably low, and fast separation was successfully demonstrated with an apparent flow velocity up to 32 mm/s. In the gradient method, five inorganic anions were separated rapidly with a high precision within 20 s.

Both two columns prepared with UV photo-polymerization at low temperature exhibited both good separation efficiency and low flow resistance. Here, we guessed that the monomer conversions to the monolith influenced the column characteristics. However, there is no method to determine monomer conversions directly for monolith fixed in a narrow capillary. In chapter 4, therefore, direct determination method for monomer conversions for monolith fixed in a capillary column was developed using pyrolysis-gas chromatography (Py-GC). The proposed method was successfully applied to determining the monomer conversions to poly(BMA-*co*-EDMA) monolith. Consequently, it was determined that the conversion of EDMA was significantly greater than that of BMA in a low-conversion UV photo-polymerized poly(BMA-*co*-EDMA) monolithic column. In other words, in the low-conversion poly(BMA-*co*-EDMA) monolith, the monomer composition did not match that of the reaction solution introduced into the capillary before polymerization.

In chapter 5, the preparation of the remarkably highly efficient poly(BMA-*co*-EDMA) monolithic column with quite low flow resistance was investigated. Here, the monomers conversions to the monolith prepared with UV photo polymerization at low temperature were reduced to utilize the low conversion polymerization. The shorter time polymerization was effective to produce both the lower flow resistance and higher column efficiency. By UV irradiation for 2 min, the monolithic column exhibited a high column efficiency of over 100,000 plates m^{-1} at a linear flow rate of 1 mm s^{-1} with 0.14 MPa of back pressure. At this condition, the conversions of BMA and EDMA were 10% and 21%, respectively. CLSM observation revealed that the prepared monolith structures were more homogenous than those prepared in chapter 2. As an application of the low flow resistance column, low pressure-HPLC (LP-HPLC) system without conventional LC pump was developed, in which low gas pressure and vacuum were used to generate mobile phase stream. The separations of alkylbenzenes and proteins were successfully achieved using a low pressure of less than 0.2 MPa.

LP-HPLC, proposed in chapter 5, has a potential to construct a highly acid-resistant system because it is free from metal and aluminum oxide which are used in conventional HPLC pump. Thus, in chapter 6, it was developed that an evaluation method for interactions between metal ions and nonionic surfactant in highly acidic aqueous solution as an application of the LP-HPLC. Prior to the construction of the LP-HPLC, a short time thermal polymerization-based low flow resistance styrene-*co*-divinylbenzene monolith was investigated as an acid-resistance column and the polymerization for 1.5 h allowed preparing the column with both high separation efficiency of 60000 plates/m for alkylbenzenes and quite low back pressure of 0.14 MPa at a linear flow rate of 1 mm/s. The column

prepared with the optimized condition was coated with the nonionic surfactant of polyoxyethylene nonylphenyl ether (PONPE, n=7.5, 15, and 20) and applied for evaluation of the interaction of PONPEs with metal ions in 6 M HCl. The interactions between PONPEs and metal ions of Au(III), Ga(III), Fe(III), Zn(II) and Cu(II) were successfully evaluated using both breakthrough and chromatographic methods. Furthermore, the study for the effect of POE chain length revealed that the magnitude of the PONPE-metal ion interaction mainly depended on the amount of OE unit, not the chain length.

In this issue, we have developed two types of highly efficient polymer monolith columns with low flow resistance, *i.e.*, methacrylate and styrene based ones. In particular for methacrylate based monolith, it was revealed that the low temperature UV photo-polymerization is effective in preparing monolithic columns with both high separation efficiency and low flow resistance. Although the column of RP and anion exchange modes were only prepared in this issue, the low temperature UV photo-polymerization will be adaptable to the preparation of other chromatographic separation modes, such as cation exchange and hydrophilic interaction modes. However, the mechanism to result the highly efficient monolith with the high permeability is not clearly elucidated. In order to figure out the detail, further studies will be necessary and the elucidation will significantly contribute the advance in the polymer monolith column.

Meanwhile, in this issue, the concept of LP-HPLC using a low flow resistance capillary column was proposed. As the application of LP-HPLC, the interaction in highly acidic solution was studied. Since a volume of a mobile phase used in LP-HPLC can be reduced less than 1 mL, a solution containing rare and/or expensive compounds will be able to use as a mobile phase, which may support the

progress in studies in various fields. Moreover, the LP-HPLC without a conventional pump will have a potential to fabricate an ultra-light weight HPLC, which will be suitable for portable use.

As described in introduction, the HPLC is a potential separation method for analysis widely used in various research areas. In order to progress a great variety of researches, the enhancement of the HPLC is considerably important. The present study successfully demonstrated that the highly efficient polymer monolithic column with low flow resistance enabled the development in HPLC which can not be done by the use of conventional packed columns. Therefore, the results in this study will contribute further progress in studies for many researches using HPLC.

List of co-workers (alphabetical order)

Ayumi Kobayashi	Graduate School of Engineering, Nagoya Institute of Technology
Hajime Ohtani	Graduate School of Engineering, Nagoya Institute of Technology
Kazuaki Nagayama	Graduate School of Engineering, Nagoya Institute of Technology
Mutsumi Takahashi	Graduate School of Engineering, Nagoya Institute of Technology
Shigendo Akita	Nagoya Municipal Industrial Research Institute
Shinya Kitagawa	Graduate School of Engineering, Nagoya Institute of Technology
Susumu Nii	Graduate School of Engineering, Nagoya University
Takehiko Kinoshita	Nagoya Municipal Industrial Research Institute
Takeo Matsumoto	Graduate School of Engineering, Nagoya Institute of Technology
Takuya Nakaza	Graduate School of Engineering, Nagoya Institute of Technology
Yuzo Ishigaki	Nagoya Municipal Industrial Research Institute

Acknowledgments

I appreciate Associate Professor Shinya Kitagawa for a lot of valuable supports and advices of my study and this thesis.

I am so grateful to Professor Hajime Ohtani for advices and assistance to my experiments.

I express gratitude to Professor Akio Yuchi for the help to the perfection of this thesis.

I am indebted to Associate Professor Tomonari Umemura for advices to my experiments.

I feel grateful my greatly thanks to Professor Takeo Matsumoto and Associate Professor Kazuaki Nagayama for support to my experiments.

I am so grateful to Associate Professor Susumu Nii, Dr. Tekehiko Kinoshita, Mr. Yuzo Ishigaki, Mr. Nobuyuki Shibata and Dr. Shigendo Akita for a lot of advice and assistance to my experiments.

I want to thank for Assistant Professor Yoshinori Iiguni for advices to my experiments.

I greatly appreciate to Ms. Mutsumi Takahashi, Mr. Ayumi Kobayashi, Mr. Takuya Nakaza for a lot of advice and assistance to my experiments.

I want to thank for Mr. Hajime Nishimura for a lot of advice and assistance to my experiments.

Thanks are offered to members in our laboratory.

Finally, I would like to express thanks to my parents.

List of publications

[The papers related to this thesis]

1. "Methacrylate-ester-based reversed phase monolithic columns for high speed separation prepared by low temperature UV photo-polymerization", T. Hirano, S. Kitagawa, and H. Ohtani, *Anal. Sci.,* **2009**, *25*, 1107-1113. (Chapter 2)
2. "Separation of small inorganic anions using methacrylate-based anion-exchange monolithic column prepared by low temperature UV photo-polymerization", M. Takahashi, T. Hirano, S. Kitagawa, and H. Ohtani, *J. Chromatogr. A,* **2012**, *1232*, 123-127. (Chapter 3)
3. "Determination of monomer conversion in methacrylate-based polymer monoliths fixed in a capillary column by pyrolysis-gas chromatography", T. Nakaza, A. Kobayashi, T. Hirano, S. Kitagawa, and H. Ohtani, *Anal. Sci.*,**2012**, *28*, 917-920. (Chapter 4)
4. "Low-flow-resistance methacrylate-based polymer monolithic column prepared by low-conversion ultraviolet photopolymerization at low temperature", T. Hirano, A. Kobayashi, T. Nakaza, S. Kitagawa, H. Ohtani, K. Nagayama, and T. Matsumoto, *Anal. Sci.,* **2013**, *29*, in press. (Chapter 5)
5. "Evaluation of interaction between metal ions and nonionic surfactant in high concentration HCl using low pressure-high performance liquid chromatography with low flow resistance polystyrene-based monolithic column", T. Hirano, S. Kitagawa, S. Nii, T. Kinoshita, Y. Ishigaki, N. Shibata, S. Akita, and H. Ohtani, in preparation for submission. (Chapter 6)

[Other papers]

1. “Preparation of Ultra Low Flow Resistance Column Based on Polymer Monolith Technology”, *Reports of Toyoda Physical and Chemical Research Institute*, **2011**, *64*, 181-184.

2. “High performance polymer monolithic columns prepared by novel polymerization methods” *J. Flow. Injection Anal.* **2012**, *29,* 30.